T H E U N I V E R S I T Y O F A L B E R T A

RELEASE FORM

NAME OF AUTHOR Michael P. Lau

TITLE OF THESIS Characteristics of Argon and Argon-Oxygen Inductively Coupled Plasmas for Trace Element Analysis of Petroleum Products

DEGREE FOR WHICH THESIS WAS PRESENTED M.Sc.

YEAR THIS DEGREE GRANTED 1981

THE UNIVERSITY OF ALBERTA

CHARACTERISTICS OF ARGON AND ARGON-OXYGEN INDUCTIVELY COUPLED PLASMAS FOR TRACE ELEMENT ANALYSIS OF PETROLEUM PRODUCTS

by

© MICHAEL P. LAU

A THESIS

SUBMITTED TO THE FACULTY OF GRADUATE STUDIES AND RESEARCH

IN PARTIAL FULFILMENT OF THE REQUIREMENTS FOR THE DEGREE

OF MASTER OF SCIENCE

DEPARTMENT OF CHEMISTRY

EDMONTON, ALBERTA

SPRING, 1981

THE UNIVERSITY OF ALBERTA

FACULTY OF GRADUATE STUDIES AND RESEARCH

The undersigned certify that they have read, and recommend to the Faculty of Graduate Studies and Research, for acceptance, a thesis entitled Characteristics of Argon and Argon-Oxygen Inductively Coupled Plasmas for Trace Element Analysis of Petroleum Products submitted by Michael P. Lau in partial fulfilment of the requirements for the Degree of Master of Science.

To my parents

ABSTRACT

The determination of various elements in crude oil and bitumen samples has been of considerable interest to both the petroleum industries and environmental protection agencies. In addition to affecting the catalyst used in the refining process, some of these elements are potential environmental hazards. Several analytical techniques that have been applied were reviewed.

A method was developed for these samples using an Inductively Coupled Plasma (ICP) as the excitation source, and a computer coupled photodiode array based spectrometer as the signal processor. The samples were diluted with xylene and aspirated directly. The parameters for simultaneous multielement analysis (SMA) were optimized, and precision and detection limits were reported.

Furthermore, the effect of the addition of oxygen gas to the argon supply on the analytical capability of the ICP was explored. Gradually increasing the amount of oxygen enhanced the analyte signal and attenuated emissions from carbon containing species and also a decrease in background continuum was observed. 20% oxygen mixed in the plasma (coolant) gas flow was determined to be optimum. Other parameters were investigated and precision and detection limits were obtained.

The analytical capabilities of both plasma discharges operating under optimal conditions were compared and the result favored the mixed oxygen-argon discharge. An

explanation was given for the observed effect of oxygen. Potential applications for the mixed oxygen-argon ICP were discussed.

ACKNOWLEDGEMENTS

The author wishes to extend his unreserved thanks and appreciation to his research group, and especially to Roger Ng, Don Hull and Dr. Naoki Furuta for many valuable discussions.

Also the author would like to thank Syncrude and Petrocan for their generosity in providing some standard reference materials, and to Sherritt Gordon Mines Ltd. for providing the MAK nebulizer.

The secretarial assistance of Kelly Vlassis in the preparation of this thesis is gratefully acknowledged.

Finally, the author is deeply indebted to Dr. Gary Horlick for his continuous support and leadership.

TABLE OF CONTENTS

LIST OF TABLES

LIST OF FIGURES

CHAPTER I

INTRODUCTION

A. Importance of Trace Elements in Petroleum Products

The trace level concentration of various elements in petroleum products is of great interest to both the petroleum industries and environmental monitoring agencies. Certain elements, if present in the refinery feedstocks, poison the catalyst during the refining process and alter the conversion and result in an undesirable shift in product distribution. Nickel and vanadium especially have been shown to poison cracking catalysts, thus reducing gasoline production and increasing coke production (1,2). Because of the large volumes of feed processed, even trace or ultra-trace concentrations gradually accumulate on the catalyst bed. The poisoned catalyst must either be replaced or regenerated, which is costly and further delays production.

On the environmental side, increasing consumption of petroleum products results in increasing amounts of elements being released into the atmosphere. Sulfur is present and oxidizes to sulfur dioxide, SO_2, either during refining or when the finished product is combusted. This highly toxic gas escapes into the atmosphere and causes "acid rain". Other elements such as lead, mercury, arsenic and cadmium are notorious for their toxicity. For example, the possible hazards to the environment from lead in gasoline have been

reviewed by the American Petroleum Institute (API)(3). The devastating effects of these elements on the environment and human life are receiving ever increasing attention.

The occurrance of metal porphyrin compounds and the unique relationship of nickel and vanadium have been studied. Baker (4) and extensive work by Falk (5) have correlated the nature of porphyrin, metal content, and nickel to vanadium ratio to the age and origin of crude oils. In identifying oil pollution sources, Brunnock et al. (6) have presented a scheme based on metal content and included nickel and vanadium data for 27 crudes. Other schemes for such applications based on metal contents and ratios have been reviewed by Adlard (7).

B. Oil Sands Importance, Composition, Origin and Trace Elements

1. Importance

The Alberta Oil Sands (AOS) are a huge natural resource. With dwindling supplies of conventional crude oil, oil sands offer a new source of petroleum which could in time help meet our nation's future energy needs. This energy self-sufficiency is vital to maintain our standard of living.

The oil sands in Alberta are not unique. There are similar deposits in the United States, the USSR, Europe, South America and Africa. Underlying an area of some 50,000 square kilometres and containing nearly 159 billion cubic metres of bitumen, the AOS are, however, the largest

deposits in the world.

The value of the oil sands was recognized long ago, but the high cost of separating bitumen from sand discouraged many early large scale extraction attempts. The rapid increase in world prices for petroleum products in the past few years has made recovery of bitumen from oil sands more economical.

2. Composition

Oil sand is composed of sand, heavy oil, mineral-rich clay and water. The sand makes up about 84% of oil sand by weight and consists predominantly of SiO_2. Water content is about 4% of the oil sand by weight and is present in the form of a film which envelops each grain of sand, keeping it separate from the oil.

The heavy oil in oil sand, called bitumen, averages about 11% by weight and is made up of 50 to 60% oil, 30 to 35% resin (fraction that is soluble in pentane), and 15 to 25% as asphaltenes (fraction that is insoluble in pentane).

In its raw state, bitumen contains more aromatic bond structures than conventional oils, and the appearance is a semi-solid, sticky black substance. Chemical alterations, such as cracking, are required to make it fluid enough to be transported by pipeline, hence the term "synthetic crude oil".

3. Origin

The AOS are believed to have been formed in the Cretaceous period, the last period of the Mesozoic Era,

which began two hundred million years ago. The layers of limestone, on which the AOS rest, date back even further.

The most widely believed theory on "how did the AOS originate?" hypothesizes the migration of oil eastward into deposits of wet sand. While the date and origin of the bitumen cannot be geologically confirmed, the AOS are considered "young" crude oil because such hydrocarbon deposits tend to become more fluid with time. The oil sands are not fluid when compared to geologically older deposits which can be extracted by traditional well drilling.

4. Trace Elements

Not unlike other "geologically older" crudes, a large variety of elements have been identified in oil sands. The source of these elements may be grouped into two categories (8). A number of organic or metallo-organic compounds are indigenous to crude oil and are found in all crudes to some degree, regardless of source. The organics include oxygen-containing materials such as naphthenic acid; mercaptans, sulfides, disulfides, etc. as sulfur-containing compounds; and both basic and non-basic nitrogenous matter. Metallo-organics, present initially or formed by interaction with surrounding mineral matter, include chelate compounds, metal soaps, and oil soluble metal alkyls. The second group consists of impurities or contaminants whose presence is not directly related to the genesis of the crude oil. These are primarily colloidal or suspended entrained inorganic material and emulsified water containing dissolved salts.

Major levels of silicon and aluminum are found predominantly in the sand or suspended mineral solid, and minor amounts of sodium and potassium ions have been identified in the water envelope. However, the majority of the elements occur in the petroleum matrix, bitumen. The minor, and trace elemental content of bitumen, although small (about 0.2%) in comparison to the organic content, is of considerable importance. Their roles both inside and outside the industry have been discussed previously.

The metal content of petroleum ash was summarized by Thomas (9) in 1924. Later, he summarized qualitative and semi-quantitative data for the metal content of crude oils (10). Hodgson et al. (11) presented semi-quantitative spectrographic analysis of an oil sand ash. They determined 14 elements and reported concentration values from 25% silicon to 0.1% chromium. The other elements determined were aluminum (12%), vanadium (8%), nickel (7%), iron (6%), copper (2%), calcium (1.6%), magnesium (1.2%), sodium (0.8%), titanium (0.8%), lead (0.6%), manganese (0.3%), and molybdenum (0.2%). A detailed survey by the U.S. Environmental Protection Agency (EPA) on potential pollutants in fossil fuels compiled all values found in the literature for the metal, nitrogen and sulfur content of petroleum (12).

C. Analytical Techniques for the Determination of Trace Elements in Petroleum Products

Numerous techniques have been applied to the

determination of trace elements in petroleum matrices. Some reviews on the subject include a chapter by Buell (13) and a book by Kyuregyan (14), both emphasizing atomic spectroscopic applications. Other reviews include books by McCoy (15), Milner (8), and one edited by Hofstader et al. (16) surveyed the development of various analytical techniques for trace and ultra-trace determinations. Braier and Eppolito (17) and Fujita (18) discussed the advantages and disadvantages of various instrumental techniques. Due to the vast number of techniques and applications reported, and excellent discussions elsewhere, only a few examples will be discussed here.

1. Chemical and Colorimetric Methods

Evidently, the methods first used were chemical and colorimetric. Using slightly modified colorimetric methods originally described by Wrightson (19), Hodgson determined iron, nickel and vanadium in 77 crudes (20). Dry ashing at 600°C followed by hydrofluoric acid dissolution was carried out. Additional information, such as depth of crude produced, API gravity, sulfur content and vanadium to nickel ratio, was tabulated and used in a study regarding age of the deposit. Similarily, Baker and Hodgson (21) analyzed 37 western Canadian crudes for magnesium as well as nickel and vanadium. The study was made in an effort to correlate magnesium present in crude with chlorophyll as a derivative for phorphyrin and magnesium. The poor sensitivity of the method was recognized when they were unable to determine

magnesium since all magnesium was present at trace levels.

However, colorimetric methods were still widely used for a number of years in view of the fact that such methods are generally sensitive, utilize relatively inexpensive equipment, and require comparatively simple skills. Overall, the methods suffer from poor selectivity and lengthy processing of the sample to the color-development stage for one-element determinations. With the advent of more elaborate and sensitive instrumental approaches, very little work has been reported in recent years.

2. Electroanalytical Techniques

One interesting early application of electroanalytical methods was reported by Samuel and Brunnock (22) based on the use of square wave polarography. The oil sample was treated with bromine, extracted with hydrochloric acid, and residual organic matter was destroyed with nitric and perchloric acids. Flato (23) discussed a "Renaissance" of electroanalytical techniques. The most sensitive technique, differential pulse anodic stripping voltammetry, is carried out with a pulse voltage superimposed upon the linearly increasing voltage in the second step. Sensitivity is excellent in the 10^{-10} to 10^{-11}M range, and a maximum of six elements can be determined simultaneously.

The major drawback of electroanalysis to petroleum matrices is incompatibility with the inorganic solution requirements. Extensive sample preparation is required, and the residual strong acid must be removed or the final

solution buffered. This often involved the addition of various reagents, and the critical consideration is the amount of contamination introduced during the entire process. Furthermore, the elements to be determined will dictate the choice of both the sample digestion scheme and the type of final analyte solution. Even at modest instrumental cost, these voltammetric methods are mainly used to complement other techniques.

3. Atomic Absorption Spectrometry (AAS)

Flame atomic absorption was used for the direct analysis of metals in oil in 1962 by Barras (24) and Sprague and Slavin (25). The sample was diluted in a suitable solvent and aspirated into the flame. The dilution ratio required to eliminate matrix effects resulted in poor sensitivity. Later in 1967, Barras and Smith (26) described a multichannel AA spectrometer for the analysis of copper, iron, nickel and vanadium. Jackson et al. (27) reported the simultaneous determination of wear metals in used lubricating oils with another multichannel AA spectrometer utilizing a silicon-target vidicon detector. An air-acetylene flame was used and precision was somewhat poorer than normal for iron, magnesium, copper and silver. Good correlation was obtained between this method and a single channel method.

A novel particle size independent procedure for the analysis of titanium and molybdenum in lubricating oil was offered by Saba and Eisentraut (28,29). The samples were

treated with a mixture containing hydrofluoric and nitric acids and shaken for two minutes before dilution with methylisobutylketone. Both accuracy and precision were reasonable.

The significant improvements in sensitivity achievable by non-flame, or electrothermal vaporization atomic absorption spectrometry (EVAAS), have provided better detection limits (up to 2 orders of magnitude better when compared to conventional flame AA), but usually at the expense of precision. Improved detection limits were reported by Runnels et al. (30) for beryllium, chromium, manganese and aluminum with a graphite furnace atomizer. The inner surfaces of the furnace were treated to provide a carbide coating. Both maximum atomization temperature and rate at which maximum temperature was attained affected the detection limit.

Thomerson and Thompson (31) reviewed the advantages and disadvantages of flame and non-flame atomization techniques and listed typical detection limits for petroleum and other matrices. Cold vapor techniques for mercury and volatile hydride generation schemes were outlined and various electrothermal atomization devices were described. Welz (32) surveyed the application of AA in industrial analysis. He covered instrumentation (flame and furnace), analysis of lubricating oil for wear methods, trace metals detection in waste water, polymer analysis, and control of metals in fuel oils for high-speed gas turbines. Modifications to spectrometers, especially electrothermal vaporization units,

have been tremendous and the number of detailed fundamental studies is still growing.

Because of the excellent detection limits (in the nanogram (ng) range), with both solid and liquid sampling capabilities, EVAAS is widely used as an ultra-trace technique in modern analytical laboratories. Inductively coupled plasma atomic emission spectrometry with ultrasonic nebulization (to be discussed later) appears to be the only competing spectrochemical technique for solution analysis with respect to part-per-billion (ppb) and sub-ppb determinations.

4. Neutron Activation Analysis (NAA)

The availability of lower cost high flux thermal neutron irradiation facilities and high resolution solid state detectors has made NAA a very attractive tool for simultaneous determinations at the trace level. In his thesis study on crude oils, Filby (33) used NAA for the analysis of 10 crudes for 15 elements: nickel, vanadium, cobalt, mercury, iron, zinc, manganese, arsenic, gold, antimony, selenium, scandium, copper, sodium, and calcium. In an oil migration and maturation study, Hitchon et al. (34) determined the concentrations of 22 trace elements in 88 crude oils from Alberta by NAA, and selected 11 for factor analysis. In some instances, as many as 30 trace elements have been identified and measured in crude oils by this technique (35). Although excellent sensitivity can be achieved for many elements, it is often necessary to carry

out a separation step after irradiation because of interferences from elements such as sodium, chlorine and bromine. NAA is mainly used to cross-check data obtained by other techniques.

5. X-Ray Fluorescence Spectrometry (XRFS)

This technique is well suited for solid samples. The main drawback in analyzing liquid samples is poor sensitivity. Meier and Unger (36) reviewed the application of energy dispersive XRFS and included a discussion on wear metal determination in lubricating oils. Kubo et al. (37) analyzed NBS fuel oil and shale oil. Spiked solutions were used for calibration of vanadium, iron, nickel, molybdenum, zinc, and arsenic. The one-element spiking method works well for samples with low viscosity while high viscosity samples require a two-element spike to correct for x-ray absorption. Determined values agree well with certified values. In an interesting paper, Krishnan (38) claimed success in analyses of samples in any matrix with standards in any convenient form by normalization involving corrections for scattering from the sample cell. Results were reported for zinc, iron, and lead in petroleum using solid or liquid standards. Although little sample pretreatment is necessary, energy dispersive XRFS can only detect elements down to the ppm region, and applications to petroleum matrices have been limited.

6. Emission Spectrometry

Emission spectrometric methods dominated the earlier

literature on trace element determinations in petroleum matrices. Shirey (39) in 1931 may be the first to have reported qualitative emission spectrometric data for seven crude oils. Rapid routine analyses with an ashing procedure were presented by Hughes et al. (40). Calkins and White (41) were the first to analyze metals in oil directly in 1946. They used a quenched electrode technique which involves preliminary heating of a graphite electrode. The electrode is then inserted immediately into the sample, quenching it and thus drawing sample into the graphite. However, it was thoroughly studied and found to have limited applications (42). Many variations have been attempted since and are too numerous to mention, except for the rotrode.

Burt (43), Pagliasotti and Porsche (44, 45) and Gambrill et al. (46), were among the first to use the rotating disc electrode (rotrode). Phosphorus, barium, calcium, and zinc were analyzed by these researchers. The porous cup was compared to the rotrode (46) and 10% accuracy was claimed for both techniques. The use of a magnesium salt of 2-ethylhexoic acid as a spectrochemical buffer and nickel as the internal standard was reported to result in no matrix dependency (45). However, this technique is admittedly subject to serious matrix effects arising from viscosity and total composition of the oil (47). Except for a few minor refinements, such as the use of argon to stabilize the spark discharge (48), direct analysis with the rotrode seems to be more universally used than any other

emission technique.

7. Other Techniques

Excellent sensitivity can be obtained with mass spectrometry and plasma spectroscopic methods. Simultaneous determinations with sub-nanogram (ng) detection limits have been reported by Morrison (49) for Spark Source Mass Spectrometry (SSMS). Petroleum samples require lengthy preparation time and the interpretation of the spectra is complex. SSMS was evaluated in an intercompany comparison project (16). Neither of the four major petroleum laboratories had SSMS capabilities, and a commercial laboratory had to be chosen for the task. To an extent, this reflects the lack of activity of SSMS in the petroleum research field.

Among the different versions of plasma spectrochemical sources, Plasma Jet Direct Current Arc (DC Plasma) spectrometry, Microwave Induced Plasma (MIP) spectrometry, and Radio Frequency Inductively Coupled Plasma (RF ICP) spectrometry have been utilized for trace level determinations for petroleum matrices.

Quantitative spectrographic determination of boron in gasoline by an all-helium DC Plasma spectrometer was reported by Vigler and Failoni (50). The concentration range studied was 0.0001 to 0.001%, and the coefficient of variation was 8.1%. Sample preparation only involved dissolution of the sample in an ethylalcohol buffer solution and addition of nickel hexoate internal standard. The

advantages mentioned include a single calibration standard for different types of compounds, a smaller volume (2 ml) for analysis, and lower cost than the rotrode method.

McElfresh and Parson (51) have analyzed wear metals in used lubricating oils with another DC Plasma source. Aluminum, chromium, copper, iron, and magnesium were determined with limits of detection of 0.01, 0.11, 0.08, 0.40, and 0.003 parts per million (ppm) respectively. The analytical curves for each element were linear up to 50 ppm. The method incorporates syringe feeding of a 1:1 xylene diluted oil sample into an all-helium arc and a photographic detection system. Potassium was added to eliminate interelement effects (suppression of ionization) on iron and chromium. A platinum line was used as an internal standard line.

A rather unusual MIP setup was used to determine iron, chromium, nickel, and silver in oil by Sermin (52). The sample was aspirated directly by a pneumatic nebulizer into a 600 w nitrogen MIP source. Calibration curves were given for concentrations up to 30 ppm iron, 20 ppm chromium or nickel, and 3 ppm silver. Standard deviations calculated were 0.04 ppm for silver and approximately 0.2 ppm for the others. High viscosity and slow vaporization rate of the sample resulted in poor sensitivity. He suggested increasing the rate of nebulization by lowering viscosity (by dilution) or by ultrasonic nebulization.

Several articles have been published for trace element analysis in petroleum matrices using RF ICP

(53-64). The earliest attempt appears to have been reported by Pforr (53). These will be discussed in the next section.

D. The Inductively Coupled Plasma (ICP) as a Spectrochemical Emission Source

The first studies of the application of the ICP as an emission source in analytical spectroscopy were made by Greenfield et al. (65) and Wendt and Fassel (66,67) in the early 1960's. The characteristics of this source include high temperature, chemical inertness, and optical thinness and these result in low detection limits, high sensitivity, and linear responses of four to five orders of magnitude with respect to concentration. Interference effects are small compared to spectrometric determinations by flame emission, atomic absorption, or arc-spark emission spectrometry.

Analytical applications of the ICP have experienced tremendous growth particularly after the introduction of the first commercial instrument in 1974 (68). Inductively Coupled Plasma - Atomic Emission Spectroscopy (ICP-AES) with the various commercial instruments has been used to simultaneously analyze qualitatively and quantitatively for up to 60 elements in 30 or more samples per hour. Excellent historical and application reviews of the ICP include Greenfield et al. (69), Barnes (70), and Dahlquist and Knoll (71).

1. Application to Organic Systems

Although most work has concentrated on aqueous samples, organic systems have been investigated by Truitt and Robinson (72,73), Greenfield and Smith (55), Warren (74), Ward et al. (75), Dahlquist and Knoll (71), and Browner et al. (76).

Truitt and Robinson (72) described the introduction of organic liquids into the ICP. A laminar flow plasma torch similar to one described earlier (60) was used. The power necessary to sustain the plasma with organics aspirating was observed to be higher than water. They concluded that approximately ten times as much sample could be handled in the coolant (plasma) stream as in the central carrier stream without extinguishing the plasma. This limitation was a result of carbon buildup on the tubes. Flow dynamics of the torch were also studied by observing yellow flares and soot resulting from the introduction of large quantitites of hydrocarbon vapor into the carrier stream.

Emission spectra of some hydrocarbons such as methane, ethane, propane, heptane, octane, and benzene introduced into the plasma were also studied (73). Four species were identified as sources of emission signals. These were elemental carbon and hydrogen, and the fragments C_2 and CN. The effects of various simple gases - argon, helium, nitrogen, oxygen, and air added to either the carrier or coolant stream - on the emission intensity of several bands and lines were recorded. Spatial emission profiles, RF power dependency, and the effect of increasing the number of

carbon atoms in the sample for these bands or lines were also studied.

In 1972, Greenfield and Smith (55) determined chromium and iron in xylene. Microlitre samples (1-25 µl) were aspirated into a 5.5 kw nitrogen cooled plasma. The calibration graph was linear for chromium up to 250 ng, but iron showed curvature even at concentrations under 100 ppm. The same procedure was also used in the analysis of trace metals in organic phosphorus compounds. Standards of acetylacetonates of aluminum and magnesium and samples were diluted (1 + 9) with methanol. The results obtained agreed reasonably well with results obtained by wet oxidation of the samples followed by determination of the metals in aqueous solution.

Warren (74) reported the determination of some trace metals in foodstuffs by a chelation/solvent extraction system employing diethylammonium diethyldithiocarbamate (DDDC) and heptan-2-one. The argon ICP was operated at 2.1 kw and copper, iron, and zinc were studied for instrumental drift but it was found to be insignificant. The sensitivity of cadmium, cobalt, copper, iron, nickel, lead, and zinc were compared in both aqueous and heptan-2-one, and found to be similar. No trouble was experienced with carbon buildup on the torch.

In another chelating/solvent extraction in complex matrices, Ward et al. (75) reported detection limits for oxine in xylene and APDC in MIBK at pH 4 and 9 for 15 elements. Other elements were studied but were not

quantitatively extracted by either solvents. With a preconcentration factor of 10, these values were equivalent or slightly better than determination in water. A comparison was made for a seawater sample, and at 50-fold preconcentration, detection limits were significantly better (1 to 2 orders of magnitude) in MIBK or xylene systems than direct analysis for applicable elements. Instrumental conditions were not reported.

Dahlquist and Knoll (71) studied the enhancement effect of organic solvents. Varying amounts of acetic acid and glycerol were added and relatively small enhancements of 1 to 10% were observed at 5% volume acetic acid for 11 elements. The use of a cobalt internal standard reduced such enhancements to negligible proportions, and thus the effect was concluded to be localized in the nebulization and transport system. Soil extracts with either neutral 1.0 M ammonium acetate solution or triethanolamine buffered DTPA solution were analyzed directly, and no difficulty was reported.

Evaporation characteristics and theorectical maximum tolerable amounts of organic solvent aerosols in the ICP were investigated by Browner et al. (76). Nebulization efficiency was compared for different solvents and a detailed discussion of various effects was presented. With the argon ICP, oxygen- or chlorine-containing solvents appear to be tolerable at higher levels than hydrocarbon solvents.

2. Application to the Direct Determination of Trace Elements in Petroleum Matrices

The direct determination of trace elements in petroleum matrices by ICP-OES has been reported. Published articles include Pforr (53), Pforr and Aribot (54), Greenfield and Smith (55), Fassel et al. (56,57), Peterson (58), Ohls (59), Varnes and Andrews (60), Ward and Mariello (61), Smith (62), Merryfield and Loyd (63), and Ohls and Sommer (64).

Pforr (53) evidently published the first paper on the direct introduction of gasoline diluted oil samples into the plasma in 1967. In a later report, Pforr and Aribot (54) reported detection limits of 3.6, 4.2, and 1.5 ppm (by weight), respectively, for aluminum, iron, and nickel. Diluted oil was introduced at 50°C and the carrier gas flow was 20 litres per hour (1/3 litres per minute, l/min). An atomizer regulated the carrier gas pressure to deliver a constant amount of aerosol having constant particle size. The plasma was operated at 40 MHz and power range from 500 to 1000 w. Spectral information was recorded with a quartz spectrograph.

Greenfield and Smith (55) determined aluminum, chromium, copper, iron, titanium, nickel, magnesium, and manganese in samples of engine oil. Calibration graphs were obtained for the first three elements at concentration ranging from 0 to 100 ppm. Except for copper, the calibration graphs were linear. All samples were diluted in the ratio of 1:2 with xylene and 25 µl samples were aspirated into the plasma using a pneumatic nebulizer. The

nitrogen cooled plasma was operated at 7 MHz and 5.5 kw.

Fassel et al. (56,57) employed a 2.1 kw at 27 MHz argon plasma for the simultaneous determination of wear metals in lubricating oil, and trace elements in liquid fuels derived from coal. In addition, the analysis of edible oil for trace elements was reported by Peterson (58). The samples were diluted 1:10 w/v with MIBK and aerosols formed from these solutions were injected into the plasma. Detection limits of 0.0004 to 0.3 ppm for 15 wear metals in lubricating oil were reported. They found that differences in viscosity for the samples did not bias the analytical results. A comparison for titanium determination by this procedure and an atomic absorption procedure (28) showed reasonable agreement.

Comparison of trace element determination in oil by ICP-AES and rotrode emisssion spectroscopy was reported by both Ohls (59) and by Varnes and Andrews (60). Rotrode excitation in a CO_2 atmosphere and an ICP with ultrasonic or pneumatic nebulizer were used to analyze the samples either directly or after ashing. Detection limits were comparable to those obtained by pressed electrodes (59).

Results reported by a commercial testing laboratory using rotrode excitation were compared to argon plasma results (60). The plasma settings were 1.8 kw at 27 MHz and the viewing height was 18 mm above the load coil. Sample dilution of 1:9 w/v in MIBK was performed and the solution was analyzed for 12 elements. Agreement with rotrode was good for some elements but poor for others.

Ward and Mariello (61) determined sulfur, iron, lead, vanadium, nickel, manganese, and zinc in National Bureau of Standards - Standard Reference Material (NBS-SRM) 1634 residual fuel oil. A 27 MHz argon ICP operating at 1700 w was used and the observation height was 18 mm above the load coil. Other than sulfur and lead, good accuracy was reported.

Another application of an argon ICP for the simultaneous determination of metals in oil was reported by Merryfield and Loyd (63). The sample was diluted 1:9 w/w with xylene and aspirated into a 1700 w plasma. The observation height was 18.5 mm above the load coil. Twenty elements were determined at sub-ppm levels in a used oil sample and the average precision was 3.8%. Significant interferences were noted and corrected for. The effects of a detergent and of an easily ionized element, potassium, were found to be negligible. NBS-SRM 1634 and General Material 5 were analyzed, and the comparison of ICP results with the certified values showed agreement within 2%. Three oil samples were also analyzed for four elements by both ICP and XRFS and both methods gave comparable results.

Ohls and Sommer (64) determined trace elements in oil samples. A 27 MHz nitrogen cooled argon plasma working at a coil power of 1.5 kw was used. The observation height was 8 mm above the load coil. Sample preparation included a 10-fold dilution with xylene and particle distribution using an ultrasonic bath. Detection limits for 13 elements ranged from 0.001 ppm for calcium to 0.1 ppm for aluminum. Except

for boron, precision ranged between 0.3% to 0.5%. No residue of carbon was noticed in the torch using nitrogen as coolant.

3. Problems and Difficulties Encountered with Analysis Involving Matrices with High Organic Content

The aspiration of organics into the plasma is not as trivial as that of an aqueous solution. This may be reflected by the limited published literature associated with analyses involving high or 100% organic matrices. In addition to gradual carbon buildup at the torch, which eventually extinguishes the plasma, certain organics, such as alcohols and chlorinated hydrocarbons, have been reported to be difficult to introduce into the plasma without rapidly extinguishing it. Even if present only in small amounts, they may cause sputtering in the plasma. A new tuning system is sometimes necessary to overcome the problem for a certain solvent, and thus limits the flexibility of the instrument. Viscosity or surface tension differences for different mixtures or solvents also affect the analytical results. For example, nebulization efficiency is different for benzene, xylenes, and nitrobenzene under free or controlled aspiration with a pneumatic nebulizer (76). This can result in the erroneous interpretation of data. The use of a peristallic pump is generally recommended to regulate the sample introduction rate for samples which differ only slightly in viscosity, for example, diluted oil samples.

In addition to the argon and hydroxyl lines, the

background spectrum increases in complexity with emission from species such as C, H, CH, C_2, and CN when aspirating organics. Spectral interference of this nature may be overcome with a high resolution spectrometer, thus increasing the instrument cost. The other approach is to introduce a certain amount of oxygen into either the carrier or coolant flows. The effects of oxygen on the reduction of intensity of background emitting species have been reported (77,72,73).

The remarkably sensitive detection limits characteristic of the ICP for aqueous determinations have not yet been realized for organic systems. Based on reported detection limits, and except for calcium, trace element determinations in oil are restricted to 100 ppb and higher, depending on the procedure. Ultrasonic nebulization with solvent desolvation has been shown repeatedly to provide the lowest detection limits in aqueous systems, but has not been applied to matrices containing high organic content. This may stem from the lack of understanding of analyte species - organic solvent interactions.

CHAPTER II

EXPERIMENTAL FACILITIES AND PROCEDURE

A. Experimental Facilities

A detailed description of the spectrochemical emission source and measurement systems used in this investigation will be presented. Basically, it consisted of a radiofrequency inductively coupled plasma as the excitation source and spectral radiation from the plasma was decoded by either a monochromator-photomultiplier tube (PMT) detector system, or a photodiode array (PDA) based direct reader system. A minicomputer with software developed in our laboratory was used for data acquisition and reduction. A schematic block diagram is shown in Figure 1.

1. ICP

A Plasma-Therm ICP-5000 (Plasma-Therm, Inc., Kresson, N.J.) radiofrequency inductively coupled plasma was employed. An itemized description is presented in Table I.

The inductively coupled plasma discharge is initiated by a tesla discharge which partially ionizes a flowing gas, usually argon. An oscillating magnetic field, induced by the alternating current in the load coil, causes additional ionization. Thus the plasma is formed (Figure 2). The plasma and auxillary gas flows are tangentially introduced into an ICP torch, which consists of three coaxial and concentric quartz tubes.

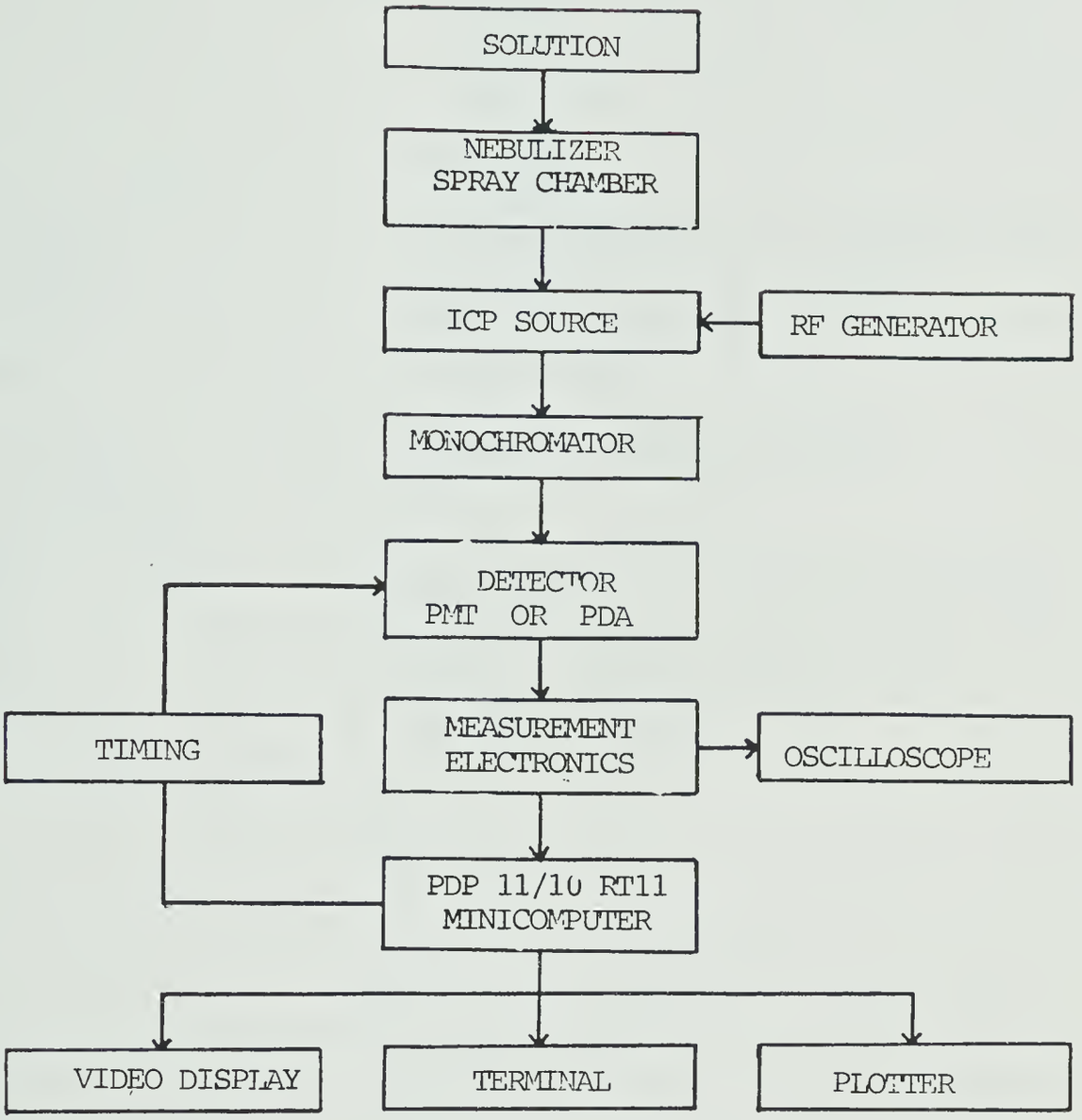

FIGURE 1. Schematic diagram for instrumentation

TABLE I

ICP Specifications

Plasma	ICP 5000
Manufacturer	Plasma-Therm Inc., Kresson, N.J.
RF Generator	Model HFS 5000D
Frequency	27.12 MHz
Power Control	Automatic, Model APCS-3
Power Available	5.0 kw
Matching	AMN-5000E Auto Matching Network
Load Coil	Silver-plated copper coil, 4 turns, 2.5 cm i.d.

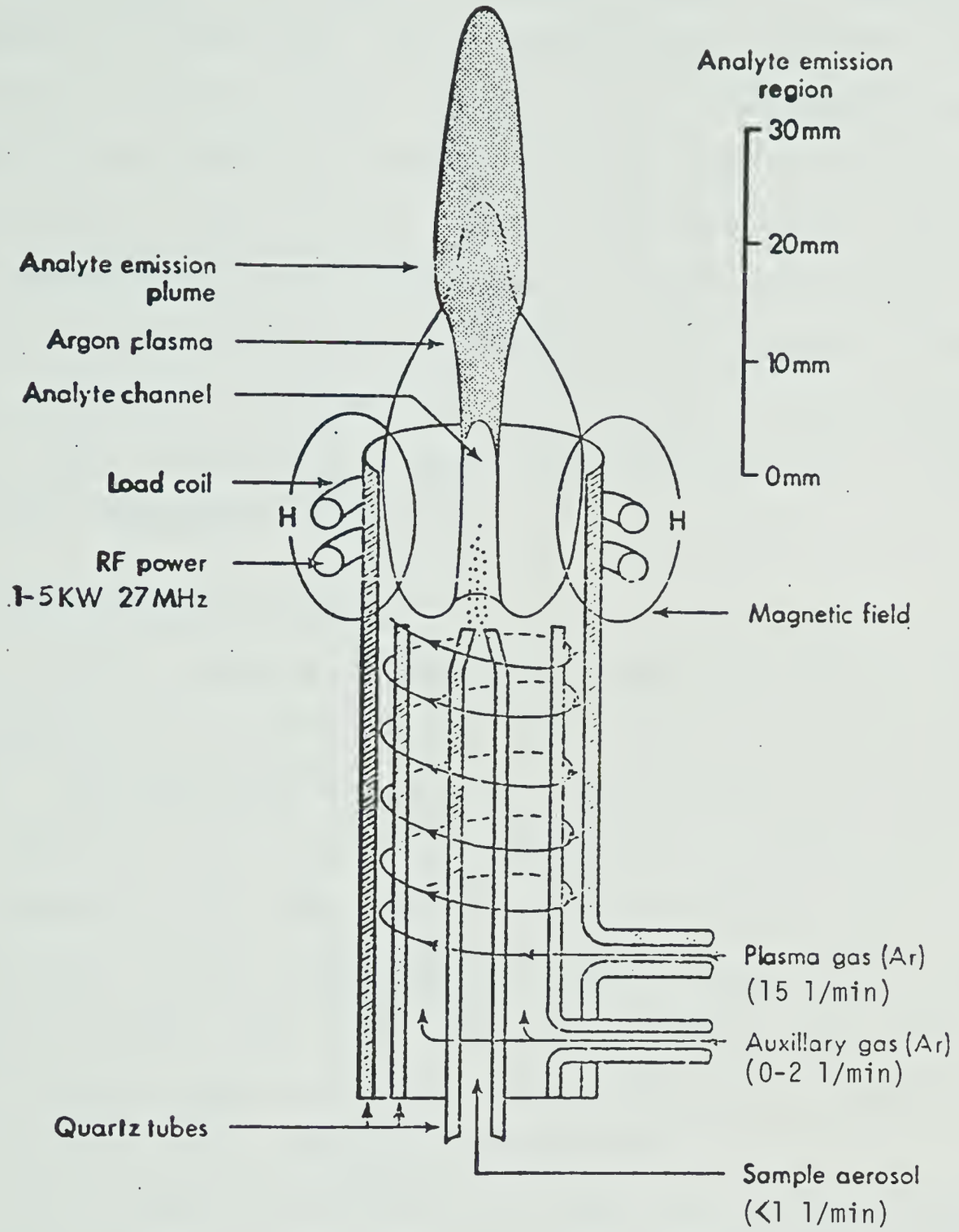

FIGURE 2. Main features of the ICP discharge

The plasma torch used is shown in Figure 3. The torch suppled by Plasma-Therm has a constricted outlet for the central, or injector tube. This central tube was replaced with a 2.0 mm internal diameter thick wall tube to provide a more laminar flow of sample carrier gas through the torch. The injector portion of this tube was ground and tapered to allow a better torodial flow at the tip, and thereby reduce salt deposit or carbon buildup. This type of torch proved to be easy to construct, and is manufactured here at the Chemistry Department Glass Shop.

2. PMT Measurement System

A Heath Scanning Monochromator Model EU-700-70 with accompanying Electronic Control Unit Model EU-700-51 were used. The plasma was imaged with a magnification of -0.5 on the entrance slit of the monochromator by a quartz lens. This monochromator has a focal length of 350 mm and is a single-pass Czerny-Turner design with folding mirrors to provide entrance and exit beams on a common optic axis. The precision plane grating of 1180 lines per mm blazed at 250 mm gives better than 0.1 nm resolution.

An 1P28 PMT was mounted at the exit slit and powered by and enclosed in a Heath Photomultiplier Module EU-702-30. The operation voltage ranged from 400 to 700 v. Spectral coverage with this PMT is from about 185 to 650 nm. Purging with nitrogen is necessary for measurement under 200 nm. The current output of the PMT was converted into a voltage signal with amplification/filtering by a Keithly Current

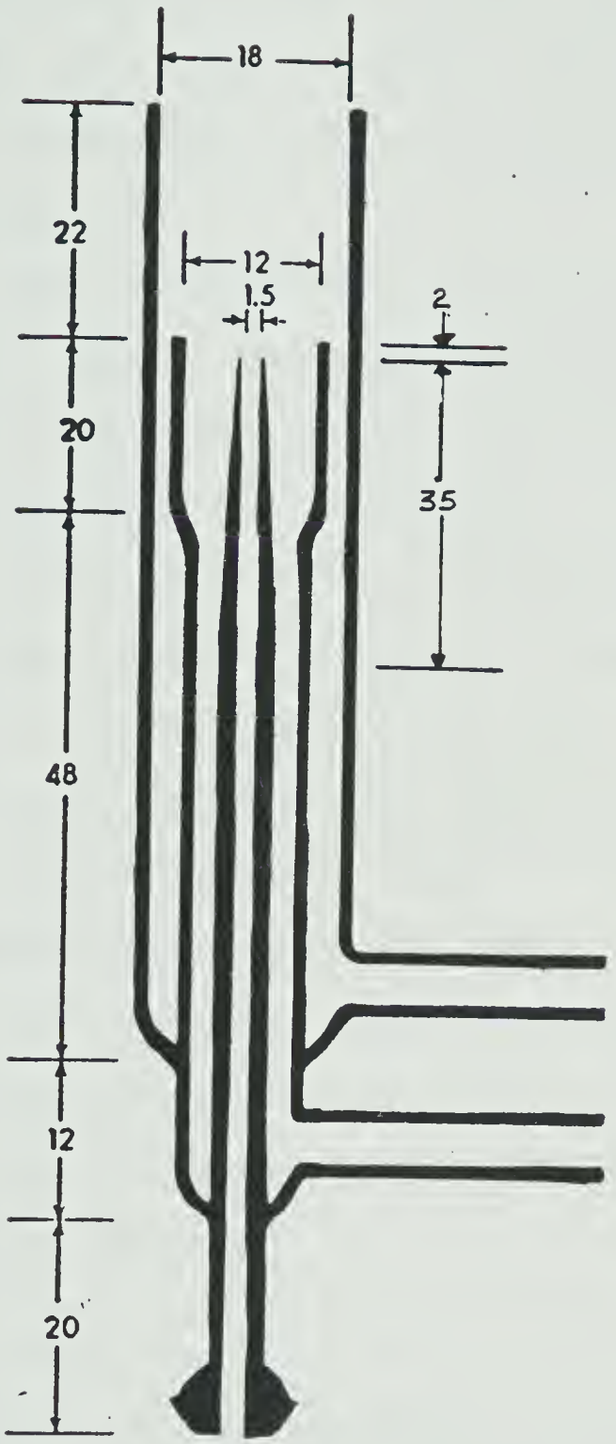

FIGURE 3. ICP torch (dimensions in mm)

Amplifier Model 427 (Keithly Instruments, Inc., Cleveland, Ohio). For spectral tracing, a Heath Strip Chart Recorder Model EUW-20A was used. Either linear or logarithmic response can be selected with the incorporation of a Heath Module EU-20-28.

Digital data conversion was performed by a Digital Equipment Corp. (DEC) Laboratory Peripheral System Model LPS11. This data acquisition unit contains all the electronic components for connection to external analog, digital, and timing signals and interfaces directly to a DEC PDP-11/10 sixteen bit minicomputer. The minicomputer was operated under the RT11-02C disk-based operating system. Programming was in Fortran and Macro assembly language. Mass storage was available by means of DEC RK-05 cartridge disks. Alphanumeric and graphic display was available with a DEC VT-55 video terminal. Hard copy output was available from the internal printer of the VT-55, a DEC Writer II, or a Zeta Incremental Plotter Series 100/1200 (Zeta Research Corp., Lafayette, Calif.)

3. PDA Measurement System

The computer coupled photodiode array readout systems used in this work have been developed in this laboratory over the last eight years. Two systems were used in decoding spectral information. A number of articles have been published about these systems by Horlick et al. (78, 79).

The first system used was the vertical spatial emission

profiling system. In this system an array of 250 photodiodes 25.4 μm (0.001 in.) wide by 25.4 μm (0.001 in.) tall is mounted vertically in the exit focal plane of a Heath Monochromator Model EU-700-70. With a magnification of -0.25 of the plasma at the entrance slit, this system allows direct readout of a 25.4 mm (1 in.) portion of the source for vertical spatial emission intensity (80,81).

The second photodiode array based system uses a 1024 element PDA. Each diode is 25.4 μm (0.001 in.) wide by 430 μm (0.017 in.) tall. This array is placed horizontally in the exit focal plane of a Heath Monochromator Model EU-700-70. As the effective width of the 1024 element PDA is 26.01 mm (1.024 in.) and the dispersion of the monochromator is approximately 2 nm/mm at 250 nm, a spectral window of roughly 50 nm is achieved. This combination allows coverage of a large spectral region with reasonable resolution. The image magnification was -0.5.

The computer-based data acquisition system operates at up to 20 kHz, and the PDA is clocked at this rate. Integration times of either array cooled to about -20°C can vary from 0.1024 to over 50 seconds between readout cycles. Individual readout cycles can be stored under computer control, or can be time averaged and background subtracted. A Tektronix Differential Amplifier AM 502 (Tektronix Inc., Beaverton, Oregon) is used to amplify and filter the photodiode array signals prior to analog-to-digital conversion. A/D conversion clocking was provided by the photodiode array electronics. The remainder

of the data acquisition and readout systems are similar to that described earlier. The program used for data acquisition was ADCPDA and PDAPLT was used for the plotting of spectral scans. These are included in the Appendix.

4. Sample Introduction

The most widely used aerosol generation system is the pneumatic nebulizer (crossflow or concentric), together with a dual cylinder Scott-type spray chamber. The aerosol produced is carried by the sample carrier gas and injected into the center of the plasma (Figure 4). Sample delivery could either be free uptake by the venturi effect, or pumped by a peristallic pump. The nebulizer breaks up the solution into small droplets, and the spray chamber of a certain geometry discriminates against the larger droplets. However, this combination results in about 3% of the aerosol actually reaching the plasma. Obviously, much of the sample solution is wasted. A more efficient system that will deliver a more uniform and finer mist may result in higher sensitivity and a more precise result. The "MAK" fixed crossflow nebulizer together with the Model 200 Expansion Chamber fitted with the removable baffle (Figure 5), is slightly more efficient and also more precise than the most popular setup (82). A separate argon supply (e.g. a 100 lb cylinder) capable of delivering 200 psi pressure provides gas flow for the nebulizer. The fixed glass bridge between the two capillaries eliminates the necessity for realignment common to most crossflow nebulizers. This results in good

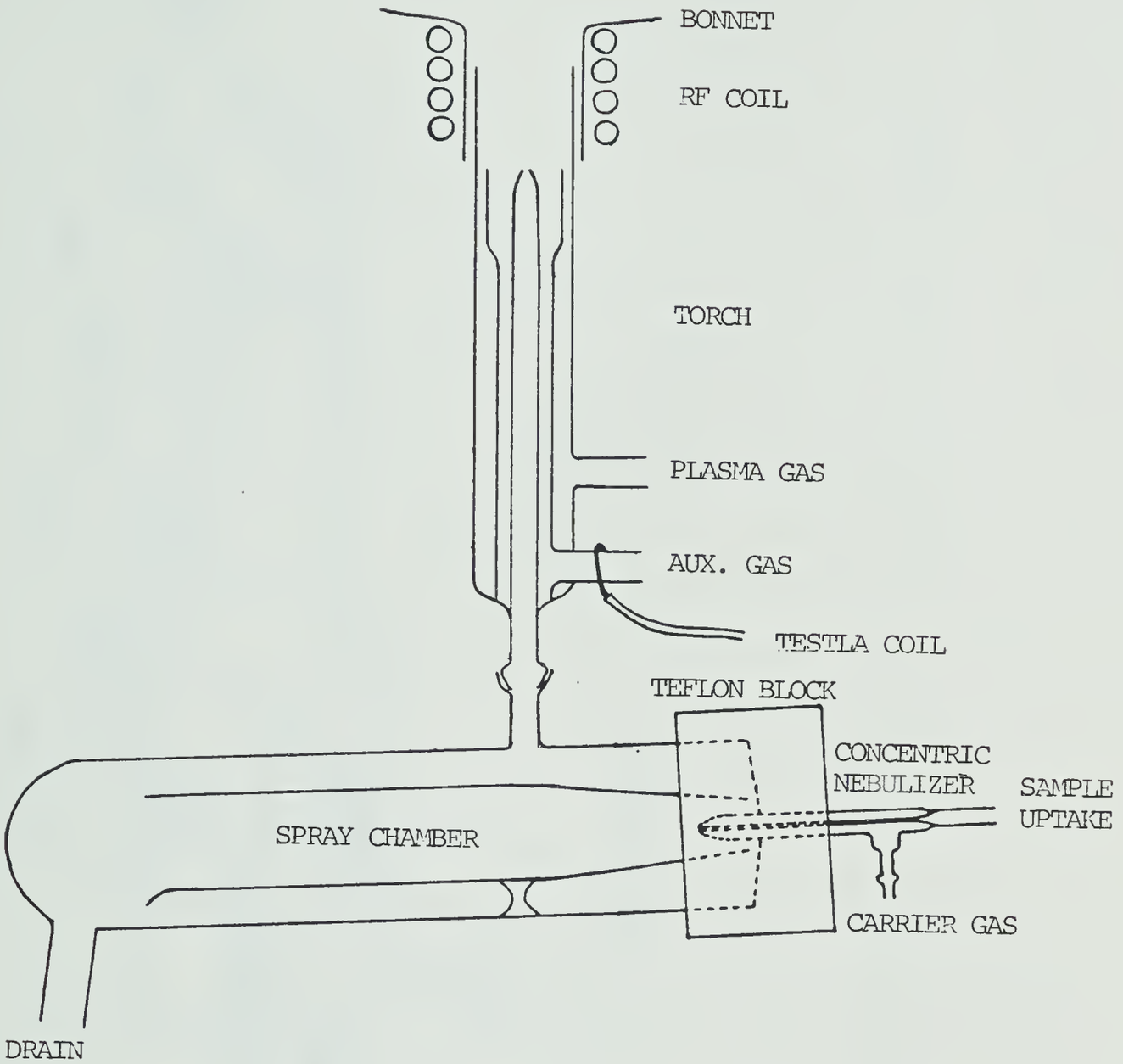

FIGURE 4. Aerosol generation system and torch assembly

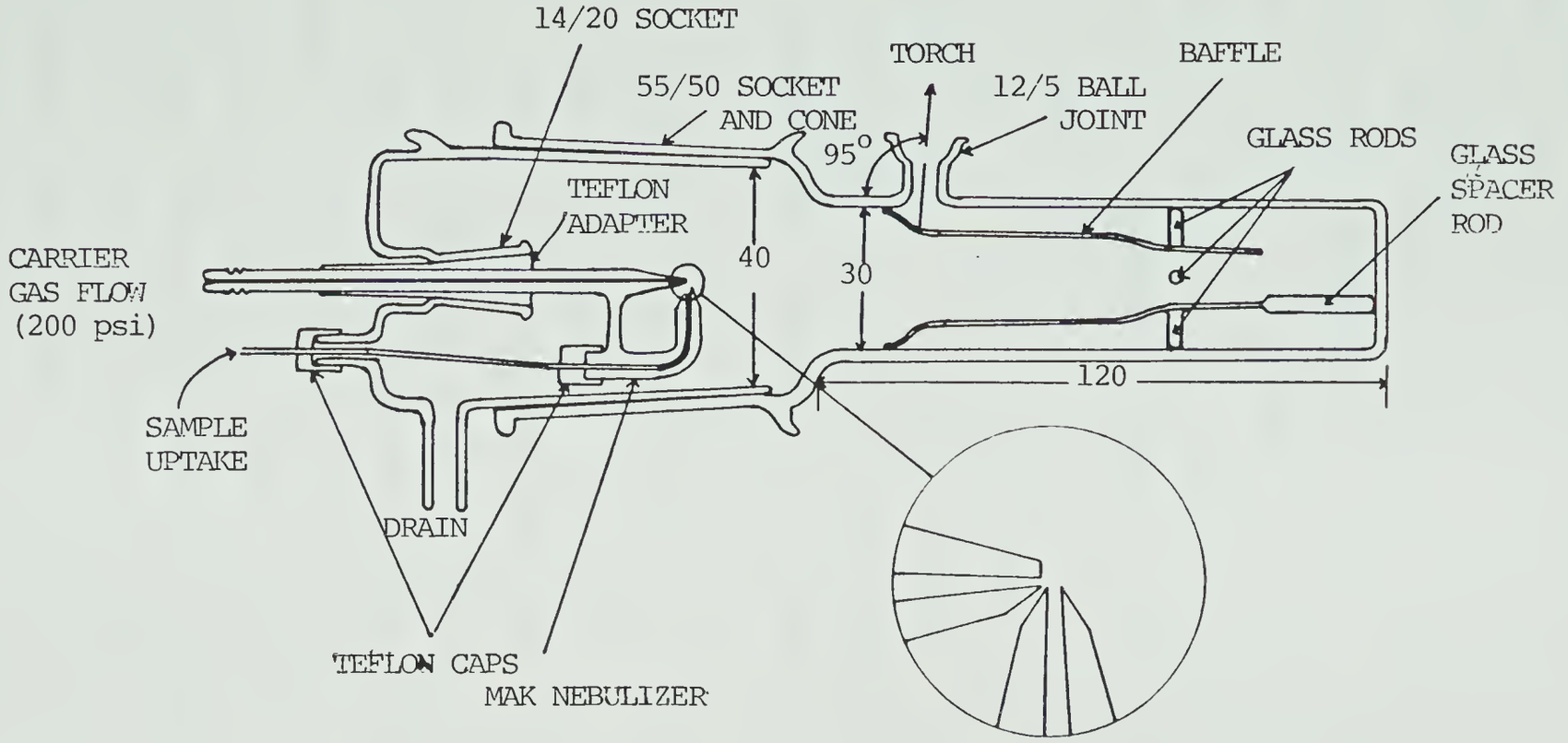

FIGURE 5. MAK Nebulizer with Model 200 Expansion (Spray) Chamber

long term reproducibility. The long and narrow capillary together with the high pressure appears to damp out variation, functionally similar to a low pass filter in electronics, and results in excellent long term stability.

The plasma is typically initially formed with only the plasma and auxillary gas flowing. Typical flow rates are 15 and 1 l/min. Two different procedures were possible for xylene introduction into the plasma. The earlier method involved aspirating water to form the central channel, and then switching over to organics. Since xylene is sparingly soluble in water, acetonitrile was aspirated immediately after water. In this manner, the spray chamber was completely saturated with acetonitrile before xylene introduction. Although this method required 3 to 4 minutes, mainly as wash-out time for the different solvents, there was more than sufficient time to gradually adjust conditions to those most suitable for organics.

The later method involved direct introduction of xylene. After the plasma was formed, xylene was aspirated to "punch a hole" in the plasma. This method requires less than 10 seconds, but care must be taken to ensure that optimum settings are selected, or the plasma may extinguish and the torch could easily be damaged. Before aspirating xylene, the tuning must be set to previously determined values that are most suitable for organics, or the abrupt introduction of xylene may extinguish the plasma. The auxillary flow must be increased slightly (greater than 1 l/min) or carbonization of the central and intermediate

tubes may occur. In more severe cases, ablation of these quartz tubes occurs instantaneously. This is due to an apparent drop in the discharge when organics are introduced.

B. Sample Preparation

1. Consideration

As discussed previously, direct analysis of the sample or a diluted form is preferred over the dry or wet oxidation approach. Risk of contamination, loss of analyte, and also sample preparation time is greatly reduced. The thick, sticky nature of raw bitumen makes it impractical to aspirate the sample directly by a pneumatic nebulizer at room temperature and atmospheric pressure. Although at elevated temperature and pressure bitumen may be fluid enough and could be force-fed, such extra handling reduces the simplicity of manipulation that is desired.

The other alternatives for direct analysis of this semi-solid substance may be limited. Recent studies of solid sampling approaches include electrothermal vaporization (83,84), laser vaporization (85,86), and direct sample insertion in a modified graphite electrode (87,64). Practical sample sizes of up to 20 mg can be analyzed. This microsampling capability is undesirable in this study due to the notorious inhomogeneity of bitumen. A large number of samples from the same batch must be analyzed in this manner in order to obtain a representative result. This would greatly increase overall analysis time.

The only viable alternative is to dissolve both the sample and standard in an organic solvent. This will ensure sample homogeneity and present it in a form that can be aspirated easily.

2. Solvent Selection

The two most popular organic solvents for oil dilution and chelation/solvent extraction are methyl isobutyl ketone (MIBK) and xylene. Chelating reagents in these solvents are used extensively in extraction or preconcentration for aqueous samples. They have also been used for dilution of oil samples. Other solvents which have excellent solubility include benzene, toluene, some ketones, and chlorinated hydrocarbons. However, the selection is limited when the "plasma burning characteristic" is also considered. Except for xylene, toluene, and some ketones including MIBK, these solvents cause sputtering in the plasma, and result in poor stability. For crude oil and bitumen, only xylene and toluene have the desired solubility. Xylene was chosen so that a comparison with other reported results may be made.

3. Sample Dilution

Different production bitumen samples may be quite different in viscosity, and must be diluted by xylene to achieve similar viscosity. A dilution factor of ten times or more is necessary. Although a more diluted solution (say, a factor of 100), corresponds more closely to a matched viscosity, such a procedure is undesirable because it increases the detection limit significantly. Thus the

following procedure was employed.

Both the sample and reference were prepared in the same manner. A 5 g sample was weighed into a nitric acid washed, dry, 3 oz glass vial. Then 45 g of ACS grade xylenes was added. The vial was then capped to prevent evaporation loss, and shaken sufficiently to ensure perfect mixing. A Mettler Top Loading Balance P1200 with a taring feature speeded the operation.

C. Standards

For the quantitative determination of elements present in the sample, the instrument must be calibrated. Since the concentration of the elements are related to the measured intensity of the analytical lines, standards of known elemental concentration must be used. Single element National Bureau of Standards (NBS) organometallic standard reference materials and Conostan standards (Conostan Division, Continental Oil Co., Ponka City, Okla.) were used. Conostan base oil was used as a blank and as a base oil for calibration standards.

The single element organometallic standards were individually prepared according to instructions supplied. Depending on the particular compound, preparation times (including drying in the dessicator) ranged from a few hours to over one day. Furthermore, some of the reagents necessary for dilution and enhanced stability were not common stock reagents, and resulted in further delays. Conostan standards, on the other hand, were available in an

oil matrix, and thus required little preparation. Their accuracy at sub-ppm levels has been questioned. However, the prepared single element solutions were all compatible and were combined to give a multielement stock solution. SRM 1634 residual fuel oil would have been appropriate for this investigation, but was unavailable because of stock depletion.

By appropriate serial dilutions of the desired combination of elements with the base oil, different concentrations of multielement reference oils were prepared. The concentrations in the reference solutions ranged from 0.01 to 1000 ppm, and contained vanadium, iron, and nickel. These solutions were used to evaluate the basic analytical performance of the ICP. The xylene dilution procedure was identical to that for the sample.

CHAPTER III

EVALUATION OF THE ARGON ICP

A. Qualitative Spectral Tracing

The appearance of the ICP discharge with xylene aspirating is quite different when compared to that when an aqueous solution is aspirating (Figure 6). The more prominent features include an intense green sheath enveloping the lower region of the plasma, a violet tail flame, and a very distinguishable central channel or bullet. It has been well established that higher power is necessary to run organics. Although it is possible to operate at 1 kw with much compromise, better stability is achieved when the power setting is 1.5 kw or higher.

Wavelength scans from 190 to 600 nm at three different heights in the analyte channel provided an insight to background emitting species when xylene (or typically hydrocarbon) was aspirated. These spectral tracings are reproduced in Figure 7. The spectra emitted were very complex, with major emitting constituents being Ar, C (193.1, 247.9 nm), OH (280-330 nm), CN (350-422 nm), CH (387-431 nm), and C_2 (437-600 nm). Nitrogen from the atmosphere or as impurities in the gas supply contributed to the intense CN emission high in the plasma. The spectrum obtained from the plasma when no organic sample was being introduced was also recorded. It consisted mainly of argon lines, OH bands, and a continuum.

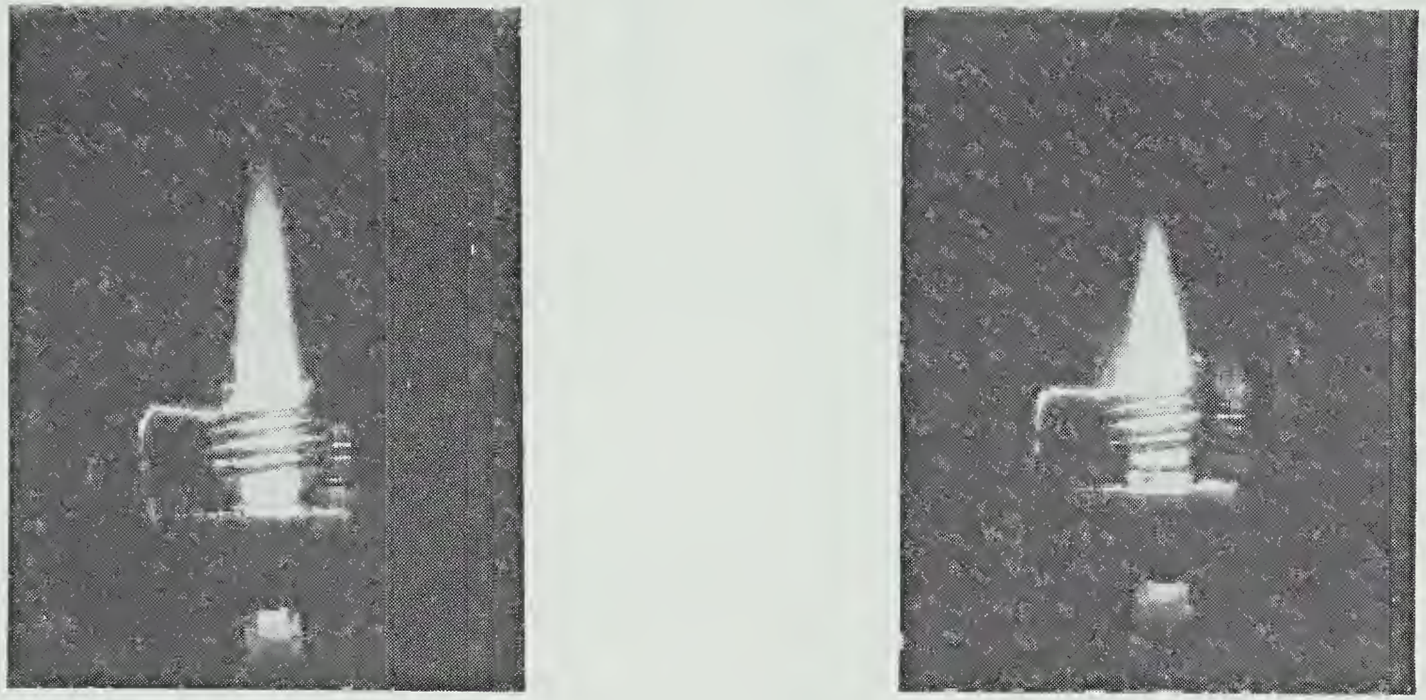

a b

FIGURE 6. Photographs taken through neutral density filters of a plasma with xylene (a) and water (b) being nebulized

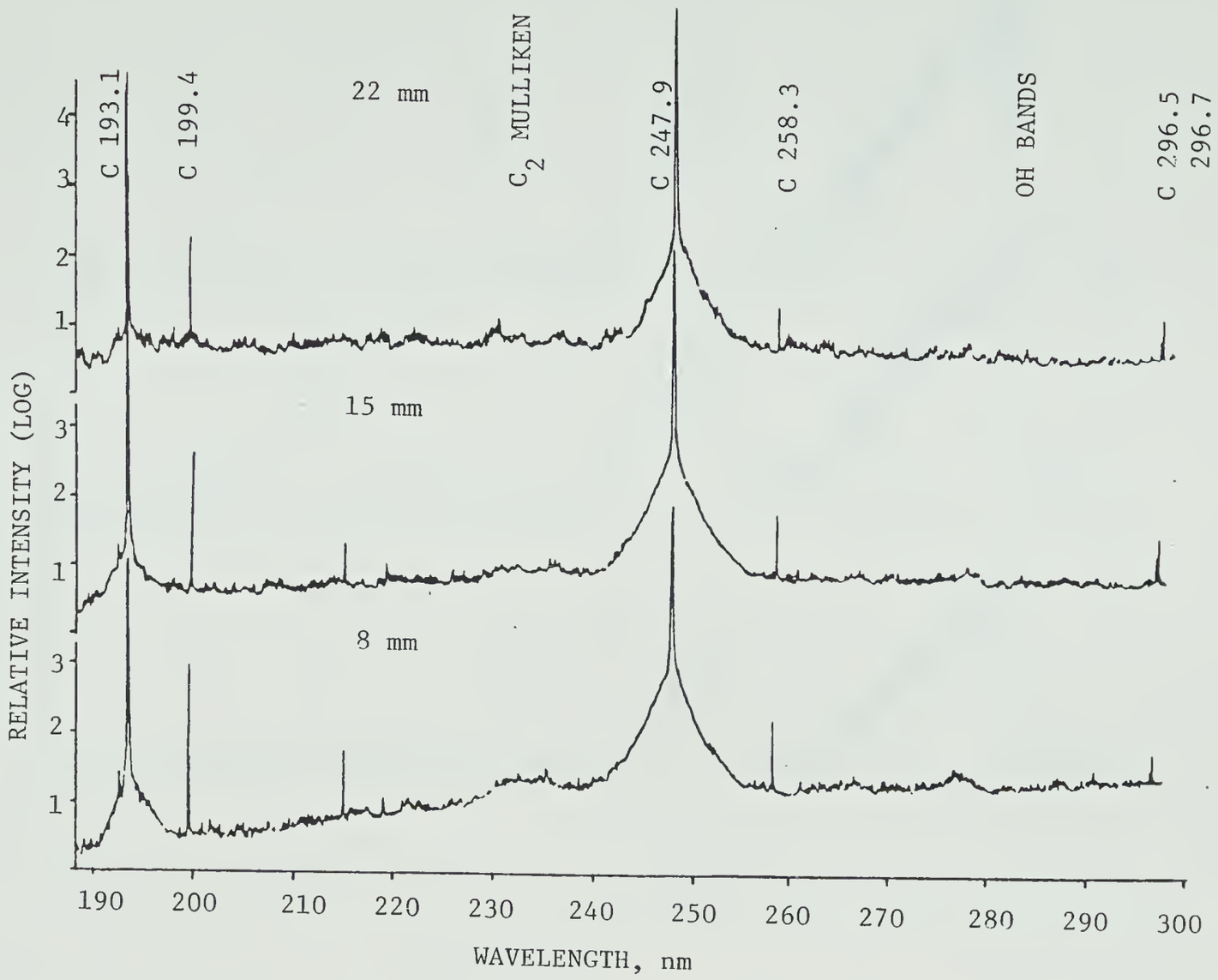

FIGURE 7. Wavelength scans from 190 to 600 nm centered at three heights in the central axial channel (22, 15, and 8 mm above coil). Scans were obtained when xylene was aspirated.

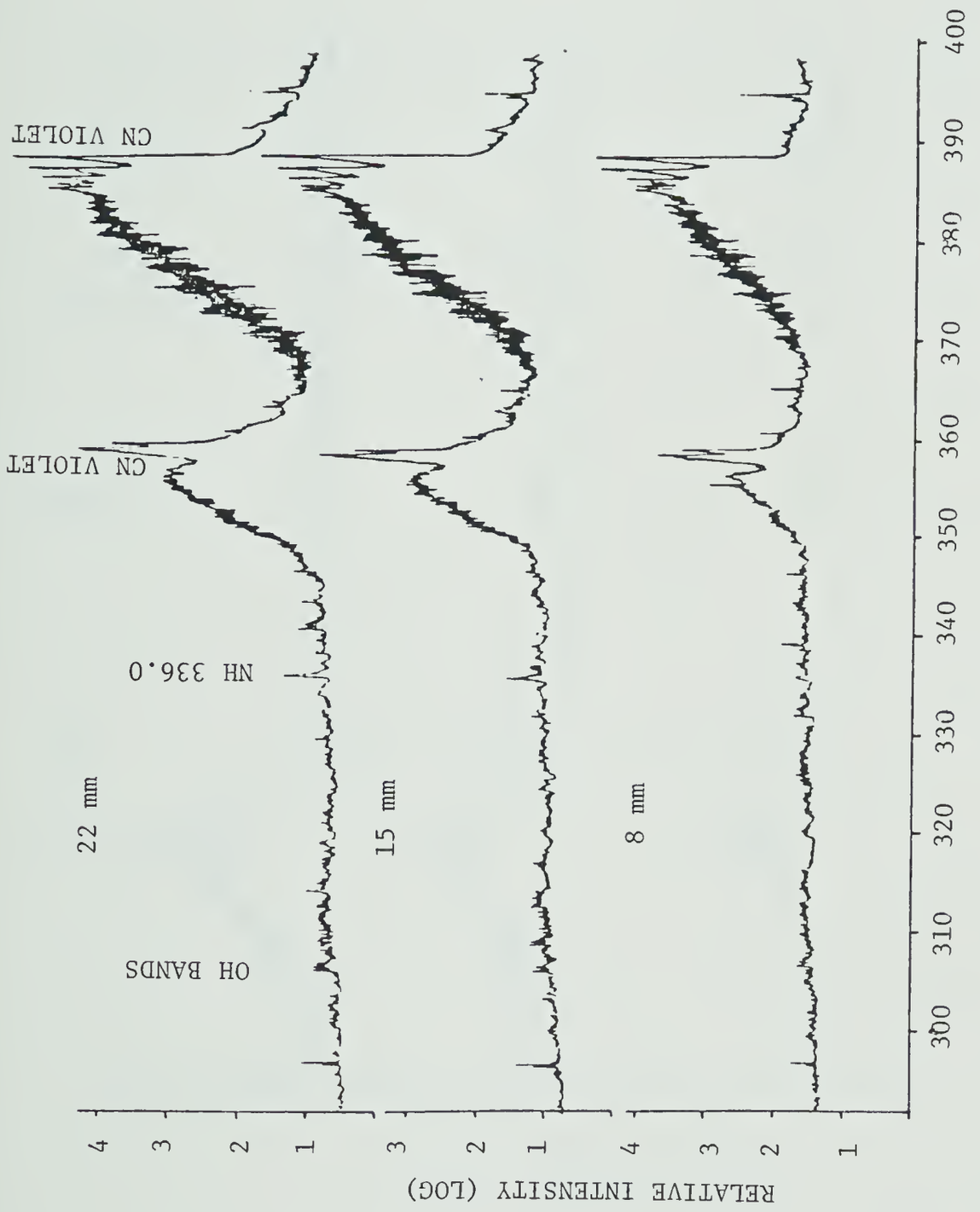

FIGURE 7. (continued)

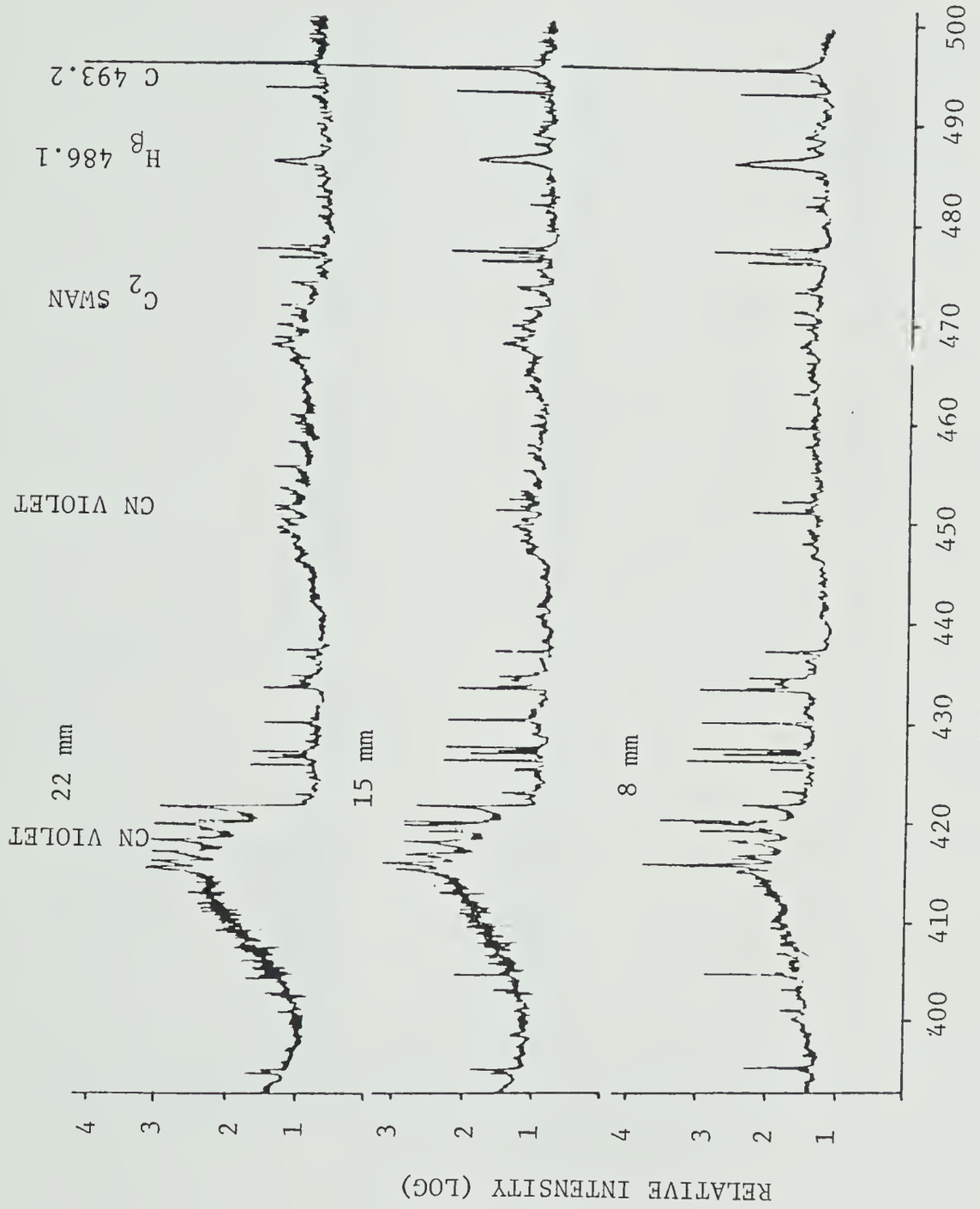

FIGURE 7. (continued)

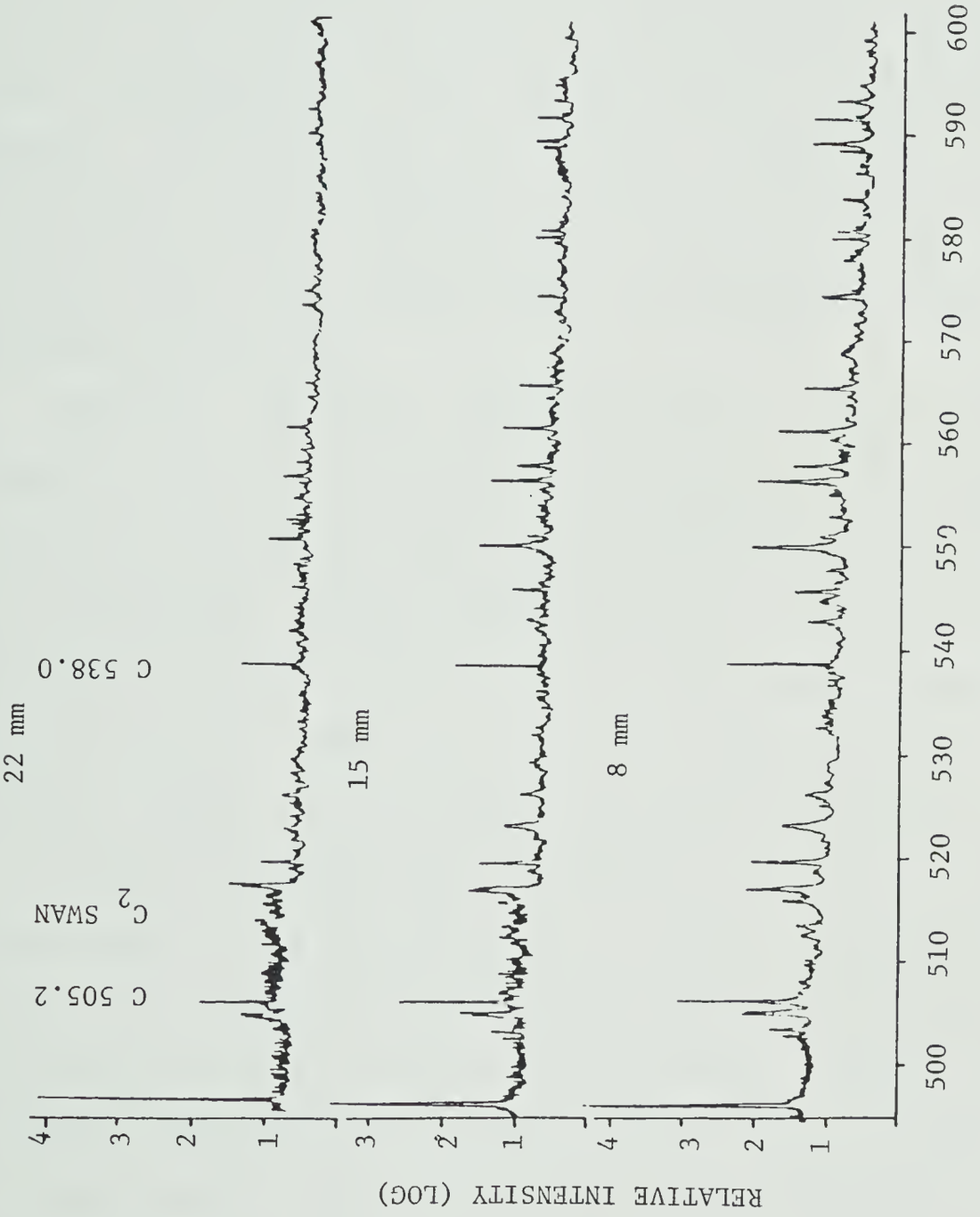

FIGURE 7. (continued)

B. Optimization of Power and Flow Rate Parameters

To accomplish simultaneous multielement analysis (SMA), we must establish a set of compromise conditions. This means selecting a common set of plasma operating parameters that will give the best overall performance for all elements being investigated. The three critical parameters that greatly influence the analytical signal are (1) the observation height above the load coil, (2) the RF power coupled into the plasma, and (3) the flow rate of the aerosol carrier gas.

Spatial emission studies which investigated the response of line intensity to changes in RF power and aerosol flow rate in aqueous systems have been reported from this laboratory. These include Edmonds and Horlick (80) and Horlick and Blades (81). This investigation employed a similar system. The instrumentation was described in the previous chapter. The concept is shown in Figure 8.

A 256 element PDA was positioned vertically at the exit focal plane of a monochromator. With a magnification of -0.25, this configuration allowed simultaneous monitoring of a 25.4 mm (1 in.) portion of the plasma. Analyte emission intensity information can thus be acquired as a function of vertical height above the load coil (Figure 9). The emission intensity porfiles for analyte species are in the general shape of a "hump". That is, the emission intensity observed initially increases, reaches a maximum and then decreases, forming an emission intensity peak or maximum.

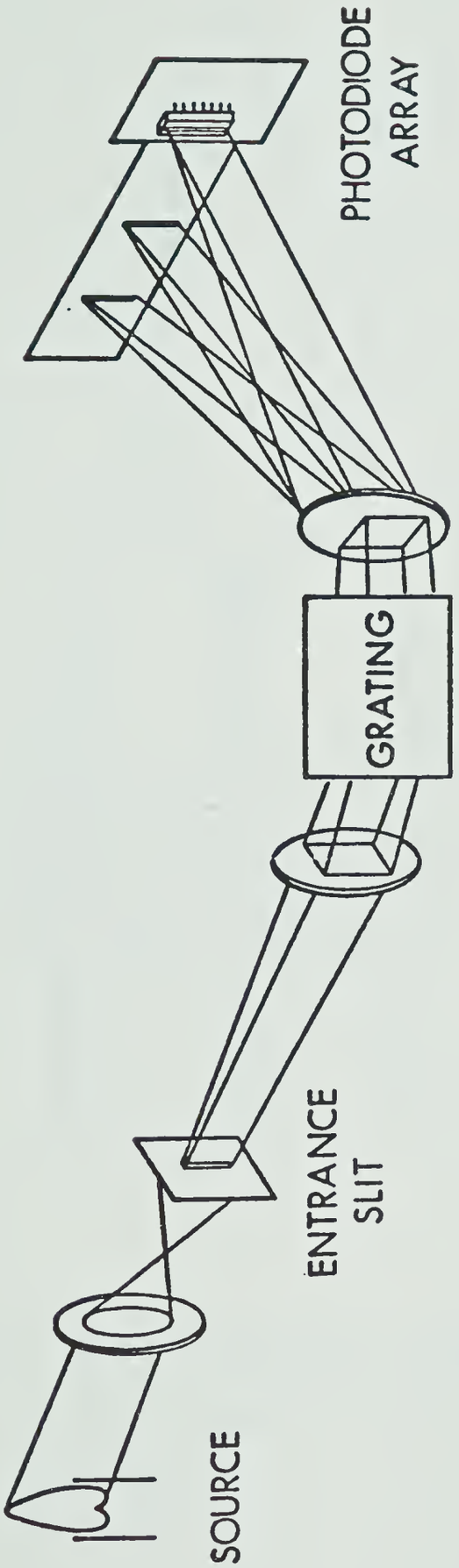

FIGURE 8. Photodiode array profiling concept

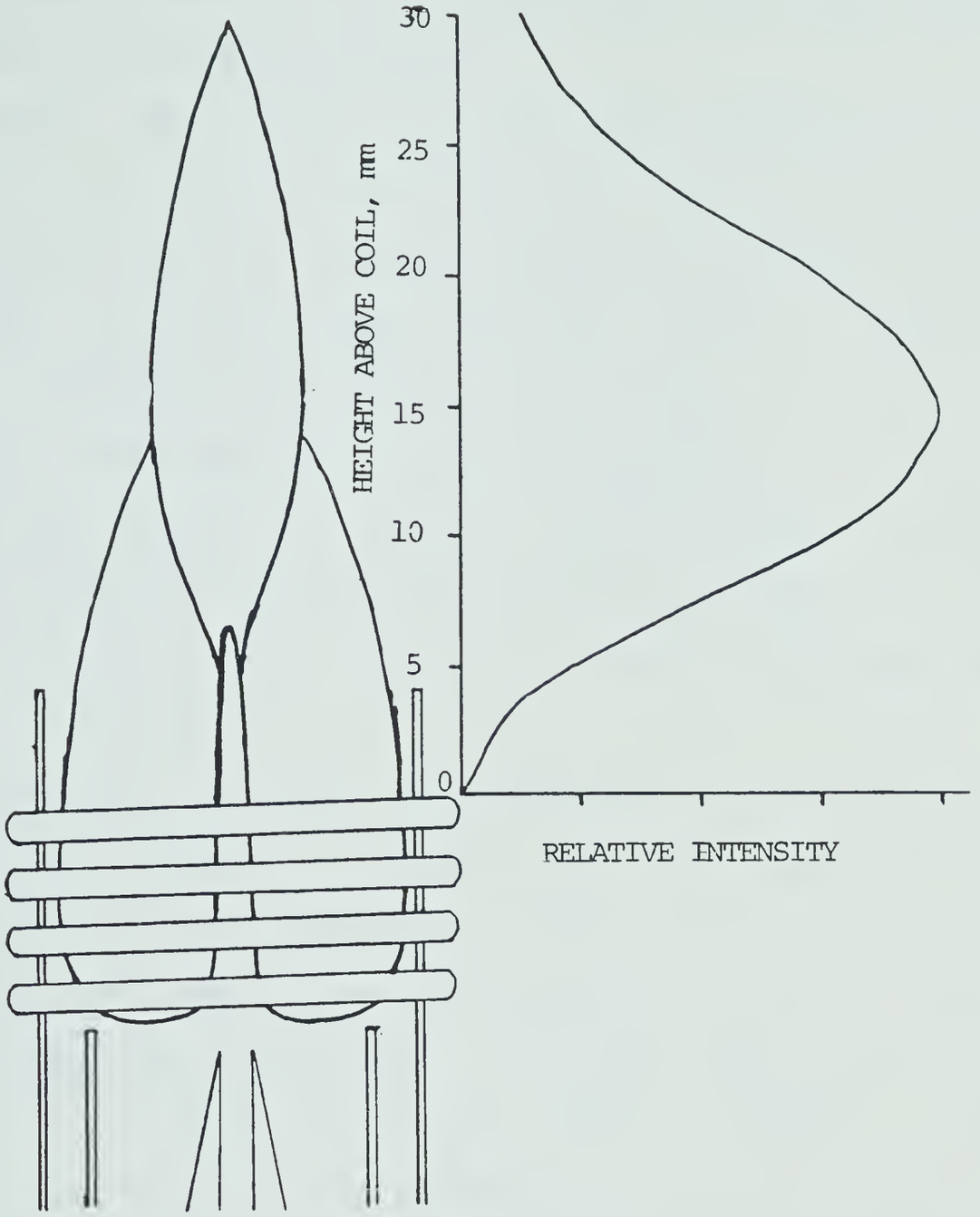

FIGURE 9. Analyte spatial emission intensity information as a function of vertical height above the load coil

Measuring the signal at the position when this peak occurs should give the best performance.

However, the position of this peak maximum is very dependent on the carrier gas flow rate. The plot in Figure 10 represents vertical spatial profiles of the VII 309.311 line when the aerosol flow rate was varied. Curves a through e represent flow rates of 0.6, 0.7, 0.8, 0.9, and 1.0 l/min. The emission intensity is plotted from 0 to 25 mm above the load coil, centered on the analyte channel. The peak intensity increases from 0.6 to 0.8 l/min, and then decreases from 0.8 to 1.0 l/min. The RF power was kept constant at 2.0 kw.

Increasing the flow rate resulted in more aerosol reaching the plasma. However, it also decreased the residence time in the discharge. Thus it is not surprising to see that the peak intensity increases and shifts higher when the flow rate increases. At higher flow rates (that is, shorter residence time), some analyte virtually passes through unexcited, and thus decreased intensity is observed.

The effect of varying RF power is shown in Figure 11. The VII 309.311 peak emission is relatively unshifted by increasing the power from 1.5 kw (a) to 2.5 kw (e). A significant enhancement in intensity is observed from 1.5 to 1.75 kw (b) to 2.0 kw (c). Further increases in RF power to 2.25 kw (d) and 2.5 kw (e) result in slight enhancement.

When other lines or elements are studied, the observed trends are similar. Although slightly improved performance and stability were achieved at 2.5 kw, this power setting

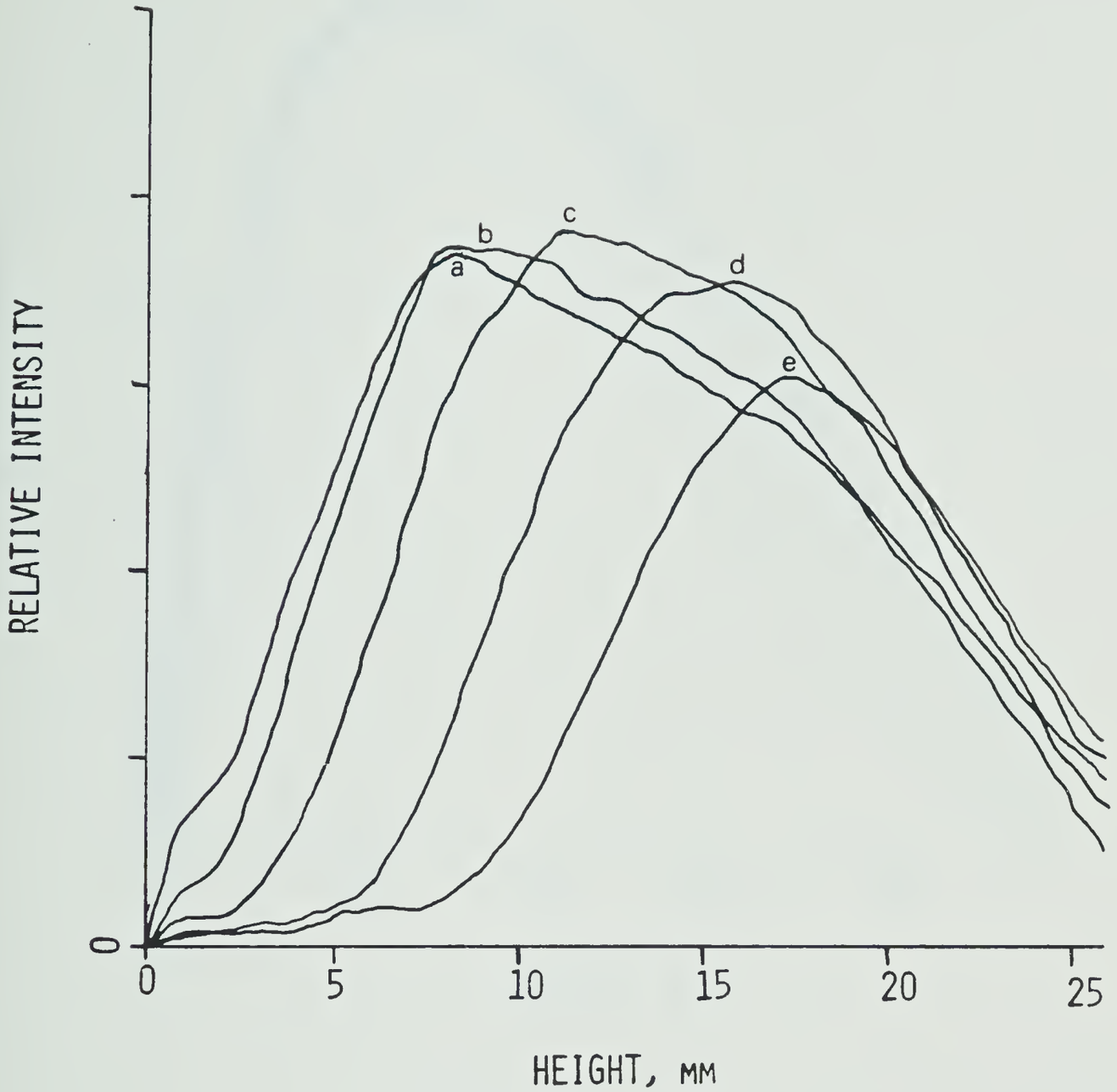

FIGURE 10. Effect of varying aerosol flow rate on vanadium spatial emission profiles at the 309.311 nm line. Curves a=0.6, b=0.7, c=0.8, d=0.9, and e=1.0 l/min.

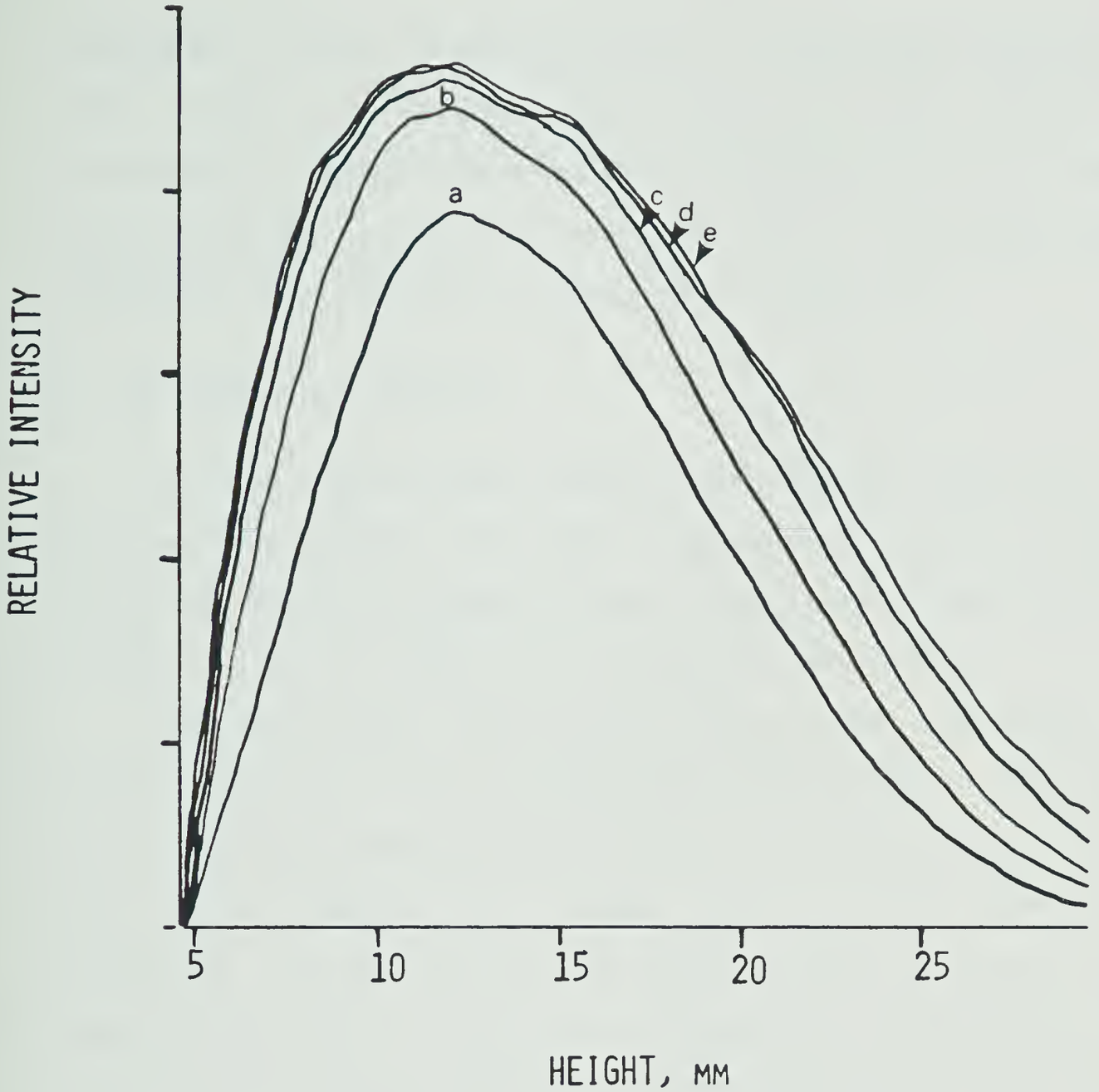

FIGURE 11. Effect of varying RF power on vanadium spatial emission profiles at the 309.311 nm line. Curves a=1.5, b=1.75, c=2.0, d=2.25, and e=2.5 kw.

required a higher plasma flow for a prolonged operation time. The 2 kw maximum power output of most commercial instruments further discouraged any comparison to be made. Thus the power setting was kept at 2 kw. The compromised condition for analysis is summarized in Table II.

C. Quantitative Results

The PDA based direct reading spectrometer described in the previous chapter was used predominantly in this study. The 50 nm spectral window allowed simultaneous detection of a large number of lines with reasonable resolution.

The analytical lines were selected on the basis of highest sensitivity with no spectral interference. They are shown with the calibration curves obtained in Figure 12. The curves obtained are linear over several orders of magnitude, and the slope of the log-log plot for V and Ni is essentially unity. Detection limits (DL), here defined as twice the standard deviation of background (i.e. 2σ), and precision (relative standard deviation) for V and Ni, are shown in Table III. The precision was determined from six consecutive runs at concentration levels approximately 100 times the DL. The minimum level that can be quantitatively determined is normally considered to be 5 times DL, or 10σ.

Although these values are not spectacular at first glance, it should be noted that these results were obtained with a PDA. It is generally agreed that the sensitivity of the PDA is roughly 2 to 3 orders worse than the PMT. Thus our results are comparable to those reported by other

TABLE II

Operating Parameters - Ar ICP

Forward incident power	2000 w
Reflected power	<1 w
Plasma gas	argon 15 l/min
Auxiliary gas	argon 1 l/min
Carrier gas	argon 0.9 l/min
Solution uptake rate	1.5 ml/min (1.3 g/min)
Observation zone above load coil	14-16 mm

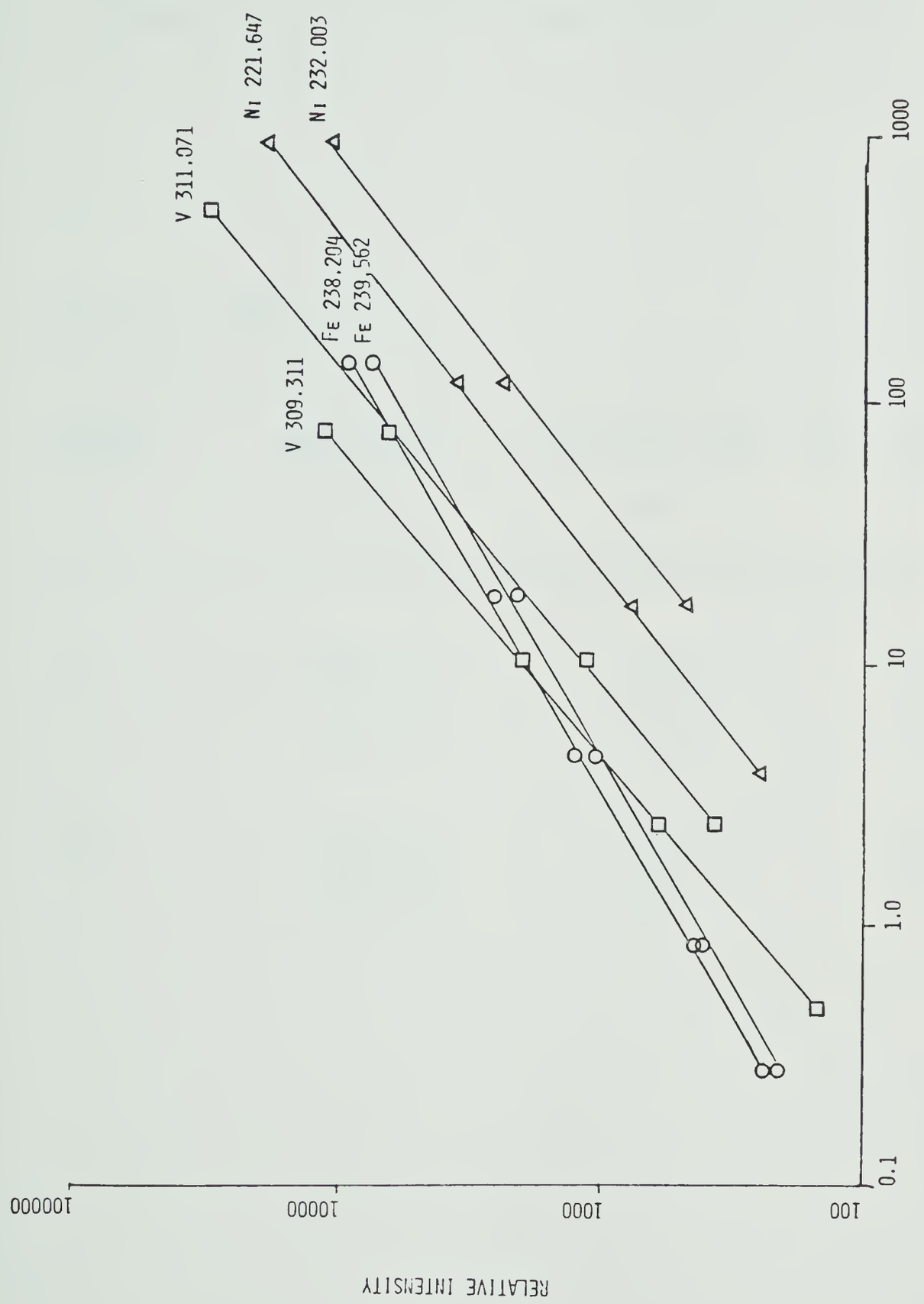

FIGURE 12. Calibration curves for vanadium, iron and nickel

TABLE III

Detection Limits and Precision Values - Ar ICP

At 15 mm, 100% Ar

ELEMENT	WAVELENGTH NM	DETECTION LIMIT PPM	REL. STD. DEV. %
V	309.311	0.26	1.0
	311.071	0.53	1.1
Ni	221.647	2.0	1.7
	232.003	4.9	2.7

workers. Although the PDA system does not provide the best in detection limits, the flexibility of the PDA as a simultaneous multichannel measurement system was required for overall system evaluation and method development.

CHAPTER IV

EVALUATION OF AN O_2-Ar ICP FOR DETERMINATIONS IN ORGANIC MATRICES

A. General Survey of "Mixed Gas" ICP

After the discovery of the ICP discharge for spectrochemical analysis, Greenfield et al. (77) in 1965 reported the first study on the use of argon, helium, nitrogen, air, and oxygen gases for the ICP. They concluded that only argon should be used to carry sample aerosol, since the other gases resulted in decreased emission intensity. The use of a 20% oxygen-80% argon mixture gave better sensitivity than a 100% argon plasma, although their attentions were focused on a high power nitrogen cooled plasma. They further concluded that oxygen could be used to remove the carbon band systems when organic solvents were aspirated. No values were given, but their findings were encouraging. Subsequent papers from Greenfield's research group (88,55,89,90) demonstrated the feasibility of such diatomic gas (nitrogen and oxygen) cooled plasmas.

The introduction of organics and the effects of nitrogen, oxygen, helium, and air in an ICP were investigated by Truitt and Robinson (72,73). In the preliminary report (72), these gases were added to an argon plasma discharge. They found that it was possible to replace all of the argon in the coolant (plasma) stream with other gases below 2 kw power. At similar power levels,

argon could be replaced completely by nitrogen or helium in the center tube, but not by air or oxygen. They found that in general, introduction of any of the gases into the center stream resulted in severe contraction of the core. A reduction in the line-to-background ratio and reduction of line and band intensities in the spectrum were observed in the core and secondary regions, and to a lesser extent from the tail flame. They observed the effects as nitrogen, oxygen, air, and helium replaced argon in the coolant stream and recorded spectra when dry nitrogen, dry oxygen, and air were used as coolant.

In a later report (73), emission spectra and spatial emission profiles of organic compounds introduced into the plasma were discussed. Four species were identified as sources to emission signals and were characteristic of hydrocarbons. These fragments were carbon, hydrogen, C_2, and CN. The effects of various simple gases (argon, helium, nitrogen, oxygen, and air, added to either the carrier or coolant stream in the presence of n-heptane) on the emission intensity of these bands and lines were summarized. The effect of RF power on emission intensity for n-octane and the effect of the concentration and number of carbon atoms on emission intensity were also discussed. However, except for carbon, there was no mention of sensitivity for other elements. Thus only spectral background information was discussed with no reference made for specific analytical lines for the elements.

Greenfield et al. (90) presented spectral background scans of an ICP plasma at different powers and with different gases in the coolant (plasma) stream. Argon gas was used for both plasma (auxillary) and nebulizer gases, with the variant being the coolant (plasma) gas. A viewing height in the tail flame of 45 mm above the base of the plasma was used. They compared the spectral background of an argon-nitrogen plasma operated at 2 to 7 kw and showed partial dissociation of molecular species at a higher power. Methanol or an aqueous solution of chromium, vanadium, and iron were aspirated into argon, oxygen, or nitrogen cooled discharges at 5 kw and the backgrounds were compared. Similar to the effect of high power, oxygen completely removed both the C_2 Swan and the CN bands, but had a fairly complicated molecular spectrum arising from O_2 and O_2^+ species. Nitrogen in the coolant resulted in a lower background continuum below 280 nm. The sensitivity of an argon-oxygen plasma was also significantly lower than an argon-nitrogen plasma. They suggested that the choice of using high power or oxygen to remove the organic species would be entirely dependent on the elemental spectral lines of interest.

Recently, Ohls and Sommer (91,64) studied the analytical application of an air-argon ICP source. The air cooled plasma was operated at 27.12 MHz and 3 kw. Although higher coolant and intermediate gas flows were used (28 l air/min and 15 l Ar/min respectively), their results on determinations in aqueous media indicated that the

performance of an air cooled plasma was slightly better than a nitrogen cooled or pure argon plasma. This air cooled plasma with a total of 16 l Ar/min flow actually offered no savings in argon gas consumption compared to most ICAP's operated at power levels below 2 kw. No explanation was given for the enhancement, but the general belief is that argon supports the discharge whereas "coolant" air prevents the hot discharge from damaging the torch.

However, all these studies involving quantitative evaluations have the discharge operated at substantially higher nominal power levels (up to 10 kw) than a pure argon ICP discharge, and thus provide no significant operating cost reduction. More recent mixed gas studies have focused on nitrogen cooled plasmas operated at lower power. These include Greenfield and McGeachin (92), Greenfield and Bums (93), Montaser and Mortazavi (94), Ebdon et al. (95,96), and Choot and Horlick (97). They all reported on the ease of operation of such nitrogen cooled plasmas and of similar performance when compared to a pure argon discharge.

In a preliminary report, Barnes and Meyer (98) sustained a 100% nitrogen ICP at 1.3 kw with a conventional spectrochemical system, similar to that described by Scott et al. (99). This nitrogen plasma was studied to verify the validity of calculated predictions by Barnes and Nikdel (100). No conclusive statements were made on the performance of this discharge, but this study may encourage other spectrochemical possibilities.

Although the addition of nitrogen to an argon ICP

decreased the argon background, a very intense emission from molecular nitrogen species can be observed at the optimum height. When organic samples were aspirated, a very intense cyanogen emission occurred. This phenomenon was reported by Truitt and Robinson (73), Greenfield et al. (90), and was also observed in our laboratory.

By using a high resolution spectrometer, Ohls and Sommer (40) analyzed wear metals in lubricants with a 1.5 kw nitrogen cooled plasma, but their results were only comparable to other studies with an argon ICP. The high plasma and auxillary flow rates, 12 l N_2/min and 10.8 l Ar/min respectively, may suggest that this approach is not superior to conventional ICP analysis although no residue of carbon could be noticed in the torch using nitrogen as coolant. The torch shown in Figure 2 provides a better flow at the injector tip and completely elminates any carbon deposit. It appears that at least with the reported results, a mixed nitrogen-argon ICP will not improve elemental determinations in organic solvents. We will thus focus on oxygen.

B. Evaluation of an O_2-Ar ICP

1. Addition of O_2

A slight modification was necessary to reroute the gas flows for the ICP 5000 for mixing in O_2. Two Matheson Rotameter-Mixers (Matheson, East Rutherford, N.J.) were employed. The one dedicated to the plasma gas supply employed Model 605 Flowtubes and the second one used for the

aerosol carrier gas supply consisted of Model 603 Flowtubes. The incorporation of these rotameter-mixers allowed for both plasma and aerosol carrier flow variations from 100% Ar to 100% O_2, or for any intermediate value to be set independently. Compensation was made for the differences in specific gravity (Ar = 1.380; O_2 = 1.105; air = 1.00) to ensure a constant volumetric flow. The new plumbing layout further allowed any gas supply other than argon to be changed even when the plasma was running.

The ICP discharge was produced by starting the plasma with argon in the plasma and auxillary gas, under impedance matching conditions best suited to the argon discharge. With the argon discharge substained, a hole was punched with either dry argon or argon with xylene aerosol. Oxygen was introduced first into the carrier gas and argon flow was reduced proportionally to ensure constant volumetric flow. Similarly, oxygen was mixed into the plasma gas. With the introduction of oxygen the automatic tuning network retuned itself and the reflected power increased. The manual tuning knob was adjusted to give the lowest reflected power. By following this simple procedure, the desired amount of O_2 could be mixed in less than 20 seconds. Welding grade oxygen was used and was satisfactory. No major contaminant was found and it was much more economical than certified grade oxygen.

A sequence of photos were taken and are reproduced in Figure 13. A 2 kw argon plasma with xylene aspirating is shown in Frame a. When a small amount of O_2 was mixed

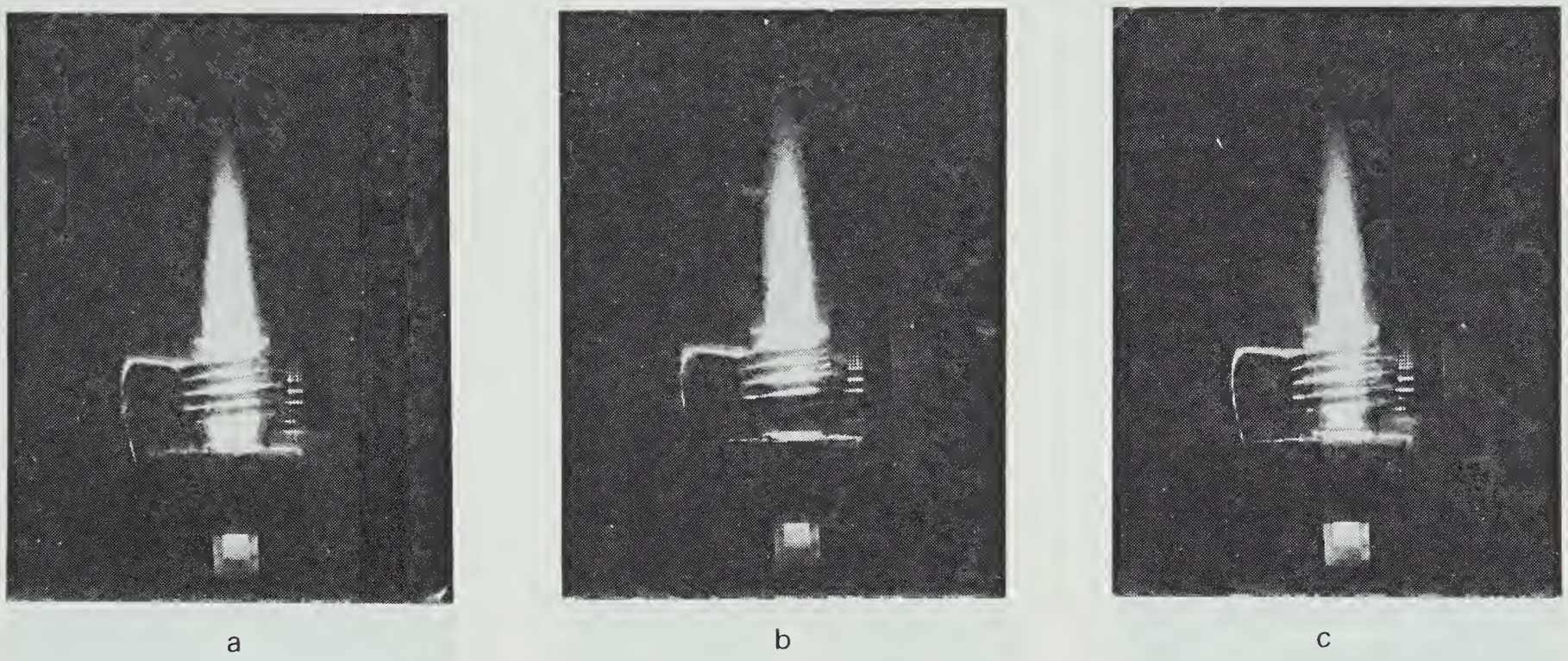

FIGURE 13. Photographs taken when increasing amount of oxygen was mixed into a plasma with xylene being nebulized. a = no O_2, b = small amount of O_2 in the aerosol carrier flow, c = small amount of O_2 in the plasma gas flow, d = small amount of O_2 added to both aerosol carrier and plasma gas flows, e = 20% O_2 in plasma gas flow, and f = 50% O_2 in plasma gas flow.

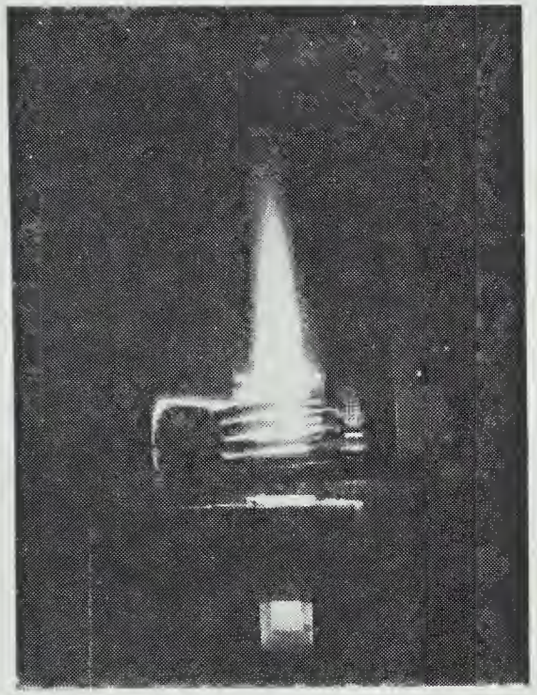

d

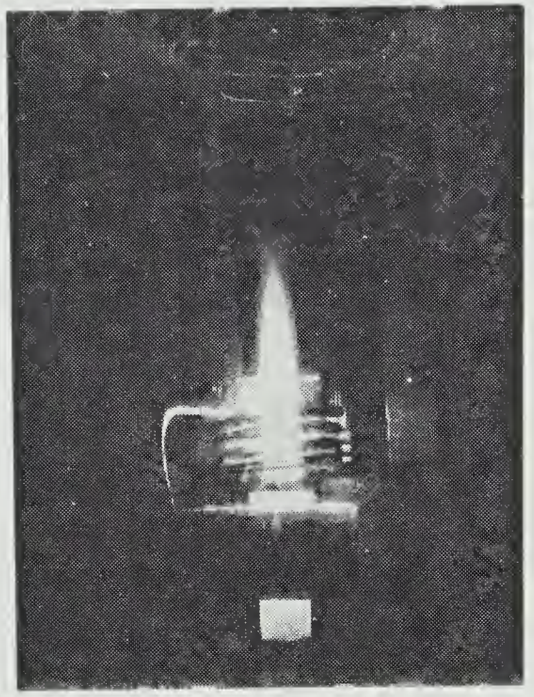

e

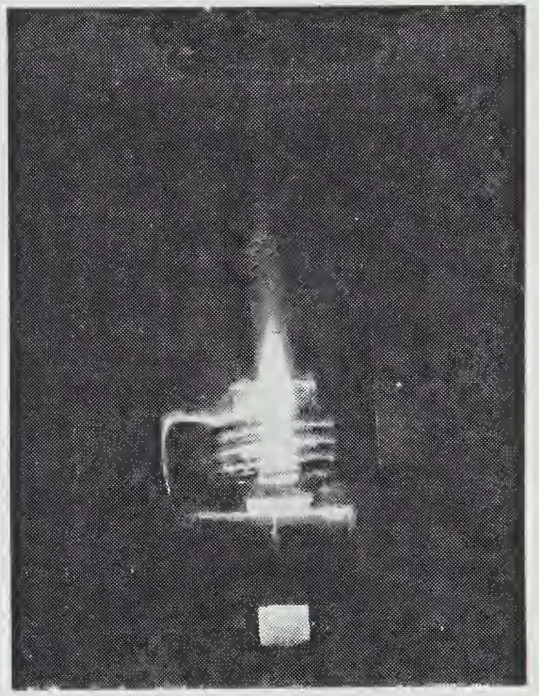

f

FIGURE 13. (continued)

with the xylene aerosol carrier argon, the central bullet diminished in intensity (Frame b). Addition of a small amount of O_2 to the plasma gas appeared to lift the whole plasma (Frame c). Introducing a small amount to both carrier and coolant flows had the combined effect (Frame d). When 20% O_2 was mixed into the coolant gas, the size of the discharge was greatly reduced (Frame e). Addition of up to 50% O_2 further reduced the dimension of the discharge (Frame f). The addition of O_2 appeared to result in a "hotter" and slightly elongated plasma. This observation is shared by Ohls and Sommer (64).

Our reasoning for only mixing O_2 in either the carrier or plasma flows was as follows. It is generally agreed that for an argon ICP, plasma gas, which may be termed coolant gas incorrectly, is responsible for sustaining the discharge. This should be obvious since it is the only gas flow necessary to initiate and sustain the plasma. The aerosol carrier flow, in addition to transporting the analyte, punches a hole and maintains the central channel in the plasma. This gas may interact with the analyte at this point in time in some poorly understood manner. The auxiliary flow lifts or lowers the plasma and the sole purpose, at least in our experimental setup, is to prevent ablation of the torch.

2. Optimization of Parameters

In order to establish the best compromise condition for analysis, a solution containing vanadium was aspirated. In

addition to the parameters previously described, the optimum amount of O_2 in both the plasma and carrier flows must be established. The instrumentation for vertical spatial profile studies was used and has been described previously.

The plasma was sustained at different levels of O_2, and the carrier flow rate was varied at each combination of O_2 and Ar. The flow rate at which maximum emission was observed was compared to those at other combinations. This result is summarized in Figure 14. Increasing the amount of O_2 from 0% (a) to 20% (d) resulted in emission enhancement, with little or no enhancement with further additions of O_2 (30%,e). The peak maxima also shifted towards the load coil with increasing amounts of O_2 in both plasma and carrier, which is expected since the actual plasma discharge visually decreases in size. Increasing O_2 further increased reflected power and decreased stability. Thus 20% O_2 in the plasma gas with a small amount of O_2 in the carrier gas operating at 2 kw (Figure 14 d) was selected. The compromise conditions after other elements were studied are outlined in Table IV.

3. Qualitative Spectral Tracing

Wavelength scans of background intensity species centered at 8 mm above the load coil were recorded (Figure 15). It is apparent that background continuum and carbon containing molecular emission are greatly reduced. A more detailed look at the effect of O_2 on the spectral background is shown in Figures 16 through 19. Curves a, b,

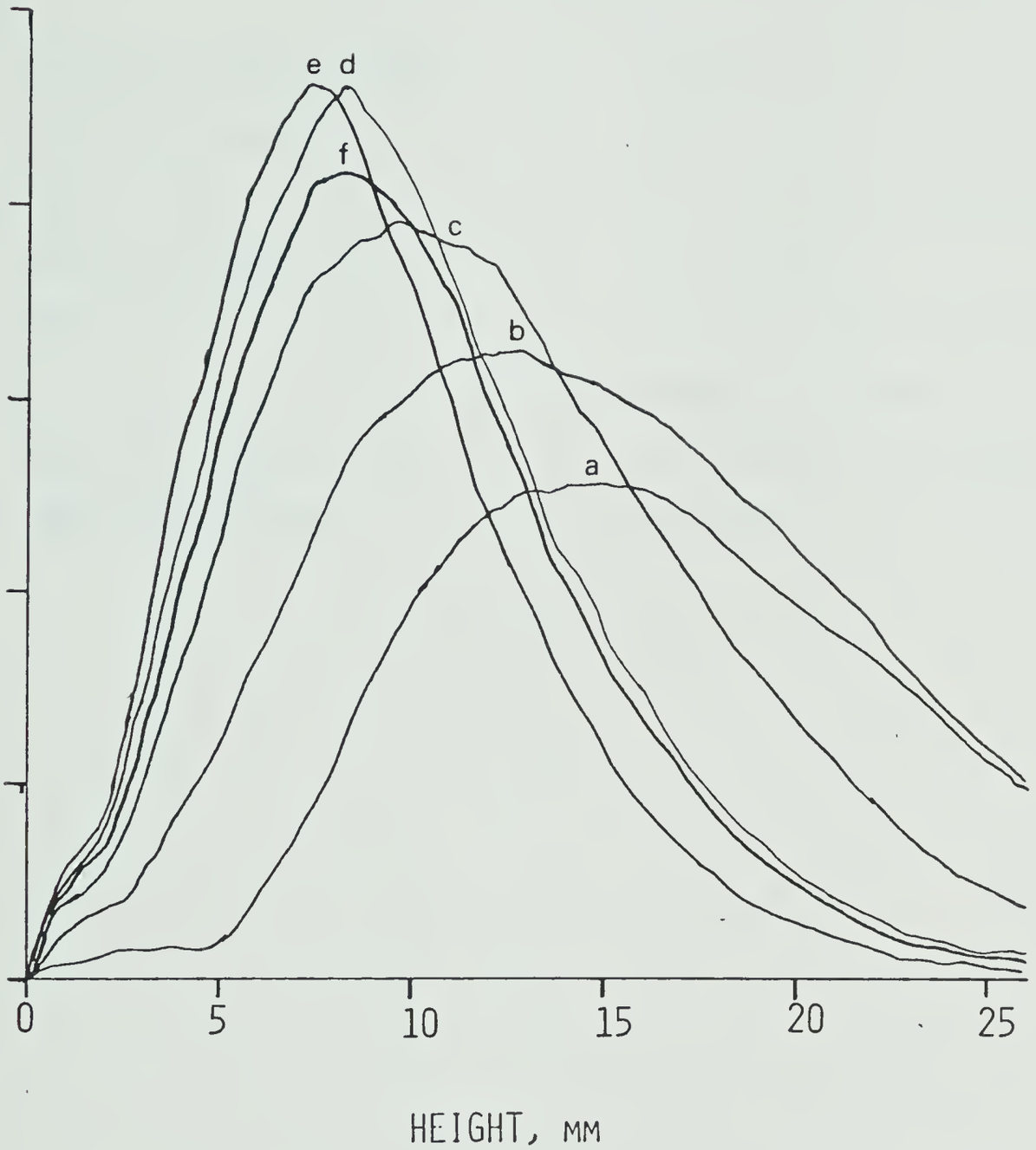

FIGURE 14. Combined effect of the amount of oxygen in the plasma flow and varying aerosol flow rate on vanadium spatial profile at the 309.311 nm line. Curves a=0%, b=5%, c=10%, d=20%, and e=30% O_2.

TABLE IV

Operating Parameters - O_2-Ar ICP

Forward incident power	2000 w
Reflected power	< 10 w
Plasma gas	O_2 3 l/min, Ar 12 l/min
Auxiliary gas	Ar 1 l/min
Carrier gas	O_2 0.1 l/min, Ar 0.6 l/min, total 0.7 l/min
Solution uptake rate	1.5 ml/min (1.3 g/min)
Observation zone	7-9 mm

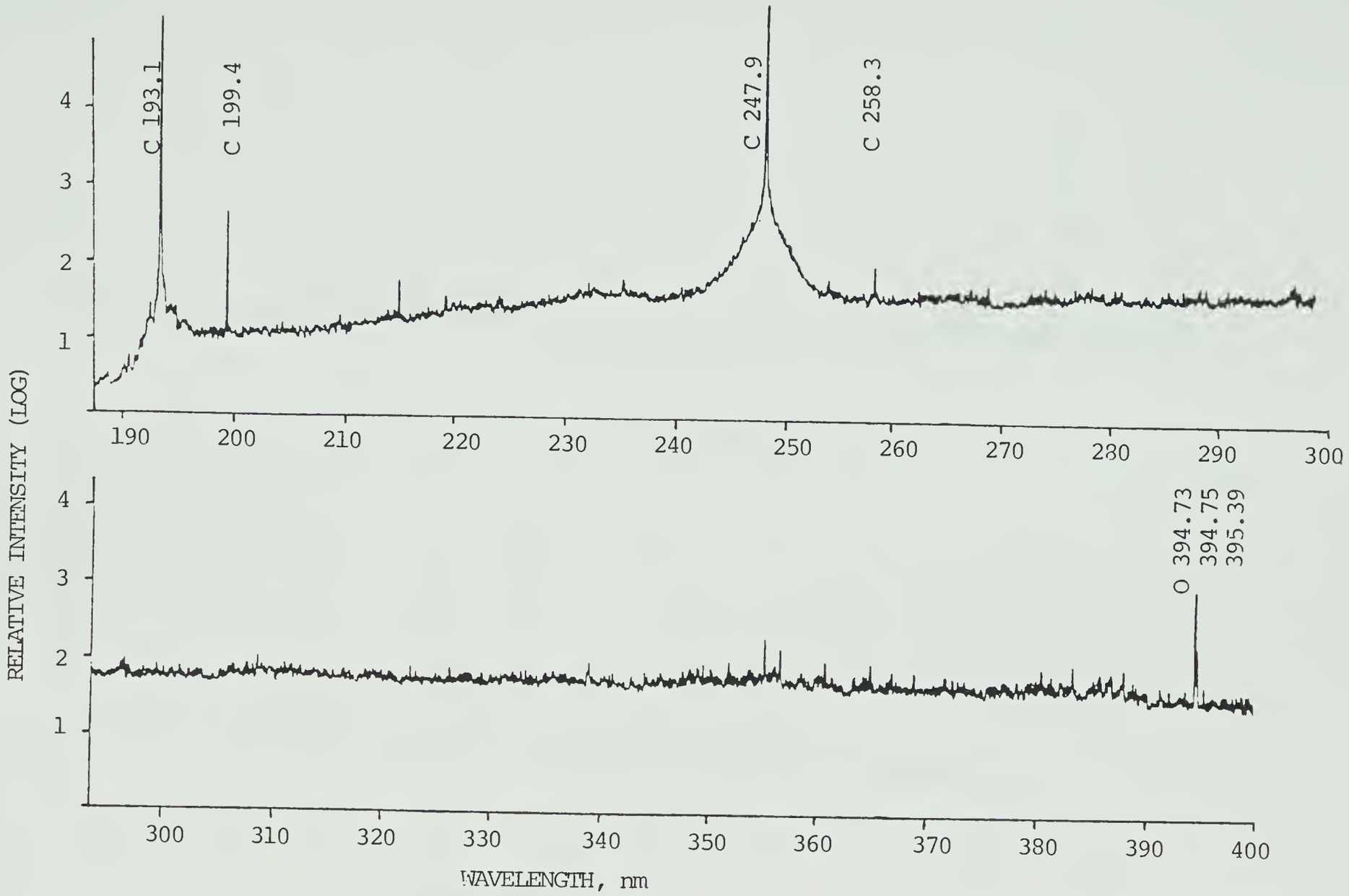

FIGURE 15. Wavelength scans from 190 to 590 nm centered at 8 mm above the load coil. Scan was obtained when xylene was aspirated.

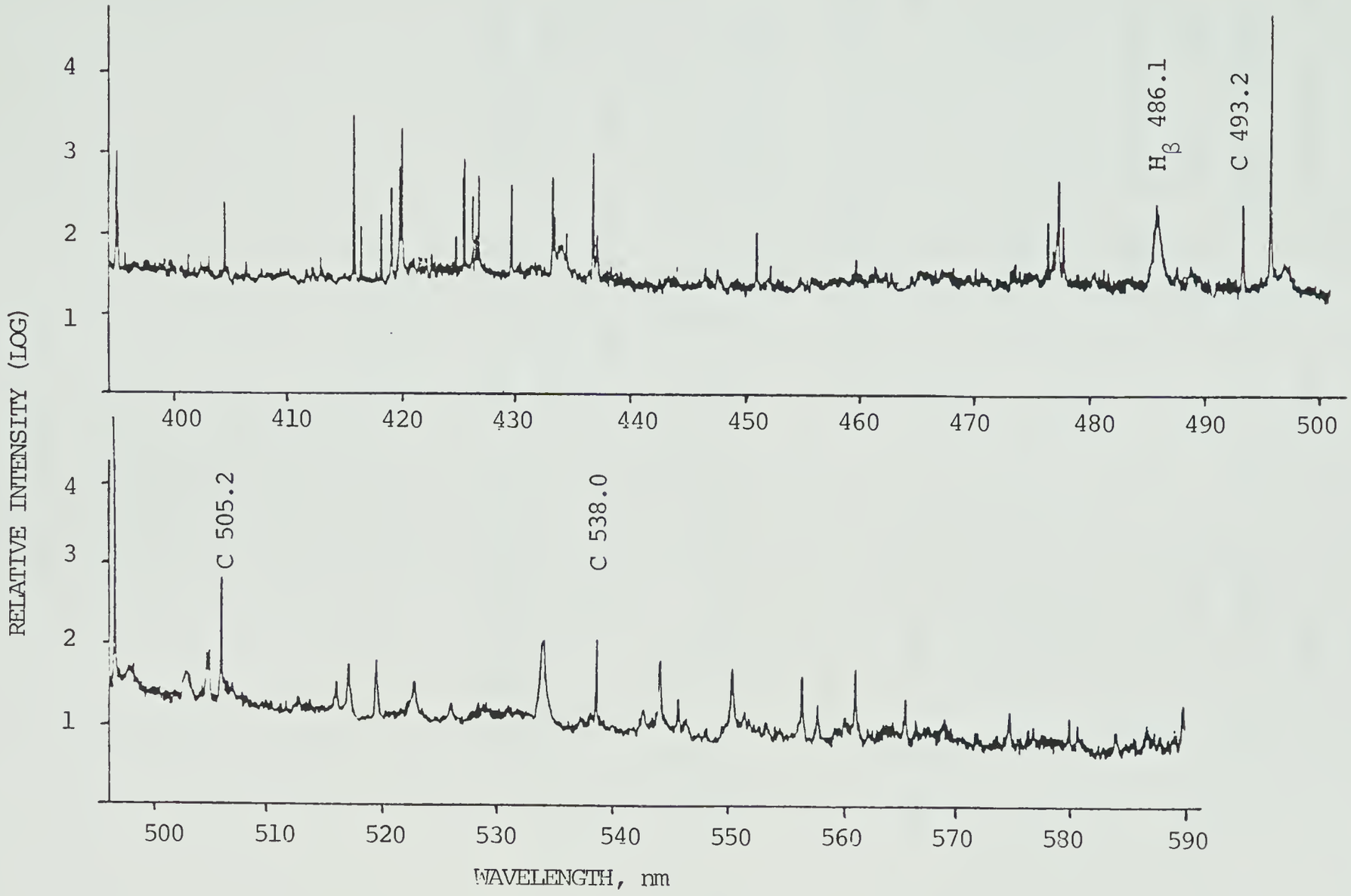

FIGURE 15. (continued)

c, d , and e represent 0, 5, 10, 20, and 30% O_2. When we monitored the region from 14 to 16 mm (centered at 15 mm) above the load coil, we observed that increasing the amount of oxygen reduced emission from cyanogen (Figure 16) and C_2 Swan bands (Figure 17). However, the background continuum level appeared to rise from 0 to 5% O_2, and a gradual decrease was observed with further O_2 additions. But when we monitored the 2 mm region centered at 8 mm above the load coil, both the background continuum and emission from cyanogen (Figure 18) and C_2 Swan (Figure 19) decreased with addition of O_2.

4. Quantitative Result

Calibration curves and the wavelengths at which they were measured are shown in Figure 20. Good linearity was obtained over several orders of magnitude, and the slopes of the log-log plots are essentially unity. Detection limit (2 σ) and precision (RSD) values are given in Table V.

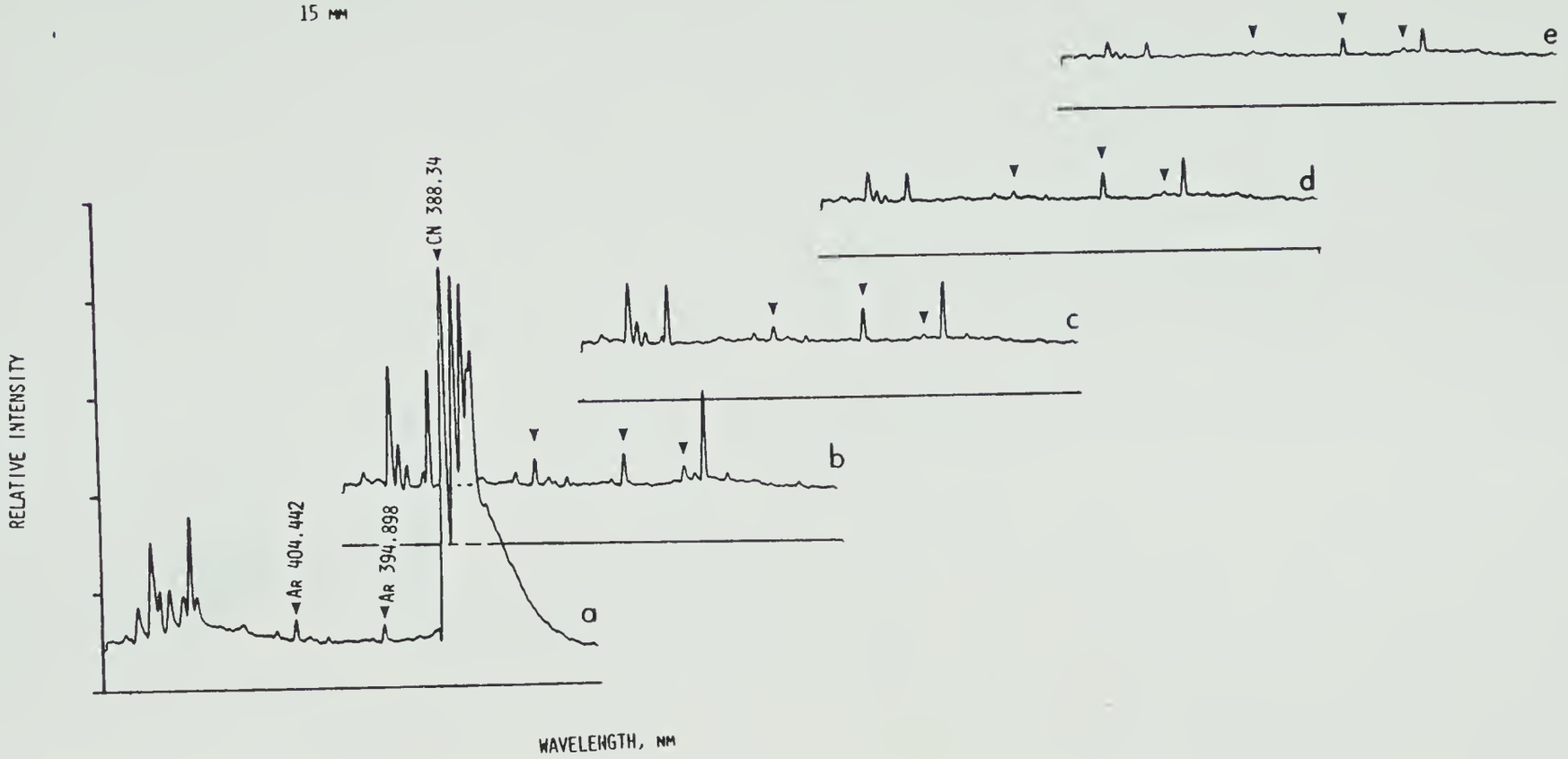

FIGURE 16. Effect of increasing oxygen on background emitting species between 375 to 425 nm. Spectra a=0%, b=5%, c=10%, d=20%, and e=30% O_2.

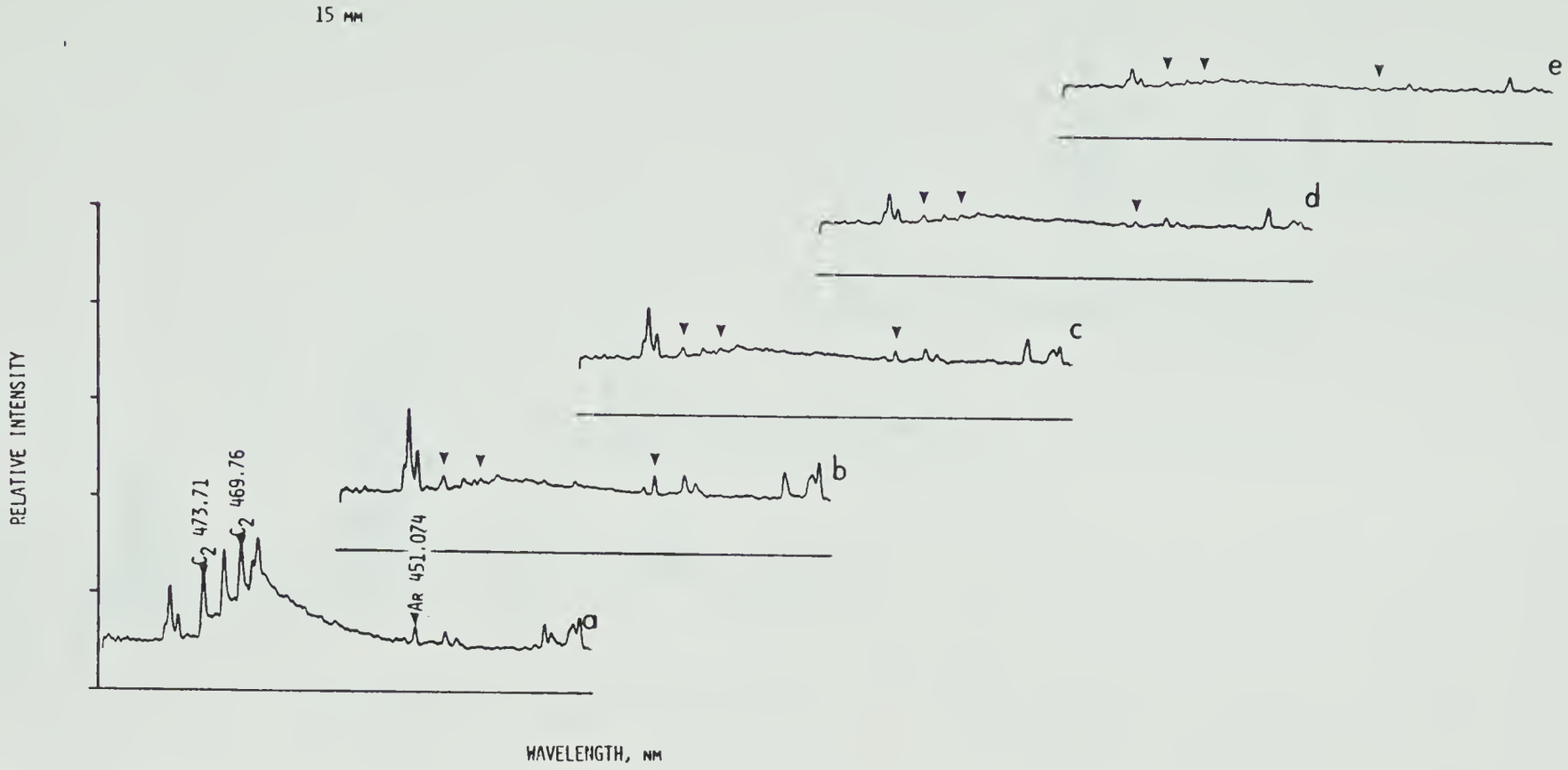

FIGURE 17. Effect of increasing oxygen on background emitting species between 435 and 485 nm. Spectra a=0%, b=5%, c=10%, d=20%, and e=30% O_2.

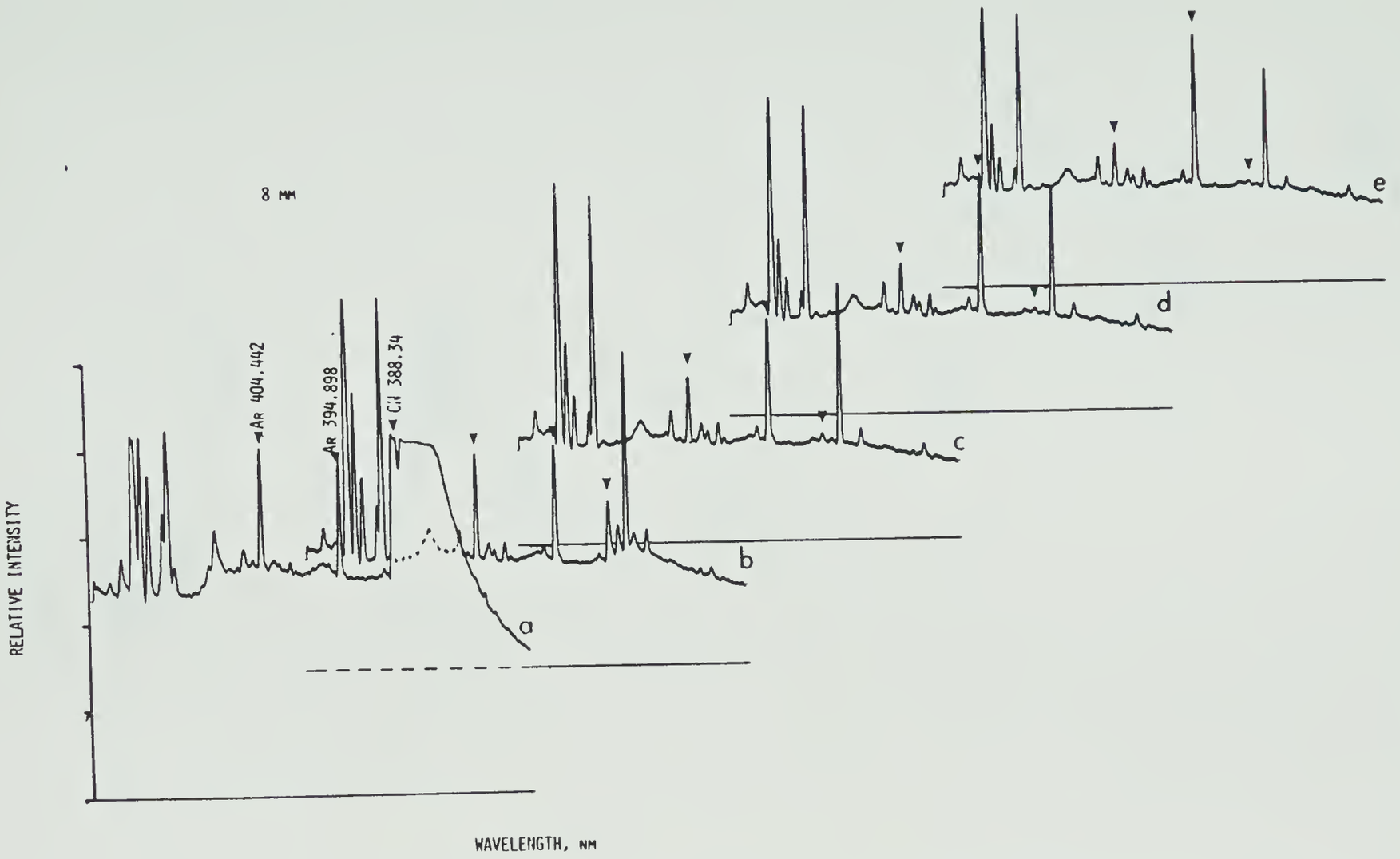

FIGURE 18. Effect of increasing oxygen on background emitting species between 375 and 425 nm centered at 8 mm. Spectra a=0%, b=5%, c=10%, d=20%, and e=30% O_2.

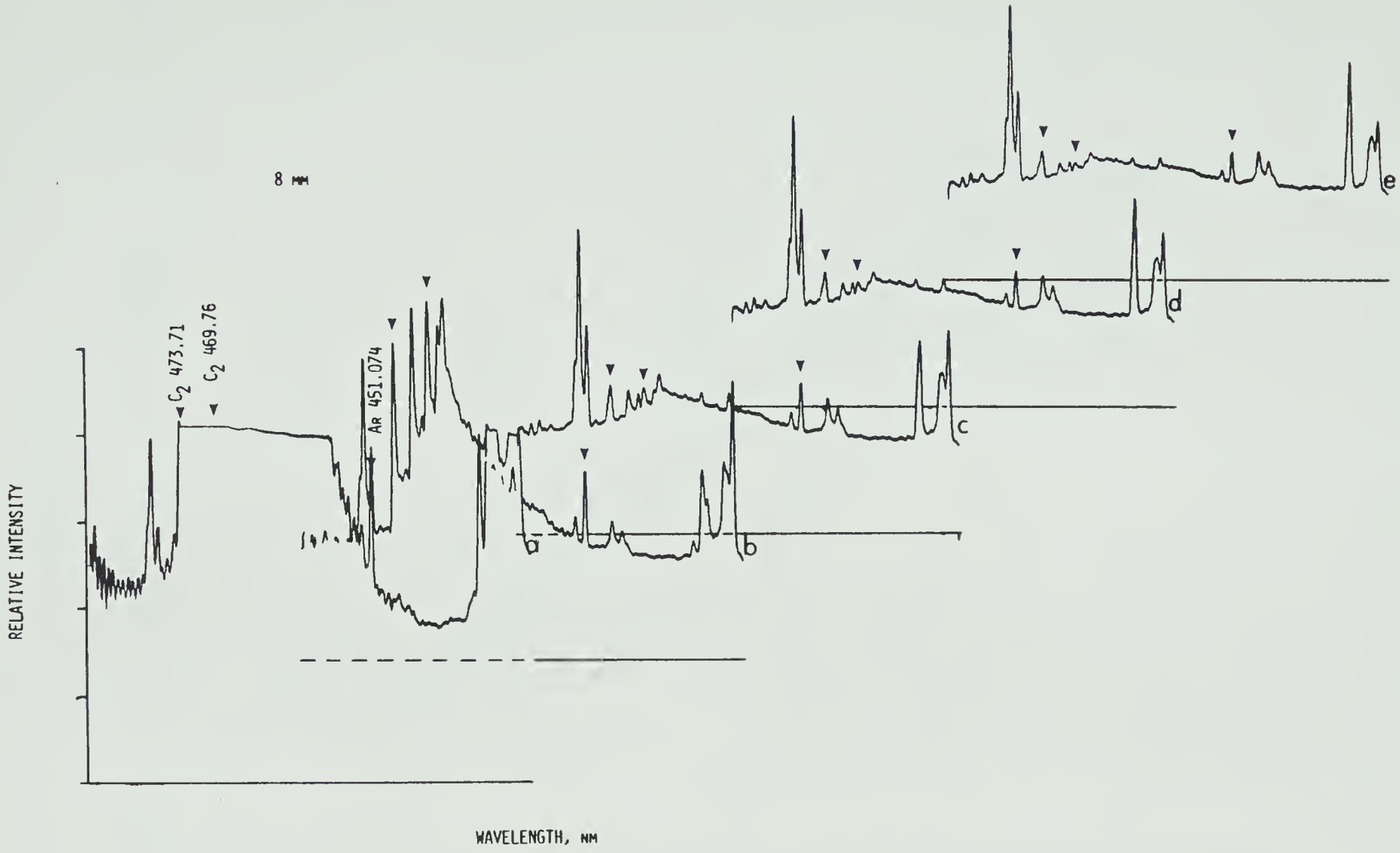

FIGURE 19. Effect of increasing oxygen on background emitting species between 435 and 485 nm centered at 8 mm. Spectra a=0%, b=5%, c=10%, d=20%, and e=30% O_2.

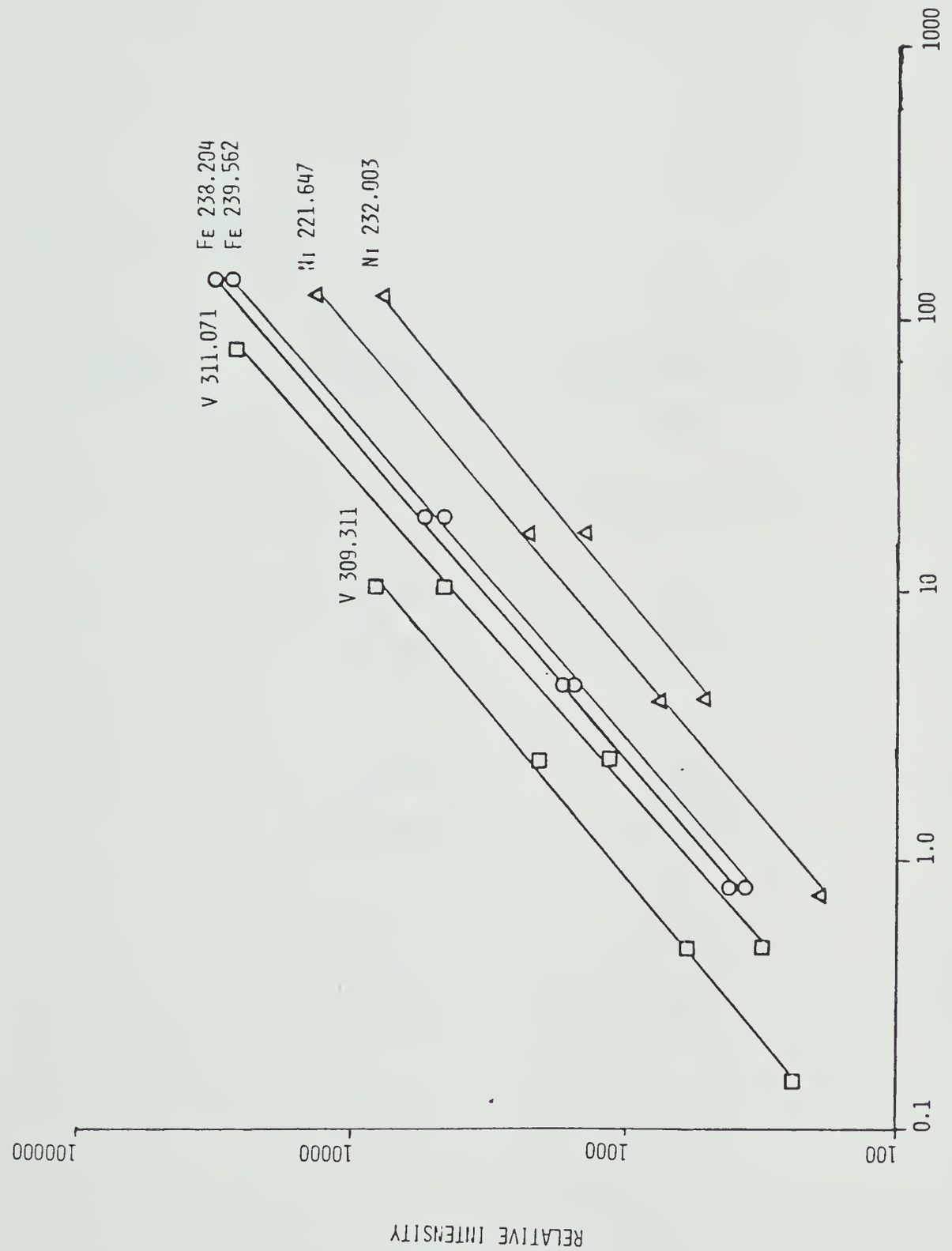

FIGURE 20. Calibration curves for vanadium, iron, and nickel obtained by a 20% O_2-Ar ICP

TABLE V

Detection Limits and Precision Values - O_2-Ar ICP

At 8 mm, 20% O_2

ELEMENT	WAVELENGTH NM	DETECTION LIMIT PPM	REL. STD. DEV. %
V	309.311	0.11	0.51
	311.071	0.26	0.50
Fe	238.204	0.46	0.78
	239.562	0.48	1.1
Ni	221.647	0.9	0.63
	232.003	1.6	1.1

CHAPTER V

COMPARISON OF EXPERIMENTAL RESULTS AND FUTURE CONSIDERATIONS

A. Comparison of 100% Ar with 20% O_2-Ar ICP

Wavelength scans from 190 to 600 nm for a 100% Ar discharge centered at 15 mm above the load coil with a 2 mm aperture and a 20% O_2 discharge centered at 8 mm show some interesting facts (Figure 21). Although the background continuum is higher at the 8 mm region for the 20% O_2 discharge, the spectrum is significantly cleaner. Less lines are observed and the molecular band systems diminish enormously in intensity. Background fluctuations are worse for the 20% O_2 discharge.

The increase in sensitivity for vanadium and nickel with a 20% O_2 plasma can easily be realized by comparing the calibration curves (Figure 22). At least a factor of 4 increase in sensitivity is observed. Detection limits are also improved by a factor of at least 2 when we ratioed the detection limits (Table VI). Also in the same table, precision values are ratioed and the 20% O_2 discharge gave more precise results. When we compared the calibration plots for iron (Figure 23), unity slope was obtained in the 20% O_2 discharge. Although no significant improvement in sensitivity was realized at concentrations under 2 ppm, the plot was linear. Thus we can conclude that a 20% O_2 ICP gives improved results when compared to a 100% Ar ICP.

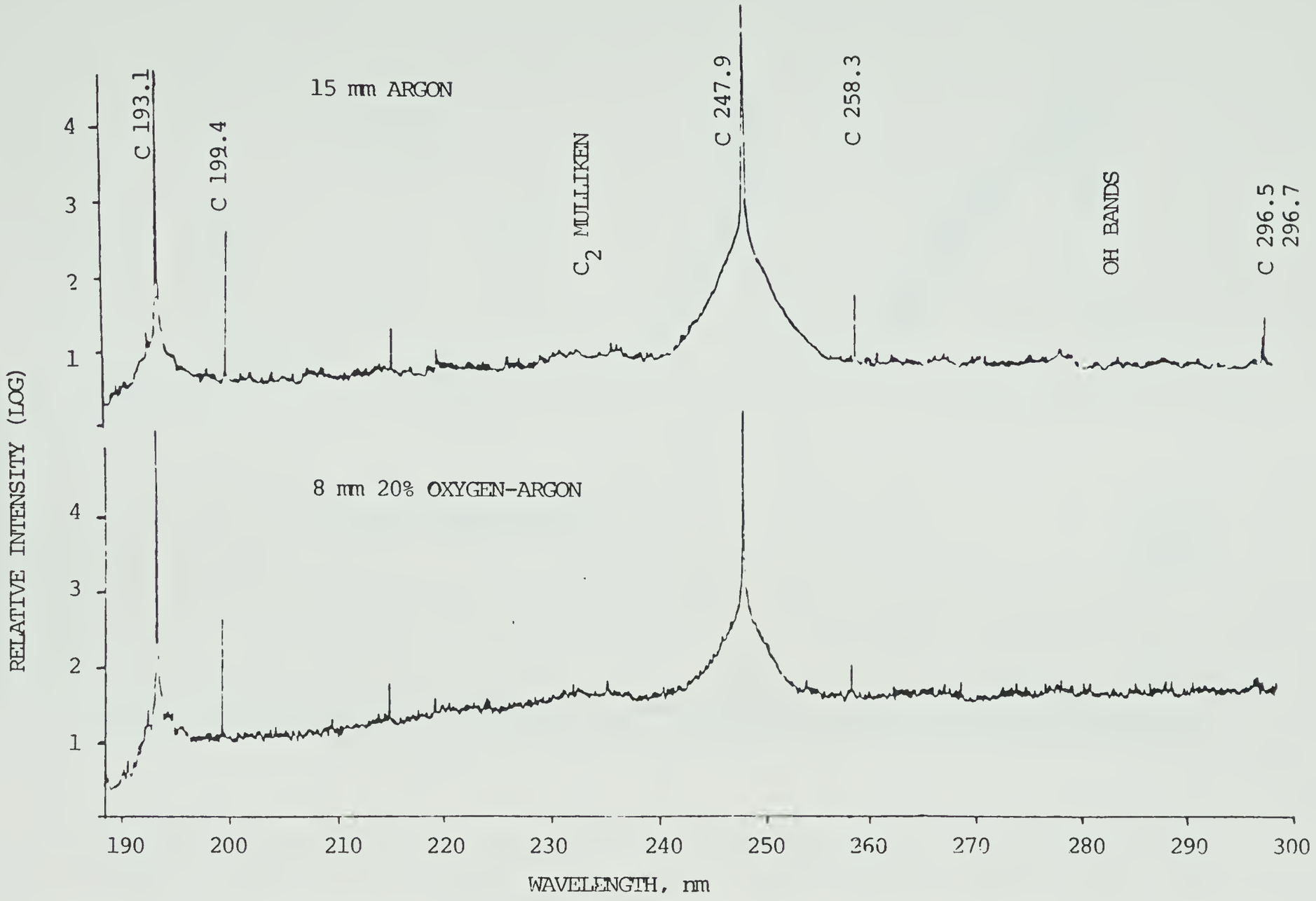

FIGURE 21. Comparison of wavelength scans from 190 to 590 nm when aspirating xylene

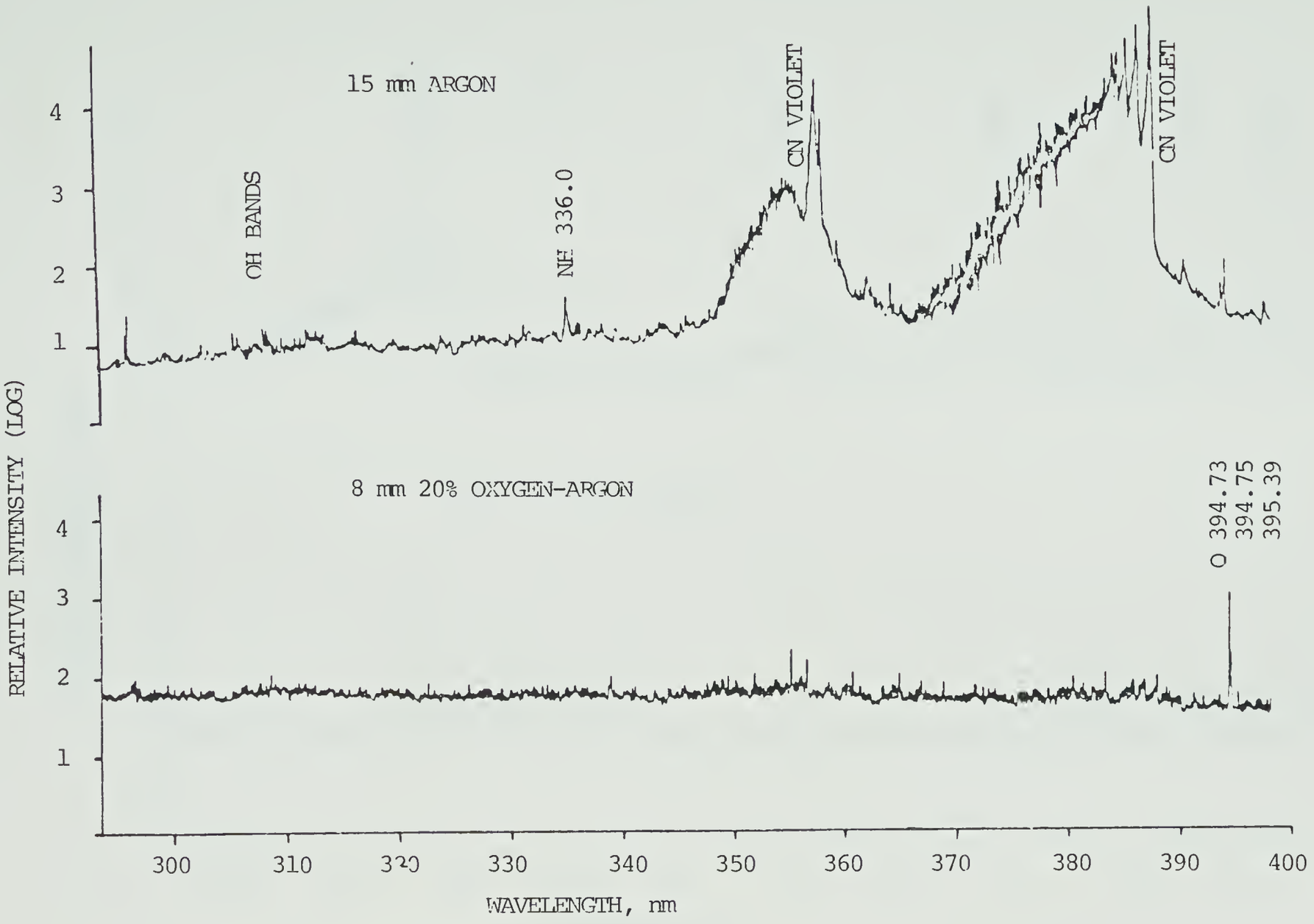

FIGURE 21. (continued)

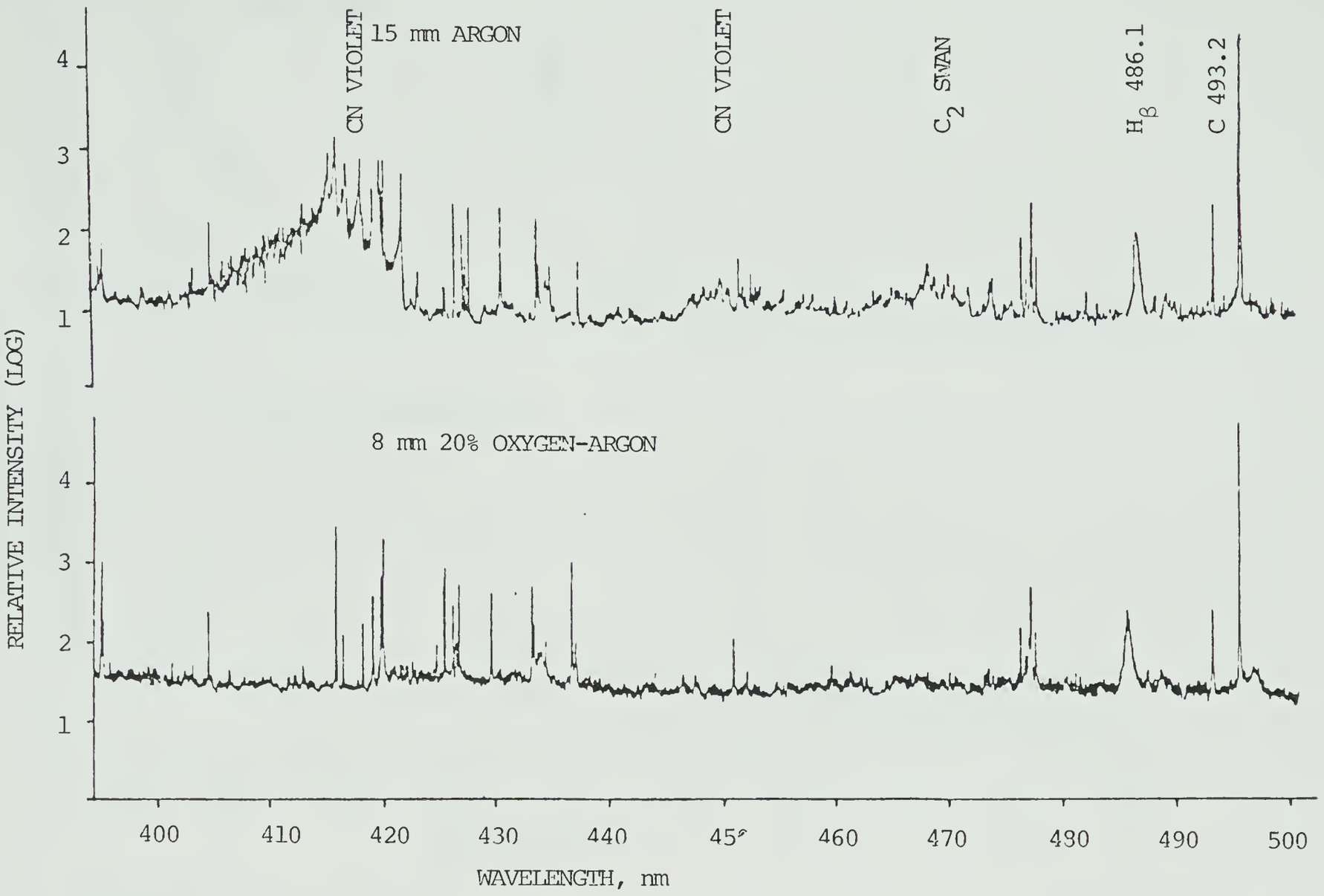

FIGURE 21. (continued)

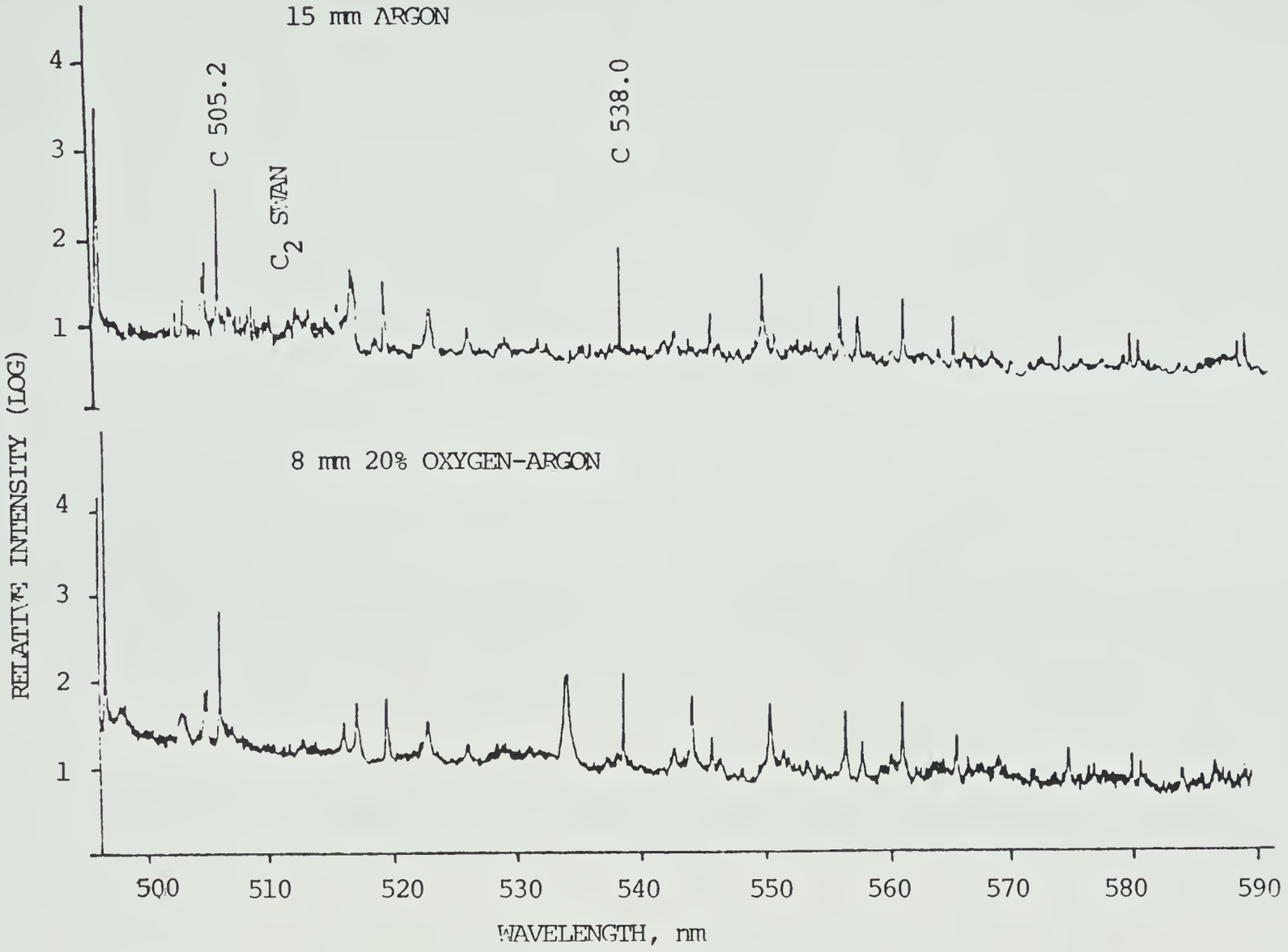

FIGURE 21. (continued)

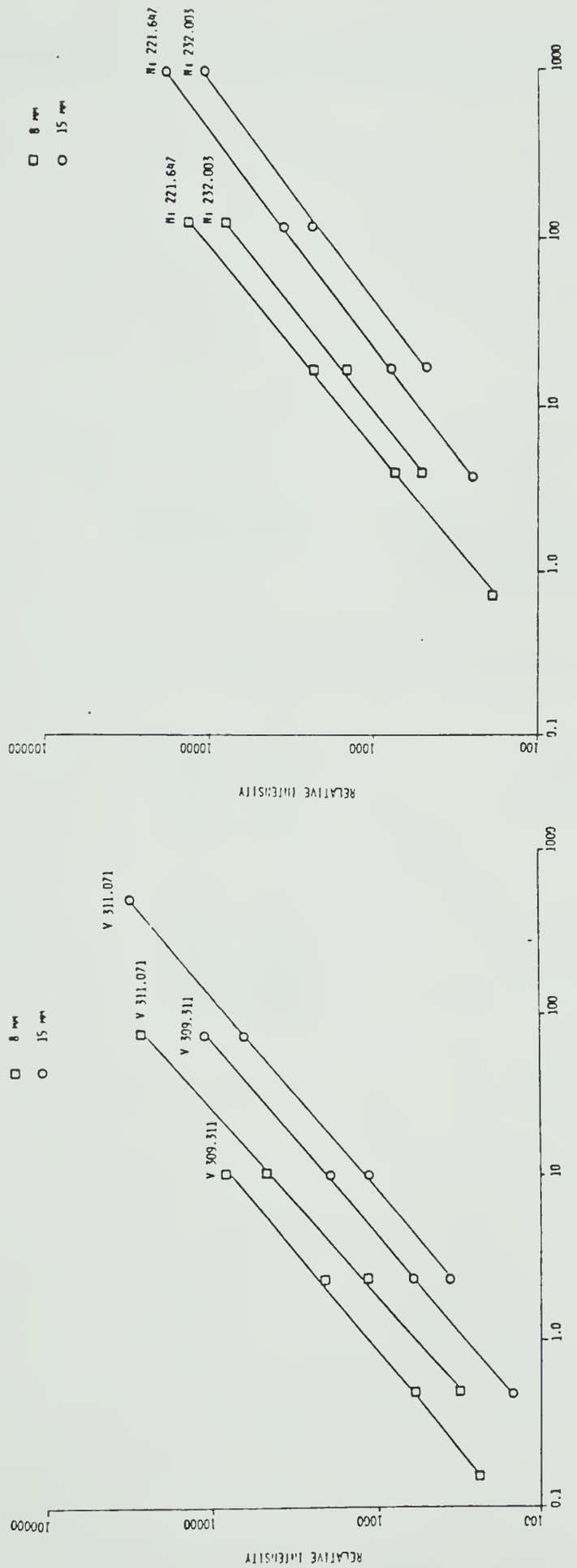

FIGURE 22. Comparison of calibration plots for vanadium and nickel

TABLE VI

Ratio of Detection Limit and Precision

ELEMENT	WAVELENGTH NM	RATIO OF DET. LIM. @ 15 MM/@ 8 MM	RATIO OF RSD
V	309.311	2.4	2.0
	311.071	2.0	2.2
NI	221.647	2.2	2.7
	232.003	3.1	2.5

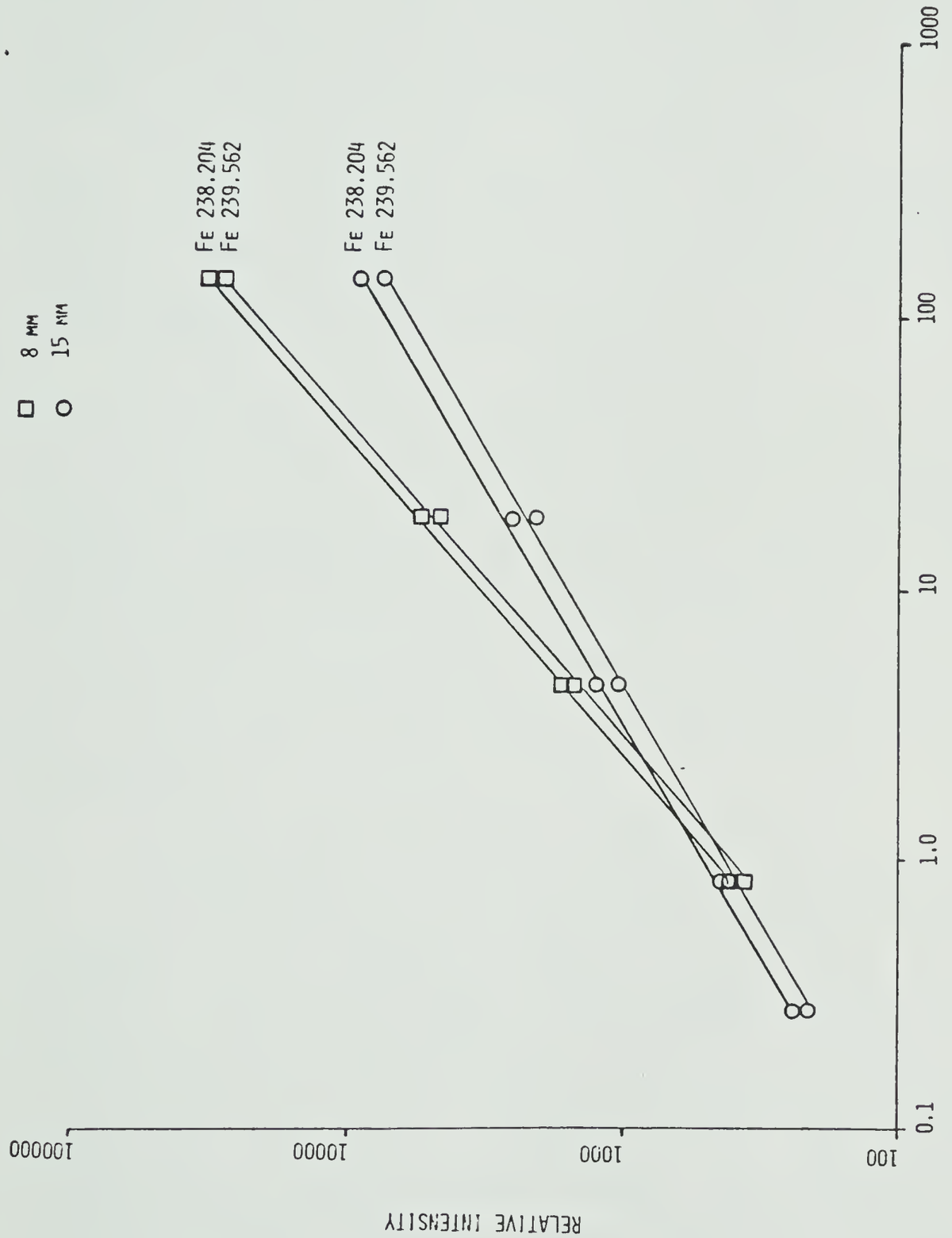

FIGURE 23. Comparison of calibration plots for iron

B. Explanation of the Effects of Oxygen

Excitation of an analyte species in a 100% argon plasma has been studied by various authors (101-103). The plasma discharge is in a state close to Local Thermal Equilibrium (LTE), in which this equilibrium exists:

$$Ar_m + e^- \rightleftharpoons Ar^+ + 2e^- \quad \text{(Equation 1).}$$

Both atomic and ionic excitations occur in the plasma. Neutral atom excitation (103) occurs by the collision of a fast electron, e^-_f with the analyte X,

$$X + e^-_f \rightleftharpoons X^* + e^-_s \quad \text{(Equation 2),}$$

with the production of an excited atomic analyte and a slow electron. Ionic excitation (102,103) is explained by Penning Ionization and the energy is available from argon metastables. Collision of a metastable with the analyte results in ionization and excitation, and the excess energy is carried away in the form of kinetic energy of the free electron.

$$X + Ar_m \rightleftharpoons X^{+*} + Ar + e^- \quad \text{(Equation 3)}$$

The discharge with the O_2-Ar mixture described in Chapter IV is visually smaller in size than a 100% Ar plasma. When O_2 is mixed in the plasma (coolant) gas, the higher thermal conductivity of oxygen as compared to argon compresses the argon discharge. This may explain the "pushing" or "thermal pinch" effect. The discharge appears smaller because molecular oxygen emission is very weak in the visible region of the spectrum, and the visible discharge still belongs to argon.

At the RF power that we are operating, argon is believed to sustain the discharge. This visually smaller argon discharge has higher electron density, and thus increases the probability of atomic excitation. This increase in electron density shifts Equation 1 to the left and produces more argon metastable, and thus Penning (ionic) ionization is also increased. This may be the reason for the observed enhancement of analyte emission intensity. The smaller argon discharge also accounts for the fact that emission maxima occurs at relatively lower regions in the plasma, as is evident by spatial studies.

The reduction in carbon, cyanogen, and C_2 emission is most likely the result of oxidation of these species by oxygen. This was also stated by Greenfield (77) and Truitt and Robinson (73). Attenuation of molecular emissions further corresponds to a lower background continuum.

C. Quantitative Bitumen Results

Determination of some elements in different bitumen samples obtained through the Alberta Research Council are summarized in Table VII. These samples are numbered in decreasing viscosity values.

Both vanadium and nickel concentrations are fairly high and this has been well documented. They are mainly concentrated in porphyrin compounds. The result for iron was somewhat surprising. No explanation could be given for the apparently extremely low levels in samples 3, 4, and 5.

TABLE VII

Quantitative Bitumen Results

Concentration, ppm

Bitumen	V	Fe	Ni
1.	163	.4	57
2.	233	108	116
3.	136	-	31
4.	74	-	11
5.	92	-	8

1. Athabasca Bitumen
   Cold-Extracted From Tar Sand with Benzene Ash = 0.07%
2. Athabasca Produced Bitumen
   GCOS Bitumen From Hot Water Process Purified by
   Dilution, Centrifuging and Naphtha Recovery Ash = 0.67%
3. Cold Lake Demulsified Bitumen
   Imperial Oil Steamflood Operation Ash = 0.08%
4. Lloydminster Heavy Oil - Sparky Formation
   Husky Primary Production Treated Crude Ash = 0.05%
5. Athabasca Produced Bitumen
   AMOCO Fireflood (COFCAW) Pilot Plant Ash = 0.07%

D. Future Considerations

1. Mixed Solvent Approach

In selecting standard reference materials for calibration, organic compounds of the elements are usually employed in a matrix that mimics the sample. The two different types of standards studied in this investigation, although widely used, still leave much to be desired. The time needed for preparation of NBS single element standards ranges from a few hours to over two days, and the reagents required are fairly exotic. Conostan standards are easy to use because they are already dissolved in an oil matrix, but their accuracy has been questioned. Stability of some Conostan standards, especially boron, is also a concern. Temporary stock depletions, as experienced for NBS SRM 1634 residual fuel oil, further necessitates the need for other standard materials.

The variation in physical and chemical properties between different matrices and solvents forbids calibration or standardization using a different matrix or solvent than the one containing the sample. The preferred procedure is to dissolve both the sample and standard in the same solvent or solution.

Certain organic solvents have good solubility for both water and other organic reagents. A three component - one phase mixed solution can be nebulized with ease. Thus we propose the following scheme. It takes advantage of the comprehensive stock of aqueous standard solutions in most

laboratories and the low purchase or preparation cost, together with the simplicity of mixed solvent for analysis.

Three components - acidified water (aqueous standard), the sample (synthetic crude or bitumen), and a "universal" solvent such as tetrahydrofuran (THF) - may be used. Preliminary multisolvent miscibility studies have shown that a system with the following composition:

10 g oil, 10 ml acidified H_2O, 70 ml THF,

is totally miscible and does not separate out during analysis. Preliminary results show that sensitivity for an element such as calcium is slightly poorer in this mixed solution as compared to single element aqueous solution determination, but the conditions were not optimized. More work is needed to verify the feasibility of such an approach.

2. Other Solvents

There is always a demanding need for the use of non-toxic or less hazardous reagents for analysis. This is to reduce risk for the analyst and other personnel. An excellent solvent for sample dissolution such as benzene, widely used in the 50's and 60's, is now regarded as an extremely dangerous material. Less toxic substituted derivates of benzene such as xylene or toluene, although still hazardous, are widely used because of desirable solubility. A plasma with either solvent or MIBK aspirating can be sustained without difficulty at power above 1.5 kw. As described in Chapter II, one can observe an intense green

sheath due to C_2 bands enveloping the plasma. With toxicity, solubility, purity, and "plasma burning characteristics" in mind, there are only a limited number of solvents available. In addition to xylene, toluene, and MIBK, acetonitrile and cyclohexanone may be considered. Acetonitrile has plasma characteristics similar to that of xylene, and offers no significant improvement. Cyclohexanone, on the other hand, is a powerful solvent, and the plasma formed with the solvent aspirating is very stable. Background continuum and molecular emission is also less intense relative to xylene. In addition, it is also desirable as the "universal" solvent as decribed in the mixed solvent approach.

3. Improved Stability by O_2 Addition

The addition of a suitable amount of oxygen improves both precision and detection limits for the elements studied. This seems to result from the formation of a "hotter" and more stable plasma. With this in mind, we attempted to aspirate other solvents into the discharge known to rapidly extinguish a normal 100% Ar ICP.

Benzene, a very powerful solvent, is widely used. A 2 kw plasma discharge with benzene uptake of 2 ml/min is very peculiar (Figure 24a). In addition to poor stability, it is extremely luminous. An elongated discharge is formed, and the axial channel appears much brighter and wider. The extra luminosity is suspected to be from combustion of carbon. Unburned carbon particles race through the

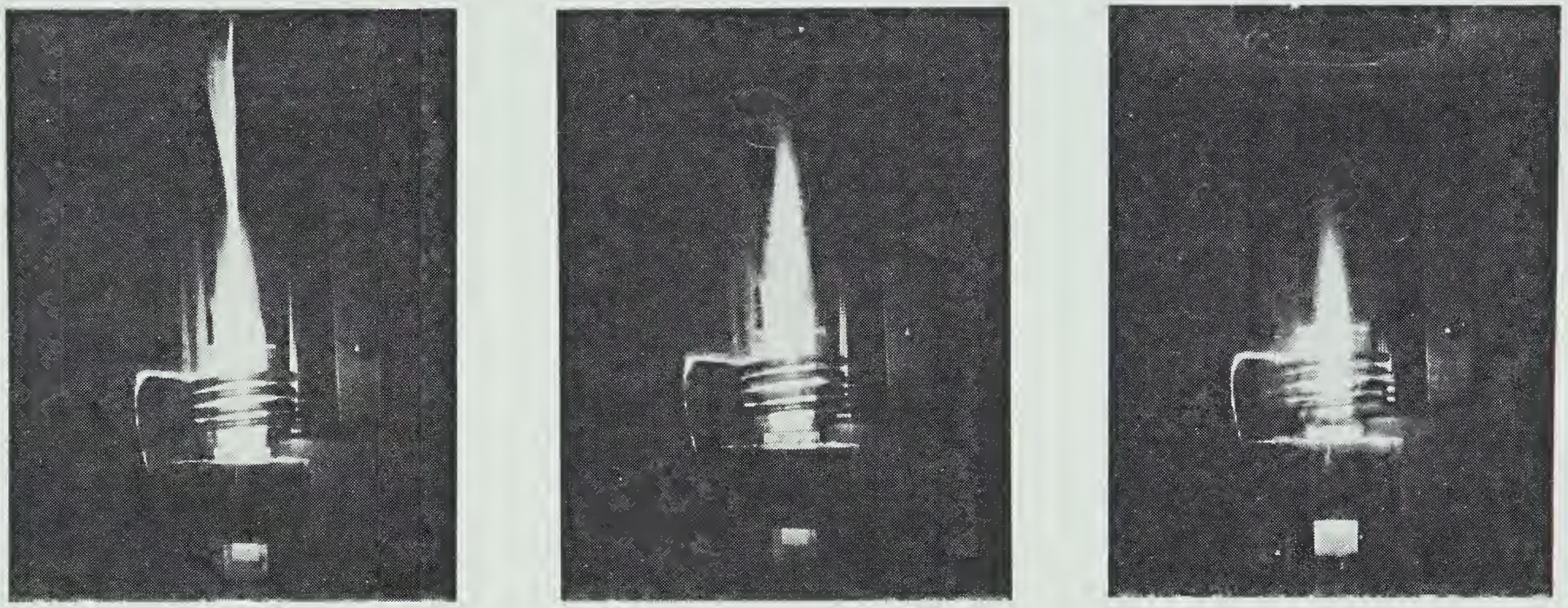

a b c

FIGURE 24. Photographs taken when oxygen was mixed into a plasma with benzene being nebulized. a = no O_2, b = small amount of O_2 in aerosol carrier flow, and c = 20% O_2 in plasma gas flow.

discharge and are noticed at the tail flame. Addition of a small amount of O_2 in the aerosol carrier flow (Frame b) resulted in a more stable discharge with no unburned carbon particles observed at the tail flame. When 20% O_2 is mixed in, the plasma formed is very stable and appears similar to one with xylene aspirating (Frame c). Similar behavior is also observed for hexane. This enhanced stability has enormous potential.

Hexane and benzene are both very common chromotographic reagents, but no reference on these solvents has been cited when HPLC is coupled to ICP (104). This may be the result of poor plasma stability. Addition of O_2 should thus enable such applications and extend the analytical capabilities of ICP.

BIBLIOGRAPHY

1. G.A. Mills, Ind. Eng. Chem., 42, 182 (1950).
2. B.J. Duffy, and H.M. Hart, Chem. Eng. Progr., 48, 344 (1952).
3. Committee on Public Affairs, "Lead in the Environment", American Petroleum Institute, New York (1967).
4. G. Eglinton, and M.T.J. Murphy, eds., "Organic Geochemistry", Springer-Verlag, New York (1969).
5. J.E. Falk, "Porphyrins and Metal Prophyrins", Vols. 1 and 2, American Elsevier Publishing Company, Inc., New York (1964).
6. J.V. Brunnock, D.F. Duckworth, and G.G. Stevens, J. Inst. Petrol., 54, 310 (1968).
7. E.R. Adlard, J. Inst. Petrol., 58, 63 (1972).
8. O.I. Milner, "Analysis of Petroleum for Trace Elements", Pergamon, New York (1963).
9. W.H. Thames, Inst. Petrol. Technol., 10, 216 (1924).
10. W.H. Thames, "Inorganic Constituents of Petroleum", Vol. 2, Oxford University Press, London (1938).
11. J. Scott, G.A. Collins, and G.W. Hodgson, Research Council of Alberta, Transactions, Vol. LVII, 34 (1954).
12. E.M. Magee, H.J. Hall, and G.M. Varga, Jr., "Potential Pollutants in Fossil Fuels", EPA-R2-73249, Office of Research and Monitoring, U.S. Environmental Protection Agency, Washington, D.C. (June 1973).

13. B.E. Buell, "Applied Atomic Spectroscopy", Vol. 2, E.L. Grove, ed., Plenum Press, New York, Chapter 2 (1978).

14. S.K. Kyuregyan, "Emission Spectral Analysis of Petroleum", Izdatelstvo Khimiya, Moscow (1969); Chem. Abstr., 74, 5285j (1971).

15. J.W. McCoy, "The Inorganic Analysis of Petroleum", Chemical Publishing Company, New York (1962).

16. R.A. Hofstader, O.I. Milner, and J.H. Runnels, eds., "Analysis of Petroleum for Trace Metals", American Chemical Society, Advances in Chemistry Series 156, Washington, D.C. (1976).

17. H.A. Braier, and J. Eppolito, "The Role of Trace Metals in Petroleum", T.F. Yen, ed., Ann Arbor Science Publishers, Inc., Ann Arbor, Mich., Chapter 4 (1976).

18. M. Fujita, Sekiyu Gakkai Shi, 20, 920 (1977).

19. F.M. Wrightson, Anal. Chem., 21, 1543 (1949).

20. G.W. Hodgson, Amer. Assoc. Petrol. Geol. Bull., 38, 2537 (1954).

21. B.L. Baker, and G.W. Hodgson, Amer. Assoc. Petrol. Geol. Bull., 43, 472 (1959).

22. B.W. Samuel, and J.V. Brunnock, Anal. Chem., 33, 203 (1961).

23. J.B. Flato, Anal. Chem., 44, 75A (1972).

24. R.C. Barras, Jarrell-Ash Newsletter, 13, 1 (June 1962).

25. S. Sprague, and W. Slavin, Atomic Absorption Newsletter, 12, 4 (April 1963).

26. R.C. Barras, and H.W. Smith, 7th World Petol. Congr., 9, 65 (1967).

27. K.W. Jackson, K.M. Aldous, and D.G. Mitchell, Appl. Spectrosc., 28, 569 (1974).

28. C.S. Saba, and K.J. Eisentraut, Anal. Chem., 49, 454 (1977).

29. C.S. Saba, and K.J. Eisentraut, Anal. Chem., 51, 1927 (1979).

30. J.H. Runnels, R. Merryfield, and H.B. Fisher, Anal. Chem., 47, 1258 (1975).

31. D.R. Thomerson, and K.C. Thompson, Chem. Br., 11, 316 (1975).

32. B. Welz, Chim. Ind., Milan, 58, 562 (1976).

33. R.H. Filby, Dissertation 1971, Washington State University, Pullman, Wash.

34. B. Hitchon, R.H. Filby, and K.R. Shah, Am. Chem. Soc., Div. Petrol. Chem., Prepr. 18, 623 (1973).

35. Al-H. Shahristani, and Al-M.J. Atyia, J. Radioanal. Chem., 14, 401 (1973).

36. H. Meier, and E. Unger, J. Radioanal. Chem., 32, 413 (1976).

37. H. Kubo, R. Bernthal, and T.R. Wildeman, Anal. Chem., 50, 899 (1978).

38. T.V. Krishnan, Indian J. Pure Appl. Phys., 15, 345 (1977).

39. W.B. Shirey, Ind. Eng. Chem., 23, 1151 (1931).

40. H.K. Hughes, J.W. Anderson, R.W. Murphy, and J.B. Rather, Amer. Petrol. Inst. Sect. III, 29M, 89 (1949).

41. L.E. Calkins, and M.M. White, Natl. Petrol. News, 38 (27), 519 (1946).

42. R.O. Clark, E.L. Baldeschwiller, G.M. Gambrill, C.E. Headington, H. Levin, J.M. Powers, and J.B. Rather, Anal. Chem., 23, 1348 (1951).

43. F.M. Burt, Diesel Progr., 1950, 68 (April).

44. J.P. Pagliasotti, and F.W. Porsche, Anal. Chem., 23, 198 (1951).

45. J.P. Pagliasotti, and F.W. Porsche, Anal. Chem., 1820 (1951).

46. G.M. Gambrill, A.G. Gassmann, and W.R. O'Neill, Anal. Chem., 23, 1365 (1951).

47. A.J. Mittledorf, The Spex Speaker, 13 (1) (1968).

48. H. van der Peipen, Spectrochim. Acta, Part B, 30, 179 (1975).

49. G.H. Morrison, "Trace Analysis - Physical Methods", Interscience, New York, N.Y. (1965).

50. M.S. Vigler, and J.K. Failoni, Appl. Spectrosc., 19, 57 (1965).

51. P.M. McElfresh, and M.L. Parsons, Anal. Chem., 46, 1021 (1974).

52. M. Sermin, Analysis, 2, 186 (1973).

53. G. Pforr, 9th International Symposium, Leipzig, Lubricants, Lubrication and Bearing Techniques, 1967; G. Pforr, "Schmierstoffe und Schmierungstechnik", No. 25, Deutscher Verlag fur Grundstoffindustrie, Leipzig.

54. G. Pforr, and O. Aribot, Z. Chem., 10, 78 (1970).

55. S. Greenfield, and P.B. Smith, Anal., Chim. Acta, 59, 341 (1972).

56. V.A. Fassel, E.M. Layton, C. Peterson, and R.N. Kniseley, Workshop Anal. Needs Future Appl. Coal Liquifaction, (Proc.), 271 (1974).

57. V.A. Fassel, C.A. Peterson, F.N. Abercrombie, and R.N. Kniseley, Anal. Chem., 48, 516 (1976).

58. C.A. Peterson, Dissertation 1977, Iowa State University, Ames, Iowa.

59. K. Ohls, Compend.-Dtsch. Ges. Mineraloewiss. Kohlechem., 77-78, 194 (1977).

60. A.W. Varnes, and T.E. Andrews, Jarrell-Ash Plasma Newsl., 1(1), 12 (1978).

61. A.F. Ward, and L. Mariello, Jarrell-Ash Plasma Newsl., 1(4), 10 (1978).

62. J.C. Smith, Jarrell-Ash Plasma Newsl., 2(3), 4 (1979).

63. R.N. Merryfield, and R.C. Loyd, Anal. Chem., 51, 1965 (1979).

64. K. Ohls, and D. Sommer, ICP Inform. Newsl., in press.

65. S. Greenfield, I.L. Jones, and C.T. Berry, Analyst, 89, 713 (1964).

66. R.H. Wendt, and V.A. Fassel, Anal. Chem., 37, 920 (1965).

67. R.H. Wendt, and V.A. Fassel, Anal. Chem., 38, 337 (1966).

68. V.A. Fassel, and R.N. Kniseley, Anal. Chem., 46, 1110A (1974).

69. S. Greenfield, H. McD. McGreachin, and P.B. Smith, Talanta, 23, 1 (1976).

70. R.M. Barnes, "C.R.C. Critical Reviews in Analytical Chemistry" (Sept. 1978).

71. R.L. Dahlquist, and J.W. Knoll, Appl. Spectrosc. 32, 1 (1978).

72. D. Truitt, and J.W. Robinson, Anal. Chim. Acta, 49, 401 (1970).

73. D. Truitt, and J.W. Robinson, Anal. Chim. Acta, 51, 61 (1970).

74. J. Warren, ICP Inform. Newsl., 2, 262 (1977).

75. A.F. Ward, H.R. Sobel, and R.L. Crawford, ICP Inform. Newsl., 3, 90 (1977).

76. A.W. Boorn, M.S. Cresser, and R.F. Browner, Spectrochim. Acta, Part B, in press.

77. S. Greenfield, I.L.W. Jones, C.T. Berry, and L.G. Bunch, Proc. Soc. Anal. Chem., 2, 111 (1965).

78. G. Horlick, Appl. Spectrosc., 30, 113 (1976).

79. G. Horlick, and E. Codding, "Contemporary Topics in Analytical and Clinical Chemistry", Vol. 1, Chap. 4 (1977).

80. J.E. Edmonds, and G. Horlick, Appl. Spectrosc., 31, 536 (1977).

81. G. Horlick, and M.W. Blades, Appl. Spectrosc., 34, 229 (1980).

82. B. Meddings, H. Kaiser, and H. Anderson, International Winter Conference on Developments in Atomic Plasma

Spectrochemical Analyses, San Juan, Puerto Rico (1980).

83. D.L. Millard, H.C. Shan, and G.F Kirkbright, Analyst, 105, 502 (1980).

84. D. Hull, Dissertation 1981, University of Alberta, Edmonton, Alberta.

85. F.N. Abercrombie, Pittsburgh Conference, Cleveland, Ohio, paper no. 406 (abstract) (1977).

86. J. Carr, and G. Horlick, Pittsburgh Conference, Atlantic City, N.J., paper no. 56 (abstract) (1980).

87. E.D. Salin, and G. Horlick, Anal. Chem., 51, 2284 (1979).

88. S. Greenfield, and P.B. Smith, Anal. Chim. Acta, 57, 209 (1971).

89. S. Greenfield, I.L.W. Jones, H. McGeachin, and P.B. Smith, Anal. Chim. Acta, 74, 225 (1975).

90. S. Greenfield, H. McGeachin, and P.B. Smith, ICP Inform. Newsl., 2, 167 (1976).

91. K. Ohls, and D. Sommer, ICP Inform. Newsl., 4, 532 (1979).

92. S. Greenfield, and H. McGeachin, Anal. Chim. Acta, 100, 101 (1978).

93. S. Greenfield, and D.T. Burns, Anal. Chim. Acta, 113, 205 (1980).

94. A. Montaser, and J. Mortazavi, Anal. Chem., 52, 255 (1980).

95. L. Ebdon, D.J. Mowthorpe, and M.R. Cave, Anal. Chim. Acta, 115, 171 (1980).

96. L. Ebdon, D.J. Mowthorpe, and M.R. Cave, Anal. Chim. Acta, 115, 179 (1980).

97. E.H. Choot, and G. Horlick, Spectrochim. Acta, in press.

98. R.M. Barnes, and G.A. Meyer, Anal. Chem., 52, 1523 (1980).

99. R.H. Scott, V.A. Fassel, R.N. Kniseley, and D.E. Nixon, Anal. Chem., 46, 75 (1974).

100. R.M. Barnes, and S. Nikdel, Appl. Spectrosc., 30, 310 (1976).

101. K.W. Bush, and T.J. Vickers, Spectrochim. Acta, 28B, 85 (1973).

102. J.M. Mermet, C.R. Acad. Sci., Ser. B281, 273 (1975).

103. P.W.J.M. Boumans, and F.J. De Boer, Spectrochim. Acta, 32B, 365 (1977).

104. I.S. Krull, and S. Jordan, American Lab., 21 (October 1980).

APPENDIX

SOFTWARE FOR PDA ACQUISITION, REDUCTION AND PLOTTING

A. ADCPDA - Data Acquisition and Reduction Routine

1. Purpose: To acquire and process data from the photodiode array.

2. Author: Originally written by D. Hull and modified by M. Lau.

3. Subroutines: PLOT55, FGDLPS and SYSLIB.

4. Operation: The operator is required to input a sample name, the number of scans, and the number of points. Background corrections can also be performed. The program accesses the system data automatically. After data acquisition, the operator then has the option of plotting the data on the VT55 screen, listing the data, locating peak of interest, subtracting spectrum, and summation of a series of channels. In addition, the operator can store the data on disk, return to the start of the program, or exit to the monitor. For further details, see the program listing.

```
      DIMENSION       TITLE(3),DAT(3),A1(30),C(1040),E(1040)
      DIMENSION       JUNK1(3),JUNK2(3)
      INTEGER*4       A(1040)
      INTEGER*2       B(1040),D(520),NDIOD(30),NDIODN(30)
      EQUIVALENCE(B(513),D(1))
      EQUIVALENCE(B(1),E(1))
      EQUIVALENCE(A(1),C(1))
      COMMON/DRH/A,NS,NP,IBKD
      INTEGER ATTACH, SELGR, STATUS, N, HGRD, VGRD, MARKER, ORIGIN,
     1 VECT, CURPOS, ERASCR, ERALIN, DISPLY, ESCCMD, UP, DOWN, HOME,
     1 ESCRN, ELIN, ENHOLD, DSHOLD, COPY, ENPRNT, DSPRNT, BELL
      DATA    DAT,TITLE/3*0.,3*0./
      DATA    ATTACH, SELGR, STATUS, N, HGRD, VGRD, MARKER, ORIGIN,
     1 VECT, CURPOS, ERASCR, ERALIN, DISPLY, ESCCMD, UP, DOWN, HOME,
     1 ESCRN, ELIN, ENHOLD, DSHOLD, COPY, ENPRNT, DSPRNT, BELL
     1/0,1,2,3,4,5,6,7,8,9,10,11,12,13,65,66,72,74,75,91,92,93,94,95,7/
      CALL DATE(DAT)
      WRITE(7,52)DAT
400   DO 91   I=1,1040
      C(I)=0.
91    B(I)=0
52    FORMAT(' ',3A4)
      WRITE(7,53)
53    FORMAT(' ','INPUT SAMPLE NAME IN 3A4-FORMAT.')
      READ(5,51,END=120)TITLE
51    FORMAT(3A4)
      WRITE(7,54)
54    FORMAT(' ','INPUT #SCANS.')
      READ(5,59,END=120)XNS
      WRITE(7,55)
55    FORMAT(' ','INPUT #POINTS.')
      READ(5,59,END=120)XNP
      NP=IFIX(XNP)
      NS=IFIX(XNS)
59    FORMAT(F10.0)
      WRITE(7,68)
68    FORMAT(' ','DO YOU WISH BACKGROUND SUBTRACTION? YES=1, NO=0')
      READ(5,59,END=120)BKD
      NS=IFIX(XNS)
      NP=IFIX(XNP)
      IBKD=IFIX(BKD)
      NP=NP+4
C
C     ACQUIRE DATA WITH SUBROUTINE FGDLPS.
C
      CALL FGDLPS
C
C     CONVERSION OF DATA FROM INTEGER*4 TO REAL
C
      DO 90   J=5,NP
90    C(J-4)=AJFLT(A(J))
      NP=NP-4
      C(NP+1)=XNS
      C(NP+2)=XNP
      C(NP+3)=BKD
C
C     CALCULATION OF MAXIMUM, MINIMUM, AND RANGE OF VALUES.
C
1010  C(NP+4)=C(1)
      C(NP+5)=1.
      C(NP+6)=C(1)
      C(NP+7)=1.
      DO 1000 I=2,NP
C
C     MAXIMUM AND SUBSCRIPT DETERMINATION.
C
      IF(C(NP+4) .LT. C(I))C(NP+4)=C(I)
      IF(C(NP+4) .EQ. C(I))C(NP+5)=FLOAT(I)
```

```
C
C       MINIMUM AND SUBSCRIPT DETERMINATION.
C
        IF(C(NP+6) .GT. C(I))C(NP+6)=C(I)
1000    IF(C(NP+6) .EQ. C(I))C(NP+7)=FLOAT(I)
C
C       RANGE DETERMINATION.
C
        C(NP+8)=C(NP+4)-C(NP+6)
        WRITE(7,56)(C(NP+I),I=4,8)
56      FORMAT(' ','MAX=',F10.0,2X,'@',F5.0,' MIN=',F10.0,
     1 2X,'@',F5.0,' RANGE=',F10.0)
C
C       PROCESSING REQUEST.
C
6       WRITE(7,57)
57      FORMAT(' ','PLOT=1, LIST=2, PEAK LOCATE=3, RESTART=4,',/,
     1 ' EXIT=5, WRITE DISK=6, READ DISK=7, TOTALS=8, SUB BKGD=9')
        CALL PLOT55(DISPLY,0,BELL)
        READ(5,58,END=120)NTEMP
58      FORMAT(I2)
        CALL PLOT55(ESCCMD,HOME,0)
        CALL PLOT55(ESCCMD,ESCRN,0)
        GO TO(100,200,300,400,500,600,700,800,900),NTEMP
        GO TO 6
C
C       DISPLAY A PLOT OF DATA ON THE VT-55 SCREEN.
C
100     NPLOT=NP
        WRITE(7,101)
101     FORMAT(' ','NORMALIZED PLOT? YES=1, NO=0')
        READ(5,59,END=120)XNORM
        IF(XNORM .EQ. 1.0)SCFAC=C(NP+8)
        IF(XNORM .EQ. 1.0)GO TO 102
        WRITE(7,103)
103     FORMAT(' ','ENTER SCALING FACTOR, F10.0')
        READ(5,59,END=120)SCFAC
102     CONTINUE
        DO 150  I=1,NP
150     B(I)=IFIX(((C(I)-C(NP+6))*100.)/SCFAC)
        CALL PLOT55(ESCCMD,HOME,0)
        CALL PLOT55(ESCCMD,ESCRN,0)
        CALL PLOT55(STATUS,547,476)
        CALL PLOT55(SELGR,0,0)
        CALL PLOT55(CURPOS,0,0)
        WRITE(7,170)TITLE,DAT,C(NP+1),C(NP+2),C(NP+3)
        WRITE(7,56)(C(NP+I),I=4,8)
        CALL PLOT55(HGRD,1,0,0)
        IF(NPLOT .LE. 512)GO TO 151
        CALL PLOT55(STATUS,551,472)
        CALL PLOT55(SELGR,1,0)
        CALL PLOT55(HGRD,1,101)
151     IF(NP .GT. 512)NPLOT=512
        CALL PLOT55(SELGR,0,0)
        CALL PLOT55(ORIGIN,0,0)
        CALL PLOT55(N,-NPLOT,B)
        IF(NP .LE. 512)GO TO 153
        NPLOT=NP-512
        CALL PLOT55(SELGR,1,0)
        DO 156  I=1,NPLOT
156     D(I)=D(I)+101
        CALL PLOT55(N,-NPLOT,D)
153     CALL PLOT55(DISPLY,0,BELL)
        READ(5,58,END=120)NSTOP
120     CALL PLOT55(ESCCMD,HOME,0)
        CALL PLOT55(ESCCMD,ESCRN,0)
        CALL PLOT55(STATUS,0,1023)
        GO TO 6
```

```
C
C       THIS SECTION LISTS THE DATA ON THE VT-55 COPIER.
C
200     CALL PLOT55(ESCCMD,HOME,0)
        CALL PLOT55(ESCCMD,ESCRN,0)
        CALL PLOT55(DISPLY,0,BELL)
        WRITE(7,170)TITLE,DAT,C(NP+1),C(NP+2),C(NP+3)
        WRITE(7,56)(C(NP+I),I=4,8)
170     FORMAT(' ',3A4,3A4,3X,'NS=',F10.0,3X,'NF=',F10.0,
     1 3X,'BKGD=',F10.0)
        DO 250  I=1,NP+8,100
        DO 251  J=I,I+95,5
        WRITE(7,63)J,(C(K),K=J,J+4)
        IF(K .GT. (NP+8))GO TO 252
251     CONTINUE
        READ(5,58,END=253)NSTOP
253     CALL PLOT55(ESCCMD,HOME,0)
        CALL PLOT55(ESCCMD,ESCRN,0)
250     CONTINUE
63      FORMAT(' ',I4,2X,'>',5(F10.0,1X))
252     CALL PLOT55(ESCCMD,HOME,0)
        CALL PLOT55(DISPLY,0,BELL)
        READ(5,58,END=120)NSTOP
        GO TO 120
C
C       THIS SECTION DETERMINES PEAK LOCATIONS AND DISPLAYS
C       THE LOCATION AND PEAK VALUE ON THE VT-55.
C
300     CALL PLOT55(ESCCMD,HOME,0)
        CALL PLOT55(ESCCMD,ESCRN,0)
        WRITE(7,170)TITLE,DAT,C(NP+1),C(NP+2),C(NP+3)
        WRITE(7,56)(C(NP+I),I=4,8)
        WRITE(7,64)
64      FORMAT(' ','ENTER THE THRESHOLD,F10.0')
        READ(5,59,END=120)THRES
66      FORMAT(' ','POINT NO.   AMPLITUDE')
        DO 320  J=1,NP
        NCNT=0
        WRITE(7,66)
        DO 310  I=J,NP
        IF(C(I) .LT. THRES)GO TO 310
        IF(C(I+1) .GT. C(I))GO TO 310
        IF(C(I) .LE. C(I-1))GO TO 310
        WRITE(7,67)I,C(I)
        NCNT=NCNT+1
        J=I
        IF(I .GE. NP)GO TO 320
        IF(NCNT .EQ. 20)GO TO 311
310     J=I
        IF(I .GE. NP)GO TO 320
311     READ(5,58,END=120)NSTOP
        CALL PLOT55(ESCCMD,HOME,0)
        CALL PLOT55(ESCCMD,ESCRN,0)
320     CONTINUE
67      FORMAT(5X,I4,6X,F10.0)
        CALL PLOT55(ESCCMD,HOME,0)
        CALL PLOT55(DISPLY,0,BELL)
        READ(5,58,END=120)NSTOP
        CALL PLOT55(ESCCMD,ESCRN,0)
        GO TO 120
C
C       THIS SECTION WRITES THE DATA ON DISK AND NAMES THE DATA FILE.
C
600     REWIND 1
        WRITE(7,170)TITLE,DAT,C(NP+1),C(NP+2),C(NP+3)
        WRITE(7,56)(C(NP+I),I=4,8)
        WRITE(7,720)
```

```
      CALL ASSIGN(1,'DK:FTN1.DAT',-1,'NEW','NC',1)
      WRITE(1)(DAT(I),I=1,3)
      WRITE(1)(TITLE(I),I=1,3)
      WRITE(1)(C(I),I=1,NP+8)
      ENDFILE 1
      CALL CLOSE(1)
      GO TO 120
C
C     THIS SECTION READS DATA FILE FROM DISK.
C
700   WRITE(7,720)
720   FORMAT(' ',' ENTER DATA FILE NAME AS *------(.DAT).',/)
      CALL ASSIGN(1,'DK:FTN1.DAT',-1,'OLD','NC',1)
      READ(1)(DAT(I),I=1,3)
      READ(1)(TITLE(I),I=1,3)
      READ(1)(C(I),I=1,NP+8)
      ENDFILE 1
      CALL CLOSE(1)
      GO TO 120
C
C     THIS SECTION READS DATA FILE FROM DISK.
C
900   WRITE(7,720)
920   FORMAT(' ',' ENTER DATA FILE NAME AS *------(.DAT).',/)
      CALL ASSIGN(1,'DK:FTN1.DAT',-1,'OLD','NC',1)
      READ(1)(JUNK1(I),I=1,3)
      READ(1)(JUNK2(I),I=1,3)
      READ(1)(E(I),I=1,NP+8)
      ENDFILE 1
      CALL CLOSE(1)
      DO 930  NQ=1,NP
930   C(NQ)=C(NQ)-E(NQ)
      C(NP+3)=1
      GO TO 1010
C
C     THIS SECTION CALCULATES THE TOTALS FOR SELECTED
C     PORTIONS OF THE DATA.
C
800   DO 805  J=1,30
      A1(J)=0
      NDIOD(J)=0
      NDIODN(J)=0
805   CONTINUE
      CALL PLOT55(ESCCMD,HOME,0)
      CALL PLOT55(ESCCMD,ESCRN,0)
      WRITE(7,170)TITLE,DAT,C(NP+1),C(NP+2),C(NP+3)
      WRITE(7,56)(C(NP+I),I=4,8)
      JR=0
      WRITE(7,882)
882   FORMAT(' ','ENTER THE STARTING POINT # AND # OF POINTS.',/,
     1 ' ENTER EXTRA CARRAGE RETURN TO COMMENCE PROCESSING.')
801   READ(5,881,END=120,ERR=801)DIODE,DIODEN
881   FORMAT(2F10.0)
      IF(DIODE .EQ. 0)GO TO 810
      JR=JR+1
      NDIOD(JR)=IFIX(DIODE)
      NDIODN(JR)=IFIX(DIODEN)
      IF(JR .GE. 30)GO TO 810
      GO TO 801
810   CALL PLOT55(ESCCMD,HOME,0)
      CALL PLOT55(ESCCMD,ESCRN,0)
      WRITE(7,170)TITLE,DAT,C(NP+1),C(NP+2),C(NP+3)
      WRITE(7,56)(C(NP+I),I=4,8)
      WRITE(7,840)
840   FORMAT(' ',' START     NP        TOTAL')
      DO 816  K=1,JR
      DO 818  L=NDIOD(K),(NDIOD(K)+NDIODN(K)-1)
818   A1(K)=A1(K)+C(L)
```

```
      WRITE(7,855)NDIOD(K),NDIODN(K),A1(K)
855   FORMAT(3X,I4,3X,I4,F12.0)
816   CONTINUE
      READ(5,58,END=120,ERR=120)NSTOP
      GO TO 120
C
C     THIS SECTION CAUSES AN EXIT FROM THE PROGRAM.
C
500   STOP
      END
```

B. PDAPLT - Plotting and Smoothing of Spectral Data

1. Purpose: To plot, with the XY-Plotter, floating point photodiode array data acquired by ADCPDA.

2. Author: Written by D. Hull.

3. Subroutines: XYLIB, SYSLIB, and /F.

4. Operation: This routine requires the number of data points, and a file name input to access a file *.DAT. Smoothing of data is carried out by simplified least squares procedures from Savitzky and Golay. See the program listing for further details.

```
      DIMENSION       TITLE(3),DAT(3),X(1040),Y(1040),F(1040)
      DIMENSION       XAXIS(7),YAXIS(7),TITP(7)
      INTEGER*2       DBLK(4)
      DATA    DAT,TITLE/3*0.,3*0./
      DATA    DBLK/3RDK0,3RDAT,3RA  ,3RDAT/
C
C     THIS SECTION RESTARTS PROGRAM BY CLEARING X & Y ARRAYS.
C
700   CALL PLOTST(0.005,'IN')
      CALL PLOT(8.5,0.0,-3)
      CALL PLOTND
      DO 701  I=1,1040
      X(I)=FLOAT(I)
701   Y(I)=0.0
      WRITE(7,110)
110   FORMAT(' ','INPUT # DATA POINTS.')
      READ(5,111)XNP
111   FORMAT(F10.0)
      NP=IFIX(XNP)
C
C     THIS SECTION SELECTS THE PART OF THE PROGRAM TO BE EXICUTED.
C
1     WRITE(7,50)
50    FORMAT(' ','READ DISK=1, AXIS=2, PLOT=3, RESTART=4,
     1 ,SMOOTH=5, EXIT=6')
      READ(5,51)NTEMP
51    FORMAT(I2)
      IF(NTEMP .LT. 1 .OR. NTEMP .GT. 6)GO TO 1
      GO TO(100,500,600,700,900,800),NTEMP
C
C     THIS SECTION READS DATA FILE FROM DISK.
C
100   WRITE(7,120)
120   FORMAT(' ',' ENTER DATA FILE NAME AS *------.DAT.',/)
      CALL ASSIGN(1,'DK:FTN1.DAT',-1,'OLD','NC',1)
      READ(1)(DAT(I),I=1,3)
      READ(1)(TITLE(I),I=1,3)
      READ(1)(Y(I),I=1,NP+8)
      ENDFILE 1
      CALL CLOSE(1)

C
C     THIS SECTION DOES BOOK KEEPING ON THE DATA ARRAY.
C
490   DO 491  I=8,1,-1
491   Y(NP+2+I)=Y(NP+I)
C
C     THIS SECTION SETS THE MINIMUM VALUE TO 0.0 AND
C     THE MAXIMUM VALUE TO BE EQUAL TO THE RANGE FOR
C     PLOTTING PURPOSES
C
C     CALCULATION OF MAXIMUM, MINIMUM, AND RANGE OF VALUES.
C
91    Y(NP+6)=Y(1)
      Y(NP+7)=FLOAT(1)
      Y(NP+8)=Y(1)
      Y(NP+9)=FLOAT(1)
      DO 1000 I=2,NP
C
C     MAXIMUM AND SUBSCRIPT DETERMINATION.
C
      IF(Y(NP+6) .LT. Y(I))Y(NP+6)=Y(I)
      IF(Y(NP+6) .EQ. Y(I))Y(NP+7)=FLOAT(I)
C
C     MINIMUM AND SUBSCRIPT DETERMINATION.
C
      IF(Y(NP+8) .GT. Y(I))Y(NP+8)=Y(I)
1000  IF(Y(NP+8) .EQ. Y(I))Y(NP+9)=FLOAT(I)
```

```
C
C       RANGE DETERMINATION.
C
        Y(NP+10)=Y(NP+6)-Y(NP+8)
        IF(NTEMP .EQ. 5)GO TO 495
        DO 492  I=1,NP
492     Y(I)=Y(I)-Y(NP+8)
        Y(NP+6)=Y(NP+6)-Y(NP+8)
        Y(NP+8)=0.0
495     WRITE(7,493)TITLE,DAT,Y(NP+3),Y(NP+4),Y(NP+5)
493     FORMAT(' ',3A4,3A4,3X,'NS='F4.0,3X,'NP=',F4.0,3X,'BKGD=',F4.0)
        WRITE(7,494)(Y(NP+I),I=6,10)
494     FORMAT(' ','MAX=',F10.0,'@',F4.0,' MIN=',F10.0,
     1 '@',F4.0,' RANGE=',F10.0)
        GO TO 1
C
C       THIS SECTION DRAWS THE AXIS OF THE PLOT.
C
500     CONTINUE
502     FORMAT(7A4)
        WRITE(7,510)
510     FORMAT(' ',' ENTER THE TITLE FOR THE XAXIS, 28 CARACTERS MAX.')
        READ(5,502)XAXIS
        WRITE(7,503)
503     FORMAT(' ','ENTER THE TITLE FOR THE Y AXIS, 28 CARACTERS MAX')
        READ(5,502)YAXIS
        WRITE(7,504)
504     FORMAT(' ','ENTER THE TITLE FOR THE PLOT, 28 CARACTERS MAX.')
        READ(5,502)TITP
        XMIN=0.0
        XMAX=Y(NP+4)
        WRITE (7,505)
505     FORMAT(' ','XMIN=0 & XMAX=NP.',/
     1 '  ENTER 1 TO CHANGE, CARRAGE RETURN IF NO CHANGE DESIRED.')
        READ(5,51)NTEMP
        IF (NTEMP .NE. 1)GO TO 506
        WRITE(7,507)
507     FORMAT(' ','ENTER NEW VALUES FOR XMIN AND XMAX, 2F10.0.')
        READ(5,525)XMIN,XMAX
506     YMIN=0.0
        YMAX=Y(NP+6)
        WRITE(7,520)
520     FORMAT(' ',' ENTER X AND Y AXIS LENGTHS, 2F10.0.')
        READ(5,525)XLONG,YLONG
525     FORMAT(2F10.0)
621     WRITE(7,494)(Y(NP+I),I=6,10)
        WRITE(7,620)
620     FORMAT(' ',' NORMALIZED PLOT=1, SCALED PLOT=0.')
        READ(5,51)NTEMP
        IF(NTEMP .EQ. 1)GO TO 550
        WRITE(7,625)
625     FORMAT(' ',' ENTER NEW VALUE FOR Y RANGE, F10.0.')
        READ(5,111)YMAX
550     X(NP+1)=XMIN
        X(NP+2)=(XMAX-XMIN)/XLONG
        Y(NP+1)=YMIN
        Y(NP+2)=(YMAX-YMIN)/YLONG
        CALL PLOTST(0.005,'IN')
        CALL PLOT(1.5,1.0,-3)
        CALL AXIS(0.0,0.0,XAXIS,-28,XLONG,0.0,X(NP+1),X(NP+2))
        CALL AXIS(0.0,0.0,YAXIS,+28,YLONG,90.0,Y(NP+1),Y(NP+2))
        CALL PLOT(XLONG,0,+3)
        CALL PLOT(XLONG,YLONG,+2)
        CALL PLOT(0,YLONG,+2)
        CALL PLOT(0,(YLONG+0.5),+3)
        CALL SYMBOL(0,(YLONG+0.5),0.14,TITP,0,28)
        CALL PLOT(0.0,0.0,+3)
        CALL PLOT(-1.5,-1.0,-3)
        CALL PLOTND
        GO TO 1
```

```
C
C       THIS SECTION PLOTS THE DATA.
C
600     WRITE(7,610)
610     FORMAT(' ',' CHANGE Y-RANGE? YES=1, NO=CARRAGE RETURN')
        READ(5,51)NQ
        IF(NQ .EQ. 0)GO TO 611
        WRITE(7,625)
        READ(5,111)YMAX
611     X(NP+1)=0.0
        X(NP+2)=XNP/XLONG
        Y(NP+1)=YMIN
        Y(NP+2)=(YMAX-YMIN)/YLONG
        CALL PLOTST(0.005,'IN')
        CALL PLOT(1.5,1.0,-3)
        CALL LINE(X,Y,NP,1,0,0)
        CALL PLOT(0.0,0.0,+3)
        CALL PLOT(-1.5,-1.0,-3)
        CALL PLOTND
        GO TO 1
C
C       THIS SECTION DOES SMOOTHING OF DATA BY SIMPLIFIED LEAST
C       SQUARES PROCEDURE FROM SAVITZKY AND GOLAY,
C       ANAL. CHEM.,36(8),P1627(1964)
C
900     WRITE(7,999)
999     FORMAT(' ','INPUT FILTER SIZE:',/,/,' 1=5 POINT FILTER',
     1 /,' 2=7 POINT FILTER',/,' 3=9 POINT FILTER',
     2 /,' 4=11 POINT FILTER',
     3 /,' 5=13 POINT FILTER',/,' 6=15 POINT FILTER',
     4 /,' 7=17 POINT FILTER',/,' 8=19 POINT FILTER',/,
     5 ' 9=21 POINT FILTER')
        READ(5,58,ERR=900,END=1)NGO
58      FORMAT(I2)
        GO TO (910,920,930,940,950,960,970,980,990),NGO
910     DO 915  I=3,(NP-2)
915     F(I)=(((-(Y(I-2)+Y(I+2)))*3+((Y(I-1)+Y(I+1)))*12
     1 +((Y(I)))*17)/35)
        DO 916  I=3,(NP-2)
916     Y(I)=F(I)
        Y(1)=Y(3)
        Y(2)=Y(3)
        Y(NP-1)=Y(NP-2)
        Y(NP)=Y(NP-2)
        GO TO 91
920     DO 925  I=4,(NP-3)
925     F(I)=(((-(Y(I-3)+Y(I+3)))*2+((Y(I-2)+Y(I+2)))*3
     1 +((Y(I-1)+Y(I+1)))*6+((Y(I)))*7)/21)
        DO 926  I=4,(NP-3)
926     Y(I)=F(I)
        Y(1)=Y(4)
        Y(2)=Y(4)
        Y(3)=Y(4)
        Y(NP-2)=Y(NP-3)
        Y(NP-1)=Y(NP-3)
        Y(NP)=Y(NP-3)
        GO TO 91
930     DO 935  I=5,(NP-4)
935     F(I)=(((-(Y(I-4)+Y(I+4)))*21
     1 +((Y(I-3)+Y(I+3)))*14
     2 +((Y(I-2)+Y(I+2)))*39+((Y(I-1)+Y(I+1)))*54
     3 +((Y(I)))*59)/231)
        DO 936  I=5,(NP-4)
936     Y(I)=F(I)
        DO 937  I=1,4
        Y(I)=Y(5)
937     Y(NP-I+1)=Y(NP-4)
        GO TO 91
```

```
940      DO 945  I=6,(NP-5)
945      F(I)=(((-(Y(I-5)+Y(I+5)))*36
     1 +((Y(I-4)+Y(I+4)))*9+((Y(I-3)+Y(I+3)))*44
     2 +((Y(I-2)+Y(I+2)))*69
     2 +((Y(I-1)+Y(I+1)))*84+((Y(I)))*89)/429)
         DO 946  I=6,(NP-5)
946      Y(I)=F(I)
         DO 947  I=1,5
         Y(I)=Y(6)
947      Y(NP-I+1)=Y(NP-5)
         GO TO 91
950      DO 955  I=7,(NP-6)
955      F(I)=(((-(Y(I-6)+Y(I+6)))*11
     1 +((Y(I-4)+Y(I+4)))*9+((Y(I-3)+Y(I+3)))*16
     2 +((Y(I-2)+Y(I+2)))*21+((Y(I-1)+Y(I+1)))*24
     3 +((Y(I)))*25)/143)
         DO 956  I=7,(NP-6)
956      Y(I)=F(I)
         DO 957  I=1,6
         Y(I)=Y(7)
957      Y(NP-I+1)=Y(NP-6)
         GO TO 91
960      DO 965  I=8,(NP-7)
965      F(I)=(((-(Y(I-7)+Y(I+7)))*78-((Y(I-6)+Y(I+6)))*13
     1 +((Y(I-5)+Y(I+5)))*42+((Y(I-4)+Y(I+4)))*87
     2 +((Y(I-3)+Y(I+3)))*122+((Y(I-2)+Y(I+2)))*147
     3 +((Y(I-1)+Y(I+1)))*162+((Y(I)))*167)/1105)
         DO 966  I=8,(NP-7)
966      Y(I)=F(I)
         DO 967  I=1,7
         Y(I)=Y(8)
967      Y(NP-I+1)=Y(NP-7)
         GO TO 91
970      DO 975  I=9,(NP-8)
975      F(I)=(((-(Y(I-8)+Y(I+8)))*21+(-(Y(I-7)+Y(I+7)))*6
     1 +((Y(I-6)+Y(I+6)))*7+((Y(I-5)+Y(I+5)))*18
     2 +((Y(I-4)+Y(I+4)))*27+((Y(I-3)+Y(I+3)))*34
     3 +((Y(I-2)+Y(I+2)))*39+((Y(I-1)+Y(I+1)))*42
     4 +((Y(I)))*43)/323)
         DO 976  I=9,(NP-8)
976      Y(I)=F(I)
         DO 977  I=1,8
         Y(I)=Y(9)
977      Y(NP-I+1)=Y(NP-8)
         GO TO 91
980      DO 985  I=10,(NP-9)
985      F(I)=(((-(Y(I-9)+Y(I+9)))*136-((Y(I-8)+Y(I+8)))*51
     1 +((Y(I-7)+Y(I+7)))*24+((Y(I-6)+Y(I+6)))*89
     2 +((Y(I-5)+Y(I+5)))*144+((Y(I-4)+Y(I+4)))*189
     3 +((Y(I-3)+Y(I+3)))*224+((Y(I-2)+Y(I+2)))*249
     4 +((Y(I-1)+Y(I+1)))*264+((Y(I)))*269)/2261)
         DO 986  I=10,(NP-9)
986      Y(I)=F(I)
         DO 987  I=1,9
         Y(I)=Y(10)
987      Y(NP-I+1)=Y(NP-9)
         GO TO 91
990      DO 995  I=11,(NP-10)
995      F(I)=(((-(Y(I-10)+Y(I+10)))*171
     1 -((Y(I-9)+Y(I+9)))*76
     2 +((Y(I-8)+Y(I+8)))*9+((Y(I-7)+Y(I+7)))*84
     3 +((Y(I-6)+Y(I+6)))*149+((Y(I-5)+Y(I+5)))*204
     4 +((Y(I-4)+Y(I+4)))*249+((Y(I-3)+Y(I+3)))*284
     5 +((Y(I-2)+Y(I+2)))*309+((Y(I-1)+Y(I+1)))*324
     6 +((Y(I)))*329)/3059)
         DO 996  I=11,(NP-10)
996      Y(I)=F(I)
         DO 997  I=1,10
         Y(I)=Y(11)
997      Y(NP-I+1)=Y(NP-10)
         GO TO 91
```

```
C
C       THIS SECTION CAUSES AN EXIT FROM THE PROGRAM.
C
800     CALL PLOTST(0.005,'IN')
        CALL PLOT(8.5,0.0,-3)
        CALL PLOTND
        STOP
        END
```